COMPARISON OF DIKES AND SCREEN UNITS WITHIN THE TRANSITION ZONE FROM EXTRUSIVES TO SHEETED DIKES OF THE TROODOS OPHIOLITE, CYPRUS

Jacquelyn E. Stevens

Submitted in Partial Fulfilment of the Requirements
For the Degree of Bachelor of Science, Honours
Department of Earth Sciences
Dalhousie University, Halifax, Nova Scotia

March 1995

Dalhousie University

Department of Earth Sciences
Halifax, Nova Scotia
Canada B3H 3J5
(902) 494-2358
FAX (902) 494-6889

DATE May 8, 1995

AUTHOR Jacquelyn E. Stevens

TITLE Comparison of Dike and Screen Units within the Transition Zone from Extrusives to Sheeted Dikes of the Troodos ophiolite, Cyprus.

Degree B.Sc. Convocation May Year 1996

Permission is herewith granted to Dalhousie University to circulate and to have copied for non-commercial purposes, at its discretion, the above title upon the request of individuals or institutions.

Distribution License

DalSpace requires agreement to this non-exclusive distribution license before your item can appear on DalSpace.

NON-EXCLUSIVE DISTRIBUTION LICENSE

You (the author(s) or copyright owner) grant to Dalhousie University the non-exclusive right to reproduce and distribute your submission worldwide in any medium.

You agree that Dalhousie University may, without changing the content, reformat the submission for the purpose of preservation.

You also agree that Dalhousie University may keep more than one copy of this submission for purposes of security, back-up and preservation.

You agree that the submission is your original work, and that you have the right to grant the rights contained in this license. You also agree that your submission does not, to the best of your knowledge, infringe upon anyone's copyright.

If the submission contains material for which you do not hold copyright, you agree that you have obtained the unrestricted permission of the copyright owner to grant Dalhousie University the rights required by this license, and that such third-party owned material is clearly identified and acknowledged within the text or content of the submission.

If the submission is based upon work that has been sponsored or supported by an agency or organization other than Dalhousie University, you assert that you have fulfilled any right of review or other obligations required by such contract or agreement.

Dalhousie University will clearly identify your name(s) as the author(s) or owner(s) of the submission, and will not make any alteration to the content of the files that you have submitted.

If you have questions regarding this license please contact the repository manager at dalspace@dal.ca.

Grant the distribution license by signing and dating below.

_____ _____

Name of signatory Date

ABSTRACT

Petrological and geochemical investigations of a series of interleaved dikes and lava screens from the Transition Constructional Zone of the Troodos ophiolite are studied to determine whether differences in magnetization of the dike and screen units are the result of primary composition or secondary alteration. Dike and screen units are hydrothermally altered equivalents to the transition alteration zone typified by the presence of chlorite and clays together. Major and trace element results show that the dike and screen units fall within a restricted basalt-basaltic andesite-andesite interval (SiO_2 46 - 62 wt %) of the Magma Group A series. Differences in primary composition cannot be responsible for the differences in magnetization. Degree of alteration, rather than style, is a probable explanation for the differences in magnetization. The results of this study indicate that magnetization can be used to interpret lithological sequences present at DSDP/ODP Hole 504B.

Keywords: Cyprus, Troodos ophiolite, Transition Constructional Zone, primary composition, secondary alteration, DSDP/ODP Hole 504B.

Table of Contents

Table of Figures

Table of Tables

Acknowledgements

I would like to thank my supervisor, Dr. Jim Hall, for his friendship, encouragement, and unending support and patience. I would also like to thank Lata Hall, James Hall, and Charlie Walls for their excellent field material, and Dr. D. B. Clarke for his editorial comments. I would like to extend a special thanks to Robbie Hicks for her encouragement and insight, and the use of her computer. Thanks also to Tom Duffett, Bob MacKay, Dr. M. Gibling, Sally Stanford, and Dr. J. Dostal. Finally, I would especially like to thank my family for their constant support and encouragement over the past 23 years; I know I haven't always made it easy.

CHAPTER 1 INTRODUCTION

1.1 General Introduction

In-situ oceanic crust is relatively thin, seven to eight kilometres thick, and is composed predominantly of basaltic lithologies. Oceanic crust consists of four major layers: 1) a surface layer of marine sediments, 2) an underlying layer of pillow basalts, 3) a zone of sheeted basaltic dikes, and 4) a layer of mafic and ultramafic rock (Nicolas 1989). Ophiolites, fragments of oceanic-type crust now above sea level, provide much of the evidence for the nature of oceanic crust. Intense study into the nature, source, and emplacement mechanism of these oceanic-type crustal suites, termed ophiolite suites has been completed over the last few decades. With the advent of plate tectonics, obduction, the emplacement of oceanic crust on the continental margin during plate convergence, explains the presence of ophiolite suites (Nicolas 1989).

The Troodos ophiolite of Cyprus is a reliable and well-studied analog for *in-situ* oceanic crust. The rocks of Troodos resemble *in-situ* oceanic crust in many ways including construction, physical properties, and hydrothermal circulation and alteration. DSDP/ODP Hole 504B, for which the Troodos ophiolite is probably a useful analog, is the deepest hole drilled in *in-situ* oceanic crust. Situated in 5.9 Ma old crust, south of the Costa Rica Rift, Hole 504B extends through 274.5 m of sediments (Layer 1) and 1836.5 m of basement rocks (Layer 2-3) (Shipboard Scientific Party 1993).

1.2 Geological Setting Of The Troodos Ophiolite And DSDP/ODP Hole 504B

The Troodos ophiolite lies in the southwestern part of Cyprus, a 9500 km^2 island in the north-east corner of the Mediterranean Sea. The ophiolite has an east-west extent of 100 km and a north-south width of just over 30 km (Fig. 1.1). The Troodos ophiolite is possibly one of the remnants of a subduction-related Mesozoic ocean basin formed between the Afro-Asian and the Eurasian plates (Dilek et al. 1990).

The ophiolite consists of two major parts, separated by the approximately east-west trending Arakapas fault zone, a possible oceanic transform fault (Simonian and Gass 1978). The southern part of the ophiolite consists of tectonized peridotites and serpentinites, mafic plutons and dikes, pillowed and massive basaltic lavas, and volcaniclastic rocks. The northern part consists of a centralized domal core of tectonized peridotite and serpentinite overlain by a pseudo-stratigraphic sequence of mafic-ultramafic cumulates, a sheeted dike complex, extrusive rocks, and sedimentary rocks (Simonian and Gass 1978; Dilek et al. 1990).

Samples for this project come from the upper northeast corner of the Troodos ophiolite, Cyprus, near the village of Kambia, along the slot canyon of the upper reaches of the Argaki tou Ayiou Onouphriou river. In this canyon continuous exposure extends over a section several kilometres in length. Rapid erosion by high-volume streams in the winter rainy season, coupled with active regional uplift, provides uniformly fresh material for sampling. A total of 136

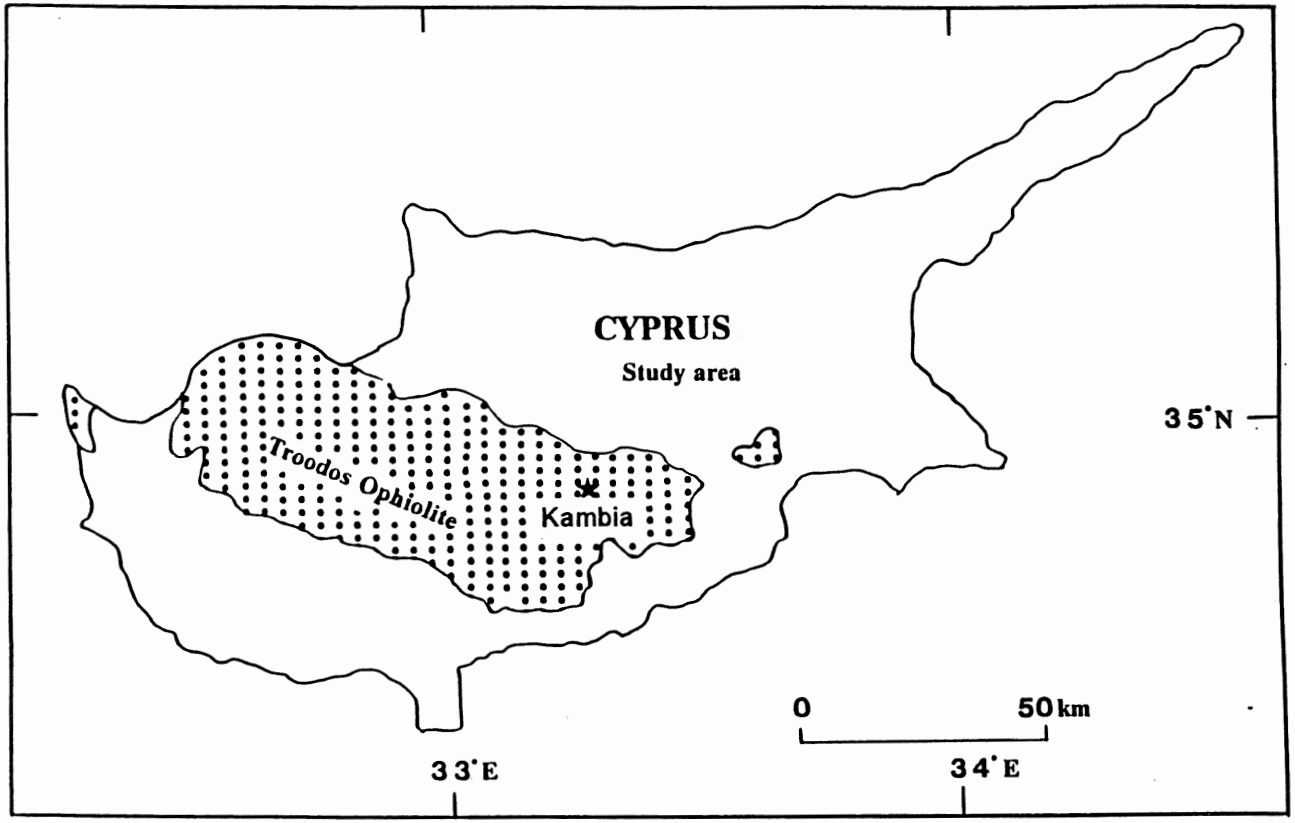

Figure 1.1 Map of Cyprus showing the Troodos ophiolite and the study area (shown as star) (from Hall 1994).

mini-core samples were taken for a parallel magnetic study using a portable gas-driven diamond drill during the summer of 1993 by J. M. Hall, C. C. Walls, and J. K. Hall. J. M. Hall and J. K. Hall completed further detailed geological studies of the section during the summer of 1994.

DSDP/ODP Hole 504B is located on the southern flank of the Costa Rica Rift at a latitude of 1° 13.611' N and longitude of 83° 43.818' W (Fig. 1.2), near the junction between the Cocos and Nazca plates, in the eastern equatorial Pacific (Leg 140 Shipboard Scientific Party 1992). The oceanic basement section, based on about only 20% recovery, is proposed to consist of 571.5 m of massive lavas and pillow lavas, 209 m consisting of mixed massive lavas, pillow lavas, and dikes forming a transitional zone, and 945.4 m of sheeted dikes (Shipboard Scientific Party 1988; Becker et al. 1989; Shipboard Scientific Party 1993).

In view of the low recovery, other interpretations are possible for the sheeted dike part of the profile for which recovery was lower than the average of 20%. Chilled margins are widespread in this interval, indicating the presence of many dikes. The country rock for these dikes could either be other dikes or screens of lava.

The present method of recovery favours physically massive units, which allows for the presence of screens of massive lavas. Screens of friable pillow lavas could well occur in the unrecovered 80%, and may have been imaged in the borehole televiewer records (Morin et al. 1989).

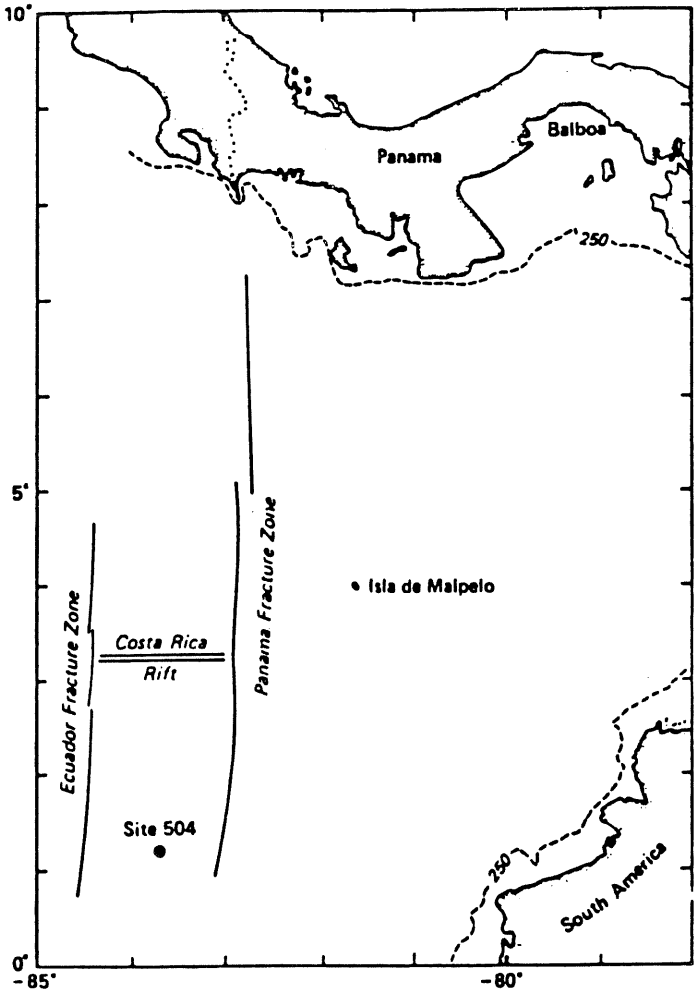

Figure 1.2 Location map for DSDP/ODP Hole 504B (from Alt et al. 1989).

With such low recovery, a better lithological profile could be based on the continuous borehole magnetometer records which are available. However, interpretation of the magnetometer records requires that any difference in the magnetization of dikes and massive- and pillow-lava screens be known.

Identification of such differences is the purpose of the parallel magnetic study. Marked differences occur in the magnetization of the dikes and screens (Fig. 1.3). Similar large differences in magnetization are evident in samples from DSDP/ODP Hole 504B and may also be evident in the magnetometer log (e.g. Table 10, page 71and Figure 78, page 80 in Shipboard Scientific Party 1993; and Table 17, page 121 in Shipboard Scientific Party 1992). The question then arises whether the observations are relevant to the interpretation of Hole 504B.

1.3 Detailed Objective

This thesis describes the primary nature and alteration of a series of dikes and interleaved lava screens occurring within the transition zone between extrusives and sheeted dikes in the Troodos ophiolite of Cyprus. In terms of physical properties and alteration, the dikes and lava screens in the Troodos ophiolite are comparable to the units in the transitional and dike zones of DSDP/ODP Hole 504B. This work constitutes part of a larger study of the magnetization of the same units with the intention of comparing the results for Troodos with those for DSDP/ODP Hole 504B.

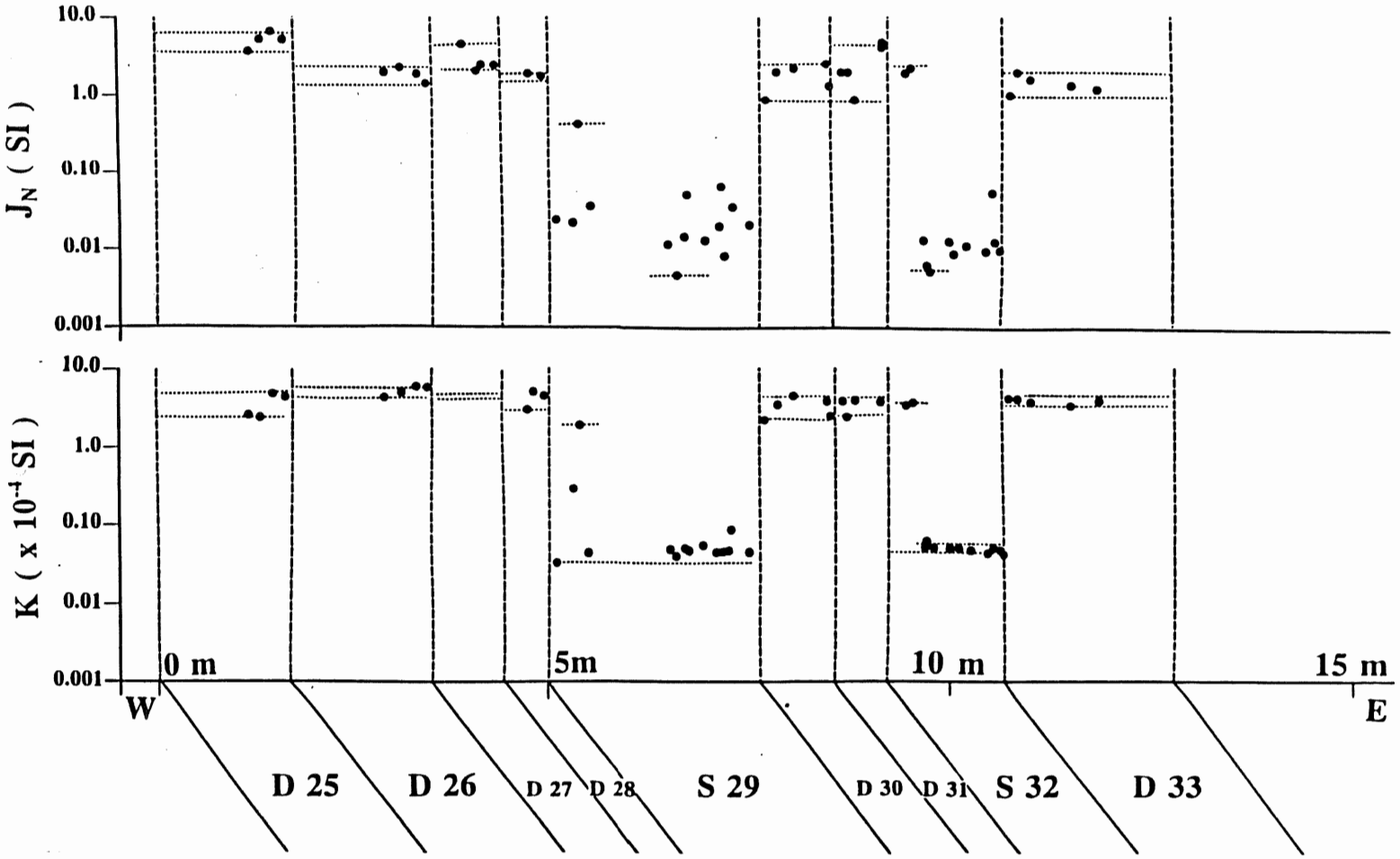

Figure 1.3 Profile showing intensity of natural remanence (J_N) and initial susceptibility (K) for Section 4 (units 25 - 33). Note the dike unit (D) magnetic properties are uniformily high. In contrast, lava screen (S) values are more scattered but generally much lower (from Hall, in press).

The focus of this study is to determine if the observed differences in magnetization of the dikes and screens are the result of primary differences, such as petrology or geochemistry, or secondary differences, such as degree or style of alteration. A simple way to separate these possibilities is to demonstrate that all of the units belong to a restricted part of one magma series. If the magnetization is a result of primary geochemical differences, the results are not relevant to the explanation of the results from Hole 504B where such differences do not occur. However, if the magnetization is a result of differences in degree of alteration, the results from Troodos can be used to provide an alternative to the currently accepted lithological model for the lower part of Hole 504B.

1.4 Composition Of The Oceanic Crustal Section Of Hole 504B And The Troodos Ophiolite

All units of the oceanic crust sampled at site 504B, whether flows or dikes, are uniformly of MORB composition (mid-ocean-ridge basalt or abyssal tholeiite) (Becker et al. 1989). However, the Troodos ophiolite is different from standard oceanic crust because it is subduction-related. Three major geochemical suites are present in the lavas: Suite A, a relatively evolved island-arc tholeiite consisting of a basalt-andesite-dacite-rhyodacite assemblage; Suite B, a depleted arc tholeiite consisting of a picrite-basalt-basaltic andesite assemblage; and Suite C, a highly depleted boninitic suite, which is petrographically similar to Suite B, although it is more chemically

depleted (Robinson et al. 1983; Mehegan and Robinson 1985; Mehegan 1988). The extrusives in the general study area being discussed in this thesis fall into Suite A composition (Robinson et al. 1983; Mehegan 1988). As a general indicator, this identification with a particular suite is very useful; however, this study requires specific information as to the composition of each dike and screen.

1.5 Alteration Zones

The alteration zones present in the Troodos ophiolite (Gillis 1986; Gillis and Robinson 1988) correspond closely to the alteration zones established for DSDP/ODP Hole 504B (Honnorez 1983; Alt et al. 1985), confirmed by later drilling legs.

The five alteration zones defined in the Troodos ophiolite, based on secondary mineral assemblages and field appearance, are: a seafloor weathering zone, a low-temperature zone, a transitional zone, an upper dike zone, and a mineralized zone (Gillis 1986; Gillis and Robinson 1988). Three alteration zones occur in DSDP/ODP Hole 504B based on mineral assemblages: a "submarine weathering" zone, a low-moderate temperature zone, and a combined transition and dike zone (Honnorez 1983; Alt et al. 1985). The "submarine weathering" zone of Hole 504B corresponds closely to the seafloor weathering zone in the Troodos ophiolite. Oxidative alteration characterizes this zone in both Hole 504B and the Troodos ophiolite. Saponite

and secondary pyrite characterize the low-temperature zone (low-moderate temperature in Hole 504B) in both Hole 504B and the Troodos ophiolite. The third and fourth zones (the transitional and upper dike zones) are equivalent to the third zone of DSDP/ODP Hole 504B, the combined transition zone and dike section. Zeolite and greenschist facies mineral assemblages are characteristic of this zone (Table 1.1). Based on the work of Gillis and Robinson (1988), Yang (1992) established contours of alteration in the area.

Dikes are present throughout the extrusive sequence; however, they generally increase in abundance downward, until they reach 100% in the sheeted dike complex. Dike density is the ratio of the net width of the dike unit to the total width of the sequence in a measured section (Yang 1992). A high number of measurements allows the construction of contours of dike abundance, leading to strong control of this aspect of the geologic setting. The area studied of the Troodos ophiolite represents the shallowest 0.5 km of oceanic crust (i.e., from the Sediment-Extrusive Interface downwards) (Hall, J. M. 1994 pers. comm.).

1.6 Scope And Methodology

The scope of the project is well constrained through geological field work already completed by J. M. Hall and C. C. Walls in 1993 and by J. M. Hall and J. K. Hall in 1994. Preliminary petrologic studies of the dikes and lava screens report the primary mineralogy and later alteration products. Electron

Table 1.1 Comparison of alteration zones for the Troodos ophiolite and DSDP/ODP Hole 504B based on definitions by Gillis (1986) and Shipboard Scientific Part (1993) respectively.

Regional Alteration Zones Troodos Ophiolite	Alteration Process and Mineral Occurrence	DSDP/ODP Hole 504B Alteration Zones
Seafloor Weathering Zone	oxidative alteration	Submarine Weathering Zone
Low-Temperature Zone	saponite and secondary pyrite	Low-Moderate Temperature Zone
Transitional Zone and Sheeted Dike Zone	zeolites and greenschist facies minerals	Combined Transition and Dike Zone

microprobe analyses were completed to determine and confirm the different mineral phases and their compositions. XRF analyses for major and trace elements were carried out to determine the whole-rock compositions and to establish whether the dikes and screens belong to one magma series.

1.7 Organization

The next chapter of this thesis contains a more detailed description of the geological setting of Cyprus, specifically the Troodos ophiolite, and a description of DSDP/ODP Hole 504B, followed in Chapter 3 by an outline of the analytical methods used. Chapter 4 describes in detail the field relations, petrological findings, and the alteration zones present in the Troodos ophiolite. Chapter 5 describes the geochemistry of the secondary mineralization. Finally, Chapter 6 provides a discussion and interpretation of the results together with the conclusions and recommendations for future work.

CHAPTER 2 GEOLOGICAL SETTING

2.1 Introduction

This chapter reviews the geology of Cyprus and the Troodos Ophiolite, and describes *in-situ* oceanic crust represented by DSDP/ODP Hole 504B. Much of the geological review of Cyprus is from the work of Gillis (1986) and Yang (1992).

2.2 Geology Of Cyprus

Cyprus consists of the Troodos ophiolite, occupying approximately one-third of the island plus three other zones making up the other two-thirds of the island: the Mamonia Complex, the Kyrenia Range, and a sedimentary succession (Fig. 2.1).

2.2.1 Mamonia Complex

The Mamonia Complex is located to the south and southwest of the Troodos ophiolite (Fig. 2.1). Two rock assemblages dominate the complex: 1) the Late Triassic Dhiarizors Group, consisting of mafic volcanic rocks, reef limestones, and hemipelagic sedimentary rocks; and 2) the Late Triassic-Middle Cretaceous Ayios Photics Group, consisting of quartzose sandstones, limestones, and pelagic siliceous sedimentary rocks. The two rock assemblages are stacked in sub-horizontal thrust sheets (Swarbrick 1980). Serpentinite and other associated igneous and metamorphic rocks cut across the Mamonia Complex in an east-west trending belt (Robertson and Woodcock 1980). Two

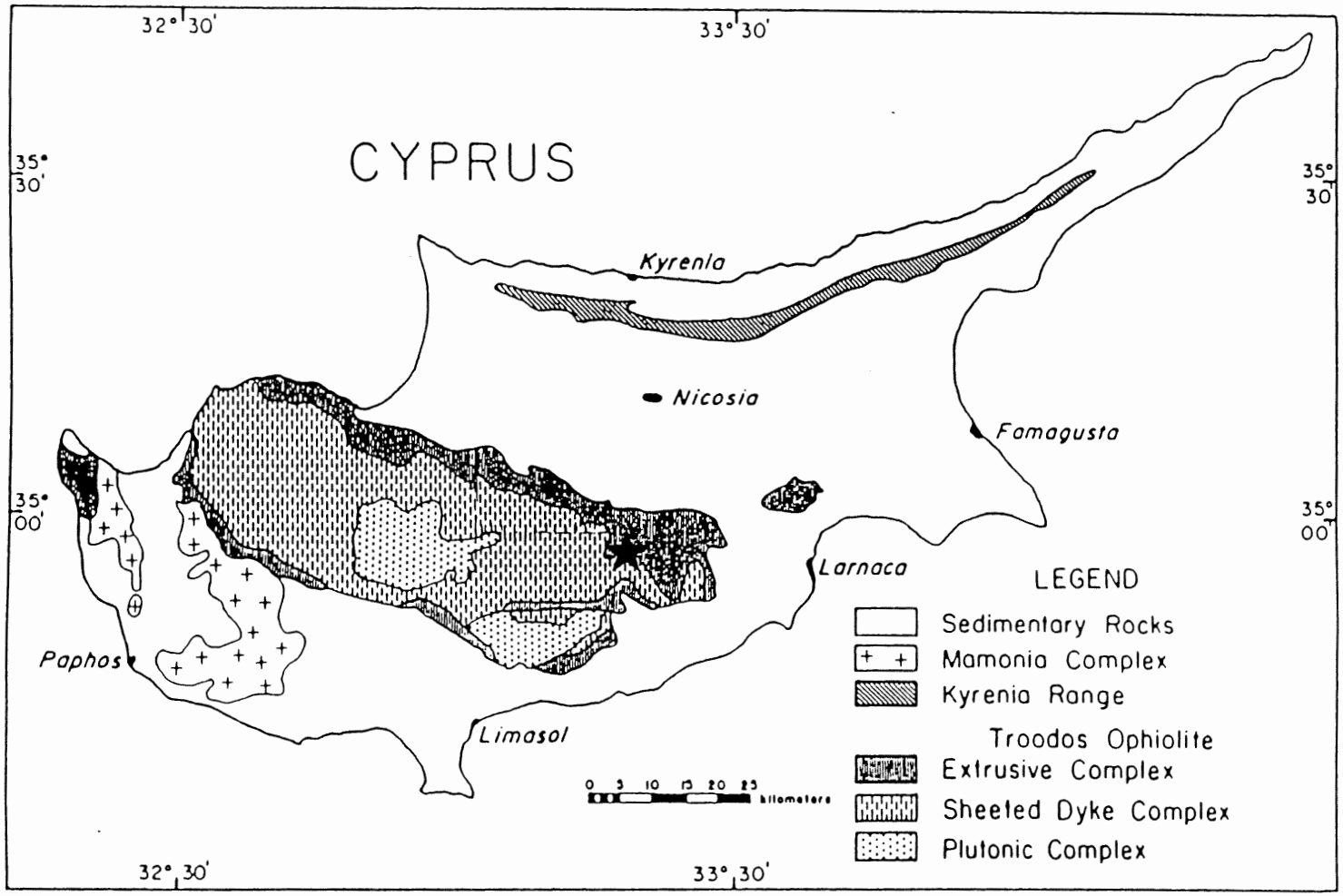

Figure 2.1 Geological map of Cyprus. Study area shown as star (after Gillis 1986).

possible mechanisms for emplacement of the Mamonia Complex in relation to the Troodos massif are: emplacement from the northeast as thrust sheets over the massif, or entrainment underneath and emplacement along with the massif (LaPierre 1975; Biju-Duval et al. 1976; Baroz et al. 1986); or emplacement from the southwest with a transcurrent fault separating them from the ophiolite (Swarbrick 1980).

2.2.2 Kyrenia Range

The east-west trending belt of allochthonous and autochthonous rocks along the northern margin of Cyprus forms the Kyrenia Range (Fig. 2.1). The rocks consist of a sequence of Permian to Miocene limestone, pelagic chalk, radiolarites, and volcanic rocks, intermingled with serpentinite and metamorphic rocks. The rocks are stacked in internally folded, north-to-northeast dipping thrust slices (Baroz et al. 1976; Biju-Duval et al. 1976). Terrigenous flysch deposits flank the stacked thrust sheets to the north and the south (Baroz 1977). Emplacement of the rocks occurred during the late Oligocene to early Miocene (Baroz et al. 1975; Robertson and Woodcock 1980).

2.2.3 Sedimentary rocks

The sedimentary sequence overlying the Troodos ophiolite and the Mamonia Complex record a very complex progression of episodic uplift, subsidence, erosion, and peneplanation occurring since the emplacement of the Troodos massif and the Mamonia Complex (Robertson 1977) (Fig. 2.1). Several major periods of sedimentation occurred during this period, creating a

varied sedimentary rock succession comprised of late Cretaceous to early-middle Tertiary chalks, Miocene reefal limestones and evaporites, and Pliocene to Recent shallow marine to terrestrial sediments.

2.3 Troodos Ophiolite

Troodos is one of the best preserved and most widely studied ophiolites in the world. It probably formed at a spreading ridge, however a question remains as to whether it was a mid-ocean ridge axis, a back-arc basin spreading axis, or some other environment. Recent study suggests that the ophiolite formed in a subduction-related spreading axis such as a back-arc basin. The Andaman Sea spreading axis is suggested as a modern analogy (Moores et al. 1984).

The Troodos ophiolite consists of two areas separated by the Arakapas Fault zone which trends nearly east-west (Fig. 2.2). The southern area of the Limassol Forest consists of tectonized peridotite and serpentinite, mafic dikes and plutons, basaltic lavas, and volcaniclastic rocks (Simonian and Gass 1978; Dilek et al. 1990). The rocks of the pseudo-stratigraphic igneous section are well preserved. The southern area will not be discussed in detail.

The northern part, the Troodos massif proper, from the bottom to the top, has a central core of tectonized peridotite and serpentinite overlain by a pseudo-stratified igneous succession composed of three main units: a mafic-

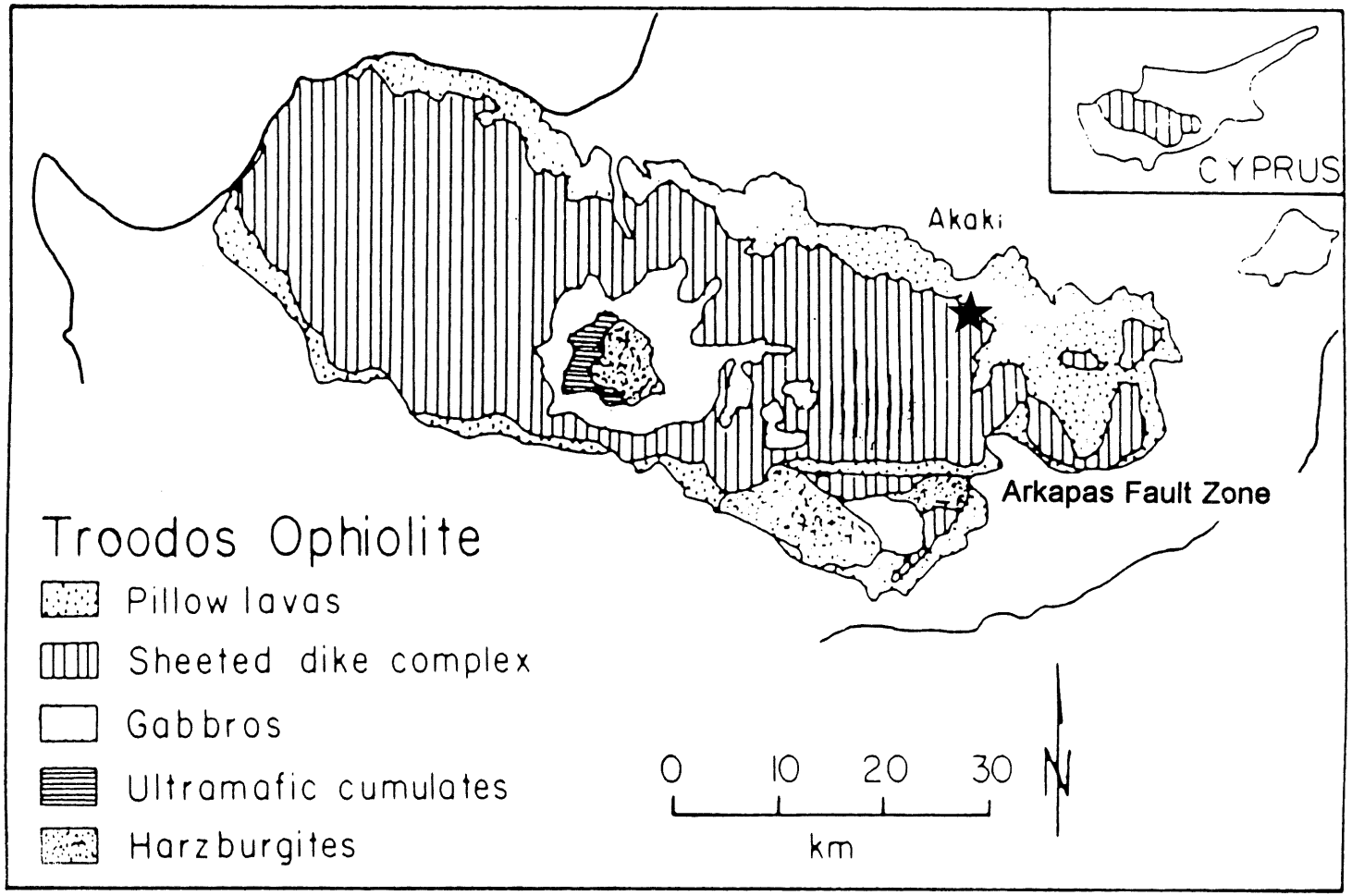

Figure 2.2 Geological map of the Troodos ophiolite (study area represented by a star). The Arkapas Fault Zone, trending east-west, separates the north and south portions of the ophiolite (after Gass 1980).

ultramafic plutonic sequence, a sheeted dike complex, and an extrusive sequence. The northern area is discussed in greater detail in the following sub-sections.

2.3.1 The Plutonic Sequence

The internal dome of the Troodos Plutonic Sequence consists mostly of tectonized harzburgite and subordinate dunite containing deposits of chrysotile asbestos and chromite lenses of economic importance (Constantinou 1980). Gass (1990) identified the internal dome as the Mantle Sequence (labelled as harzburgite in Fig.2.2). Serpentinization is pervasive throughout this sequence.

The Mantle Sequence underlies the Plutonic Complex. A series of cumulates, from dunite at the base, through wehrlite and pyroxenite to gabbro at the top, is present in the plutonic complex (Thy 1987). The ultramafic rocks are overlain by an extensive exposure of gabbroic rocks. Smaller ultramafic bodies intrude the high level gabbros (Searle and Panayiotou 1980). The small ultramafic bodies, magma chambers from which the mafic lavas were erupted, consist of layered wehrlite, lherzolite, and olivine gabbro (Malpas and Langdon 1984). Also occurring in the area is an older series of deformed plutonic rocks which is intruded by a series of undeformed cumulate rocks (Thy 1987; Malpas et al. 1989). On the margins of some areas, between the gabbro and Sheeted Complex, plagiogranites are exposed. U-Pb dating of zircon from two plagiogranites gives dates of 90.3±0.7 and 92.4±0.7 Ma (Mukasa and Ludden 1987).

2.3.2 The Sheeted Complex

A dense linear dike swarm consisting, in its central part, entirely of dikes separates the Plutonic and Extrusive Sequences. The Sheeted Complex surrounds the plutonic rocks on all sides, forming the largest exposed area of the Troodos massif (Constantinou 1980). The Plutonic Complex cuts, and is cut by, the dikes of the Sheeted Complex, making the lower boundary of the Sheeted Complex difficult to establish. The individual dikes range in width from a few centimetres to a few meters, but most are 1-1.5 metres wide. The cooling relations are clear and the chilled margins are commonly preserved (Baragar et al. 1990). The dikes have variable orientations, both strike and dip, as demonstrated by several studies (Searle and Panaziotou 1980; Smith and Vine 1990); however, an approximate north-south direction dominates. The studies have also revealed cross-cutting relationships between some dike swarms. Most of the dikes are basaltic and andesitic in composition (Desmons et al. 1980; Baragar et al. 1988).

2.3.3 The Extrusive Sequence

The Extrusive Sequence overlies the Sheeted Complex. A transition constructional zone of mixed dikes and lava screens, ranging from a few tens of metres (Gass 1980) up to a few hundred metres (Baragar et al. 1990) in thickness, separates the Extrusive Sequence proper from the Sheeted Complex.

The Extrusive Sequence consists of pillow lavas, massive and sheet lava flows, and minor volcanic breccia and hyaloclastites. Subdivision of the sequence is on the basis of field criteria, petrological, mineralogical, and geochemical differences between the lavas, and on the basis of unconformable local contacts between the divisions (Constantinou 1976; Gass 1980). The field mapping subdivisions, from the bottom up, are the Basal Group, the Lower Pillow Lavas, and the Upper Pillow Lavas (Bear 1960; Gass 1960; Carr and Bear 1960; Pantazis 1967).

The Basal Group consists of interlayered screens of pillowed or massive lava flows and steeply inclined dikes. The abundance of pillow or massive lava flows increases away from the contact with the Sheeted Complex (Carr and Bear 1960). The presence of lava screens is the only factor distinguishing the Basal Group from the sheeted dikes (Govett and Pantazis 1971). The Lower Pillow Lavas have a far greater proportion of lavas than the Basal Group. The Basal Group generally represents a transitional zone between the Sheeted Complex below and the Lower Pillow Lavas above.

The Lower Pillow Lavas are commonly deeply weathered but otherwise little altered, silica-oversaturated, aphyric basalts (Bagnall 1960; Gass and Smewing 1973; Smewing 1975), whereas the Upper Pillow Lavas are silica-undersaturated, olivine-bearing basalts with more ultrabasic varieties occurring in the upper part of the sequence (Gass and Smewing 1973; Smewing 1975).

The boundary between the Upper and Lower Pillow Lavas is taken here as being transitional because of the ambiguity associated with placing the boundary. Different authors have defined it as being dependent on dike density or the alteration facies present (Bagnall 1960; Gass 1960; Pantazis 1967). The present transitional boundary is largely the boundary between extensive, upper, and minor degrees of alteration, lower, of the lavas as a result of the draw-down of cold sea water (Hall 1994).

Gass and Smewing (1973) and Smewing et al. (1975) originally divided the Extrusive Sequence into an axis sequence consisting of the Lower Pillow Lavas and the Basal Group as well as the Sheeted Complex, and an off-axis sequence consisting of the Upper Pillow Lavas. This subdivision was based on Ti-Zr ratios for the Upper and Lower Pillow Lavas. The boundary between the axis and off-axis sequences, defined in this way, varies laterally from unconformable to transitional.

More recently Robinson et al. (1983), Schmincke et al. (1983), Mehegan and Robinson (1985), Thy et al. (1985) and Mehegan (1988) have used major element data from preserved glass and whole rock samples to define rather different divisions and to show that the historic division between Upper Pillow Lavas and Lower Pillow Lavas is unjustified in terms of geochemistry. Two distinct geochemical suites exist for the northern flank of the ophiolite: Suite A consisting of basalt, andesites, dacites, and rhyodacites of arc tholeiite origin; and Suite B consisting of an upper picritic basalt-andesitic basalt assemblage

with a depleted arc tholeiite origin. In some instances these two suites occur interleaved. Mehegan and Robinson (1985) also recognized a highly depleted boninitic suite on the southern flank of the ophiolite.

2.4 DSDP/ODP Hole 504B

DSDP/ODP Hole 504B is located on the southern flank of the Costa Rica Rift, in oceanic crust approximately 5.9 Ma old (Fig. 1.2). Hole 504B penetrates 274.5 m of oceanic sediments composed of siliceous nanofossil chalk, and an interlayered sequence of nanofossil chalk, limestone, and stringers of chert (CRUST 1982; Shipboard Scientific Party 1983, 1993). The hole further penetrates 1836.5 m of MORB consisting of three major lithostratigraphic zones. From the bottom up, they are: a zone of sheeted dikes and massive basalts showing greenschist facies alteration; a transition zone of pillow lavas, thin flows, massive basalts and dikes displaying extensive greenschist facies alteration; and a zone of pillow lavas and thin sheet flows intermixed with pillow breccias, hyaloclastites, and massive basalts showing low-temperature alteration (Fig. 2.3) (Alt et al. 1985; 1986; Shipboard Scientific Party 1988; Becker et al. 1989; Leg 140 Shipboard Scientific Party 1990; Shipboard Scientific Party 1993).

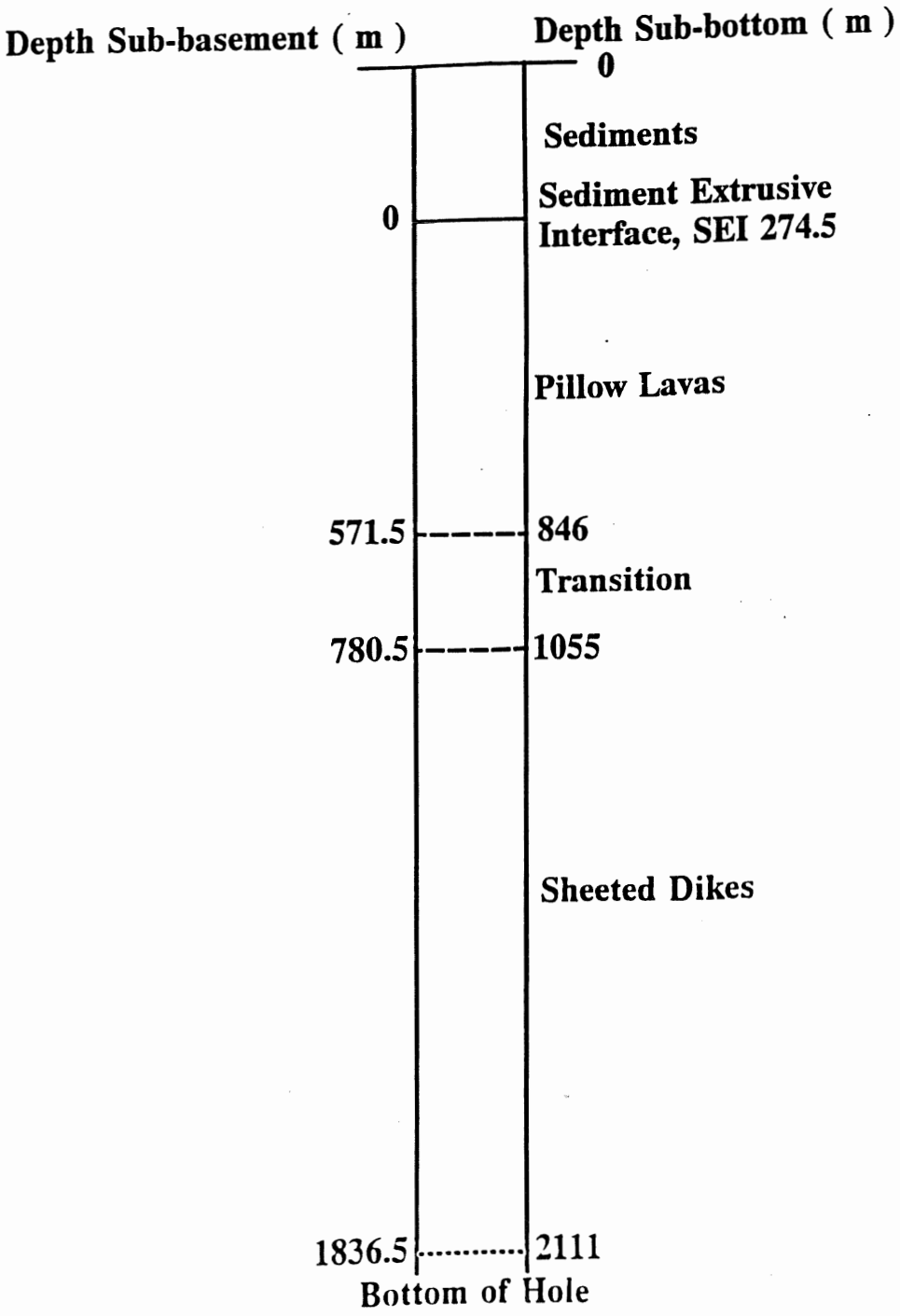

Figure 2.3 Lithological units of DSDP/ODP Hole 504B (after Shipboard Scientific Party 1993).

2.5 Summary

From the above description, the composition of the rocks from the Troodos ophiolite and the oceanic crust from DSDP/ODP Hole 504B are different. However, in terms of construction processes, magnetics, and hydrothermal alteration, they are similar. The similarities, conclusions from the parallel magnetic study, and petrological and geochemical data described in this thesis, allow for the development of an alternative interpretation of the crustal section penetrated in ODP Hole 504B.

CHAPTER 3 ANALYTICAL METHODS

3.1 Introduction

This chapter describes the analytical methods for sample collection and selection, X-ray fluorescence analyses of whole rocks, and electron microprobe analyses of minerals.

3.2 Sample Collection And Selection

In 1993 J. M. Hall, C. C. Walls, and J. K. Hall collected 136 mini-core samples representing 20 cooling units (Table 3.1) from four sections at different crustal depths, using a portable, gas-driven, diamond drill. Section 4.2 describes the different cooling units . Polished thin sections were made from 40 of the mini-core samples. A group of 20 of the 40 samples, one from each unit described in detail by J. M. Hall in 1994 (Appendix A), was selected for petrological description, XRF analyses, and electron microprobe analyses in this study (Table 3.1). The selection criteria were that samples should be magnetically typical of a unit so that the results would be relevant to both this study and a parallel study of the magnetic properties of the samples, and that they had minimal sulphide mineralization.

3.3 X-Ray Fluorescence

3.3.1 Sample preparation

Standard procedures in the Department of Earth Sciences, Dalhousie

Table 3.1 Samples used for thin sections, XRF, and microprobe analysis.

Section	Thin Section#	Unit
1	CY93 13-007	dike
1	CY93 14-015	screen
1	CY93 15-003	dike
2	CY93 16-003	dike
2	CY93 18-001	dike
2	CY93 19-008	screen
3	CY93 20-004	dike
3	CY93 21-003	dike
3	CY93 22-008	screen
3	CY93 23-002	dike
3	CY93 24-003	screen
4	CY93 25-002	dike
4	CY93 26-003	dike
4	CY93 27-003	dike
4	CY93 28-002	dike
4	CY93 29-002	screen
4	CY93 30-002	dike
4	CY93 31-002	dike
4	CY93 32-001	screen
4	CY93 33-003	dike

University, were used to prepare samples for XRF analysis. Specifically, samples were broken into < 1 cm size fragments using a chisel and hammer. Approximately 15 g of each sample was crushed in a tungsten carbide swing mill. Powders were collected after passing through a 100 mesh sieve. Any material that did not pass through the mesh was recrushed and resieved.

3.3.2 Elemental analysis

Analyses were performed at the Regional XRF Centre located in the Department of Geology at St. Mary's University, Halifax, Nova Scotia. Each sample was analyzed for 10 major and minor element oxides (SiO_2, TiO_2, Al_2O_3, FeO, MnO, MgO, CaO, Na_2O, K_2O, and P_2O_5) and 14 trace elements (Rb, Sr, Y, Ba, Zr, V, Nb, Zn, Cu, Ni, Cr, Th, Ga, and S) using a Philips PW1400 sequential X-ray fluorescence spectrometer with a Rh-anode tube. Analysis of major and minor element oxides was carried out on fused glass discs, whereas pressed powder pellets were used for trace elements. International (Govindaraju 1989) and in-house standards were used for calibration of the equipment. Analytical precision is generally better than 5% for major and minor element oxides and approximately 5% for trace elements, with the exception of lead and thorium which are slightly higher and for barium which is 10%. Loss on ignition (LOI) at 1050° C was determined by measuring the weight loss in a sample after heating the sample for approximately 1 1/2 hours (Stanford 1995 pers. comm.).

3.3 Electron Microprobe

The JEOL 733 Electron Microprobe is equipped with four wavelength dispersive spectometers and an Oxford link EXL energy dispersive system and is located at Dalhousie University, Halifax, Nova Scotia, under the direction of Mr. R.M. MacKay. The microprobe was used to analyze some of the constituent minerals in the samples used in this study. The operating conditions were 15 kv accelerating voltage, 15 nA beam current, and a 40-second counting time. The raw data was corrected using the Link ZAF matrix correction program. The instrument was calibrated using cobalt metal and an instrument precision of +/- 0.5 % at 1 standard deviation was obtained. Mineralogical standards were routinely run during the operation of the microprobe to monitor data quality. The standards were as follows: sanidine was used for Si, Al, and K; KK (amphibole) was used for Mg, Ca, and Ti; Garnet 12442 for Fe; MnO_2 for Mn; and Jadeite for Na. The relative accuracy for major elements is +/- 1.5 to 2.0 % (MacKay 1995 pers. comm.).

CHAPTER 4 FIELD RELATIONS AND PETROLOGICAL DESCRIPTION

4.1 Introduction

This Chapter presents the field relations of the dike and screen units, the mineralogical and textural characteristics, and a description of the alteration zones defined by Gillis (1986).

4.2 Field Relations

Samples for this project come from the upper northeast corner of the Troodos ophiolite, 3 to 5 km south of the village of Kambia along the slot canyon of the upper reaches of the Argaki tou Ayiou Onouphriou river (Fig. 4.1). In this slot canyon, continuous exposure of the screen and dike units occurs for several kilometres. Rapid erosion by high-volume streams in the winter rainy season, coupled with ongoing regional uplift, provides unweathered material for sampling. Figure 4.2 show a section of the slot canyon with excellent exposure.

The units of the slot canyon are divided into four sections based on field observations of location, dike density, and alteration. Field observation suggest that Sections 1 to 3 lie in the transition alteration zone, and Section 4 lies in the greenstone alteration zone. These assignments appear to conflict with the contours shown in Figure 4.1. However, it is noted that generally in Yang's (1992) study area, the T/G and L/T boundaries closely follow the 0.5 and 0.25 dike density contours respectively. Local departure from these contours is

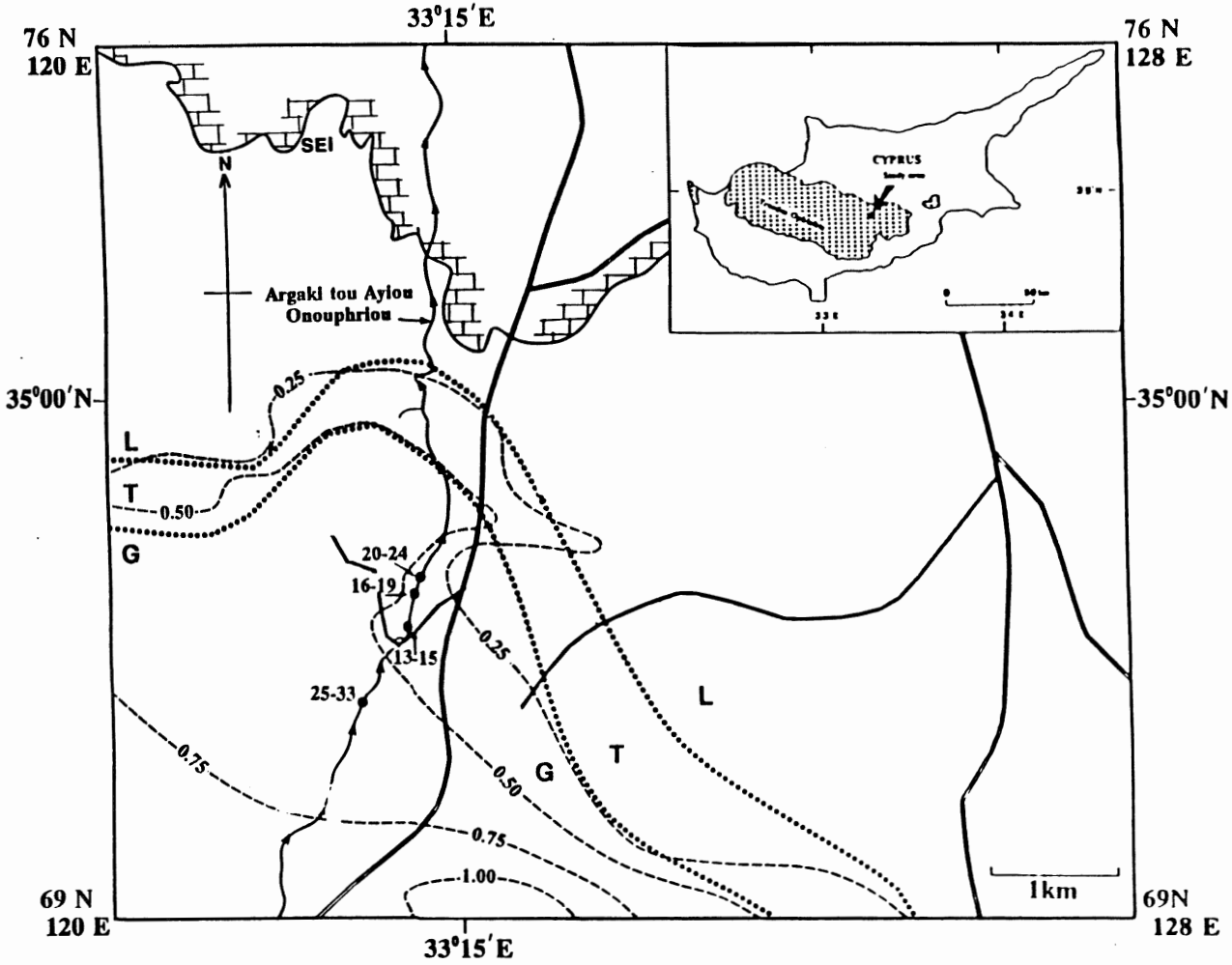

Figure 4.1 Location map for samples from the study area. Insert shows the study area with respect to the ophiolite. (--- dike abundance contours (Yang 1992); ... alteration boundaries (Yang 1992) (L - low temperature, T - transition; G - greenstone); SEI - sediment extrusive interface; ➘ Argaki tou Ayiou Onouphriou) (after Hall 1994).

Figure 4.2 A well-exposed sequence along the Argaki tou Ayiou Onouphriou river showing, from left to right, dike Unit 28, screen Unit 29 and dike Unit 30. Scale 1 cm = 36 cm.

probably the result of an insufficient number of observation in an area where these contours vary rapidly in location. Sections 1 through 3 lie in the 0.25 to 0.50 dike density zone and Section 4 lies in the 0.50- 0.75 dike density zone (Yang 1992). Table 4.1 gives a brief description of type of unit, thickness, and general characteristics for each cooling unit. Appendix A gives a more detailed description of each unit.

Dike units generally consist of fine- to medium-grained, blue-grey to green-grey, cross-jointed material. Figure 4.3A shows a characteristic dike unit. Screen units consist of a variety of morphologies including massive lavas, large- and small-pillow lavas, and pillow breccias. The lavas are fine grained, and dark grey-green, to pale blue-grey-green, in colour. Figure 4.3B shows a characteristic screen unit. Some units have a rusty appearance as a result of the alteration of sulphide minerals (e.g., screen unit in Figure 4.3A).

4.3 Petrology

The dike and screen rocks of the transition zone of the Troodos ophiolite, along the Argaki tou Ayiou Onouphriou slot canyon, consist of the primary mineral assemblage plagioclase, clinopyroxene, quartz, opaque oxides, and a fine-grained mesostasis. The secondary/alteration mineral assemblage consists of chlorite, albite, alkali feldspars, quartz, opaque oxides, and minor amounts of calcite, titanite, sulphides, epidote, and zeolites. A discussion of the textural characteristics of the samples follows the mineralogical descriptions.

Table 4.1 Unit Thickness and Structural information for the dike and screen units.

Unit	Thickness (m)	Description
Section 1	71.30N, 122.37E	
Unit 13	2.00	Dike
Unit 14	3.50	Variably fractured and mineralized screen
Unit 15	1.80	Dike
Section 2	71.60N, 122.50E	
Unit 16	0.60	Dike
Unit 18	0.95	Dike - unit 18 made up of units 17 and 18, probably one singe dike
Unit 19	5.90	Screen consisting of massive lava, and small and large pillows
Section 3	71.85N, 122.60E	
Unit 20	1.30	Dike
Unit 21	0.53	Dike
Unit 22	1.60	Massive lava screen with some pillow type outlines
Unit 23	0.60	Dike
Unit 24	2.00	Screen of variably mineralized pillow breccia overlain by brecciated massive lava
Section 4	71.75N, 122.04E	
Unit 33	1.70	Dike
Unit 32	1.77	Screen of pillow lava with tendency toward massive lava
Unit 31	0.53	Dike
Unit 30	0.75	Dike
Unit 29	2.15	Screen of massive and pillow lavas
Unit 28	0.45	Dike
Unit 27	0.75	Dike
Unit 26	1.4	Dike
Unit 25	1.4	Dike

Figure 4.3A A characteristic dike unit (Unit 13), upper, and a screen unit (Unit 14), lower, showing the sulphide mineralization common to the screen units. Scale 1 cm = 50 cm.

Figure 4.3B A characteristic screen unit (Unit 32) showing pillow outlines. Scale 1 cm = 8 cm.

A

B

Microprobe analyses were completed to identify and confirm the mineral phases and to establish their compositions (Appendix B).

4.3.1 Mineralogy

Plagioclase is the dominant primary phase in all samples. It occurs as small phenocrysts, intergranular grains, fragmented grains, and microcrystalline grains in the groundmass (Fig. 4.4). Unaltered plagioclase is labradorite (An_{50}-An_{70}) (Fig. 4.5) (Table 4.2A). The labradorite has partially altered to chlorite/smectite in all samples and to albite (Table 4.2B) and alkali-feldspar (Table 4.2C) in certain samples from Sections 2 and 4. The alteration of plagioclase does not follow a consistent pattern between field sections; within one field section, fresh plagioclase, K-feldspar, albite, and chloritized plagioclase may all be present.

Clinopyroxene appears as small subhedral phenocrysts in six of the twenty samples (Fig. 4.6). They are of calcic composition (Table 4.3) (Fig. 4.7), ranging from pigeonite to diopside, as indicated by their composition and are colourless to pale green colour in plain polarized light. Of the six samples, five are from dike units in Section 4, and one is from a dike unit in Section 1. These units show fewer chlorite pseudomorphs, suggesting that in clinopyroxene-free samples, the primary clinopyroxene has altered to pseudomorphic chlorite.

No fresh olivine is present , but altered olivine is present in three samples from dike units. It occurs as former phenocrysts which have been

Figure 4.4 A. Sample 21-003: Primary labradorite (some grains intergrown), and secondary albite and/or K-feldspar altered by chlorite (elongate, light coloured laths), small, light coloured, approximately equidimensional quartz grains (some showing chlorite alteration) set in chlorite, chlorite/smectite ± epidote (?) groundmass.
Magnification 1 cm = 0.2 mm. X-nicols.

B. Sample 20-004: Primary labradorite (some grains intergrown, and partially altered to chlorite), and secondary albite and/or K-feldspar (elongate, light coloured laths), plagioclase phenocryst slightly altered within and at the ends, small, light coloured, approximately equidimensional quartz grains (showing some chlorite alteration) set in chlorite, chlorite/smectite ± epidote (?) groundmass.
Magnification 1 cm = 0.2 mm. X-nicols.

C. Sample 19-008. Primary labradorite (some grains intergrown), and secondary albite and/or K-feldspar altered to chlorite (elongate, light coloured laths), plagioclase phenocryst showing distinct Carlsbad twinning (centre of photo), small, light coloured, approximately equidimensional quartz grains, set in a groundmass of chlorite, chlorite/smectite, quartz ± epidote (?).
Magnification 1 cm = 0.2 mm. X-nicols.

A

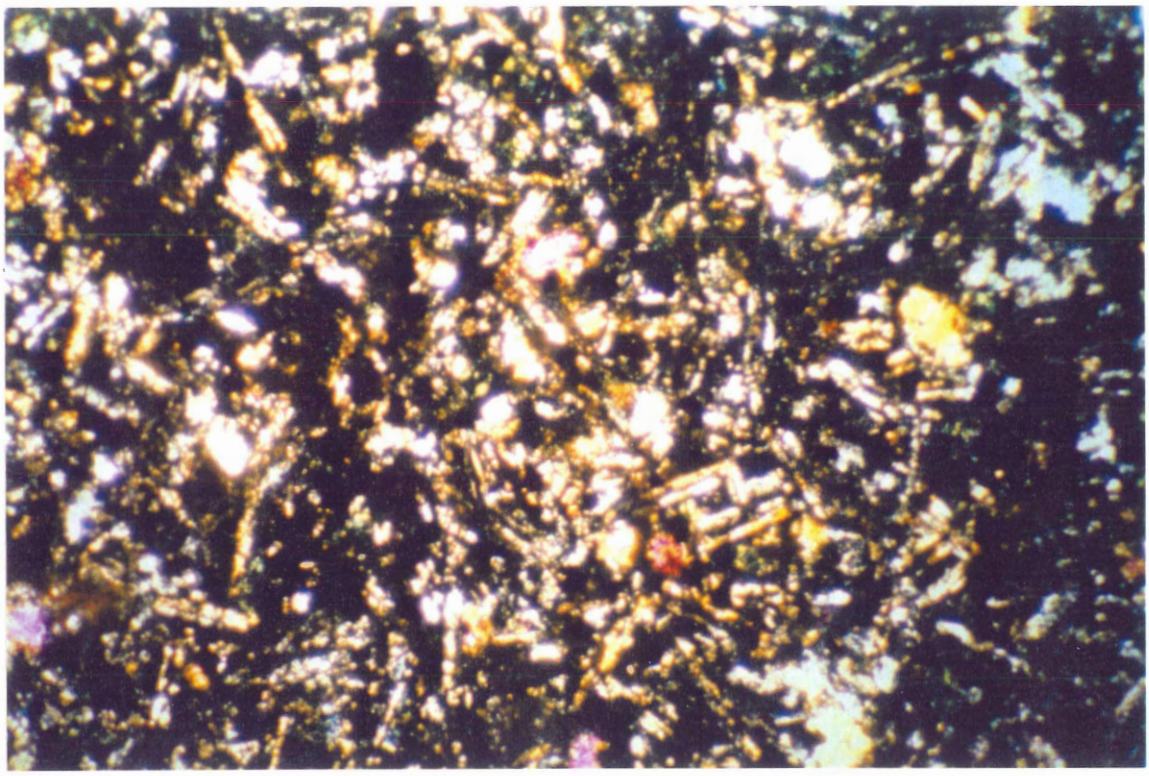

B

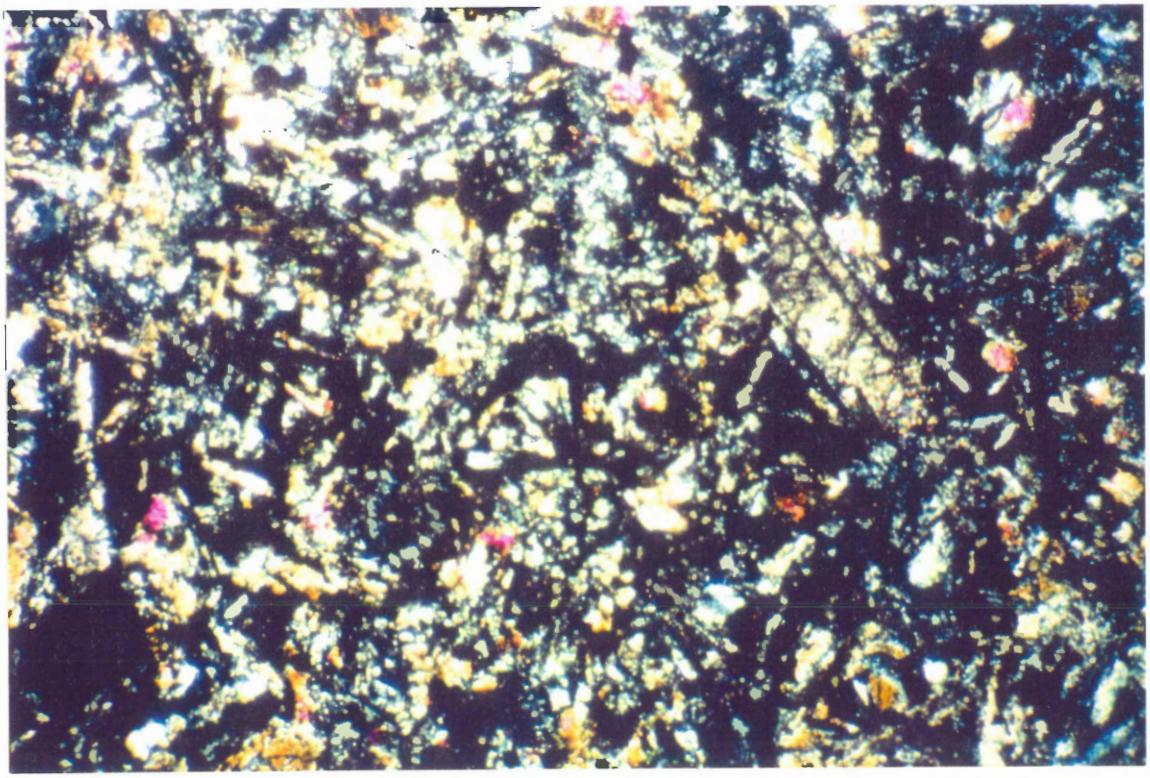

C

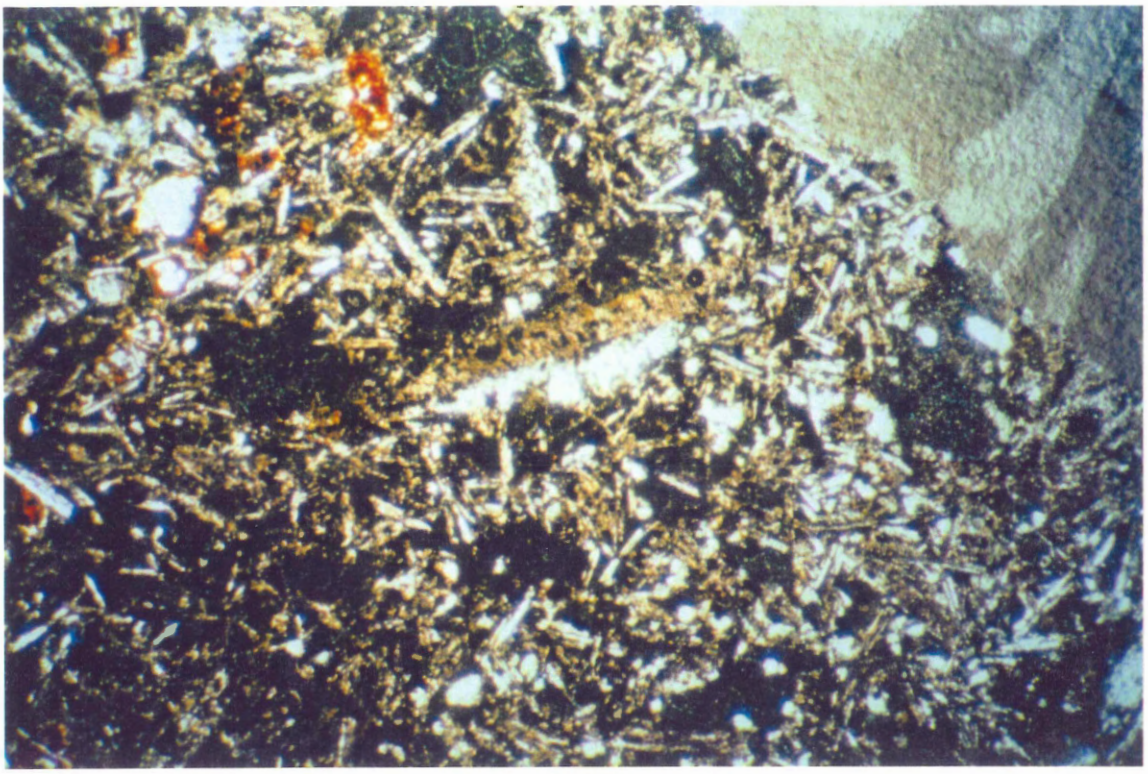

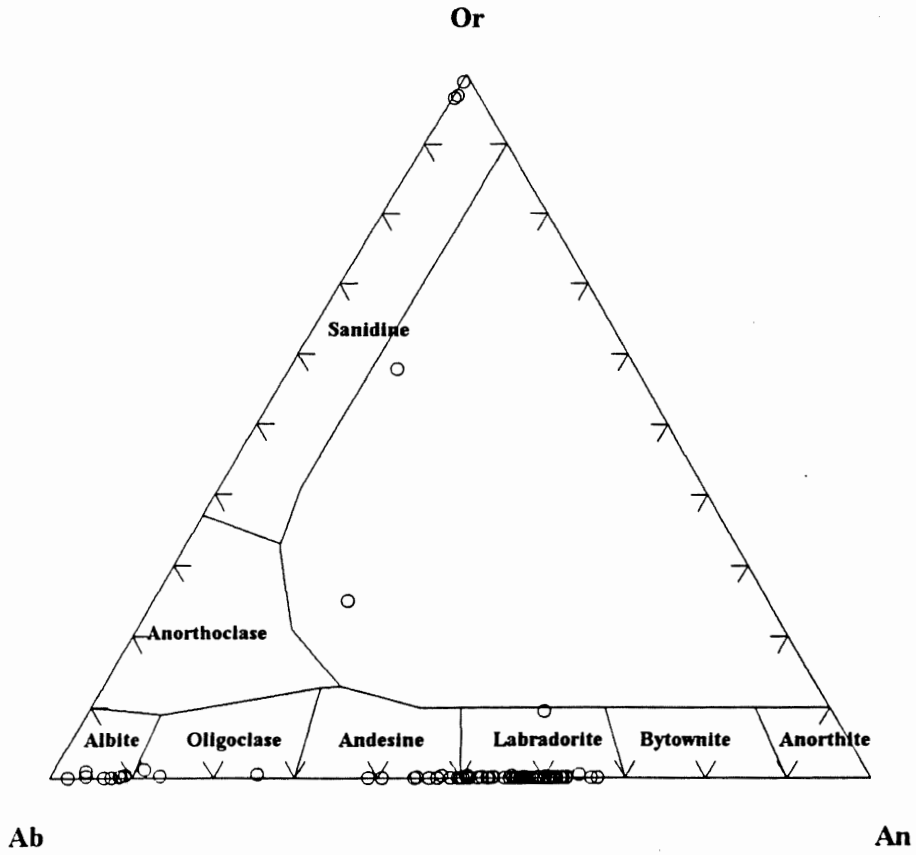

Figure 4.5 Compositional ternary diagram for feldspars with end-members Albite-Anorthite-Orthoclase for the samples from this study.

Table 4.2A Representative Labradorite Analyses

Sample	15-003	20-004	22-008	25-002	28-002	32-002
SiO2	54.1	54.9	54.9	55.7	55.3	56.4
TiO2	0.0	0.1	0.1	0.0	0.0	0.2
Al2O3	28.5	27.9	27.8	27.4	27.4	26.6
FeO	1.0	1.0	0.9	0.9	1.0	1.1
MnO	0.1	0.1	0.1	0.0	0.0	0.0
MgO	0.1	0.2	0.1	0.2	0.2	0.1
CaO	11.5	10.8	11.3	10.3	10.8	10.1
Na2O	4.9	5.4	4.9	5.5	5.2	5.5
K2O	0.0	0.0	0.0	0.0	0.0	0.0
Total	100.1	100.5	100.1	100.2	99.9	99.9
Ab	43	47	44	49	47	50
An	57	53	56	51	53	50
Or	0	0	0	0	0	0

Table 4.2B Representative Albite Analyses

Sample	25-002	27-003	30-003	32-002
SiO2	68.6	65.9	66.3	66.4
TiO2	0.1	0.1	0.1	0.1
Al2O3	21.1	21.2	20.9	20.7
FeO	0.1	0.4	29.0	0.6
MnO	0.0	0.0	0.0	0.0
MgO	0.2	0.1	0.0	0.1
CaO	1.1	2.1	1.7	1.6
Na2O	5.7	9.3	9.5	10.6
K2O	0.0	0.2	0.1	0.0
Total	99.8	99.2	98.9	100.0
Ab	93	88	91	92
An	7	11	9	8
Or	0	1	0	0

Table 4.2C Representative K-feldspar Analyses

Sample	16-003	19-008	28-002	30-003
SiO2	64.5	63.7	64.9	64.7
TiO2	0.1	0.0	0.0	0.0
Al2O3	18.6	18.3	18.6	18.5
FeO	0.2	0.3	0.3	0.3
MnO	0.0	0.1	0.0	0.0
MgO	0.0	0.1	0.0	0.0
CaO	0.2	0.1	0.1	0.1
Na2O	0.3	0.3	0.3	0.1
K2O	16.2	16.5	16.2	16.2
Total	100.1	99.5	100.5	99.8
Ab	3	3	3	1
An	1	0	0	0
Or	96	97	97	99

Figure 4.6 Sample 31-002: Fresh rhomboidal clinopyroxene phenocryst (bottom, centre of photo), plagioclase laths replaced by chlorite, small, light coloured, approximately equidimensional quartz grains partially altered by chlorite, and opaques set in a groundmass of chlorite, chlorite/smectite, quartz ± epidote (?). Magnification 1 cm = 0.2 mm. X-nicols.

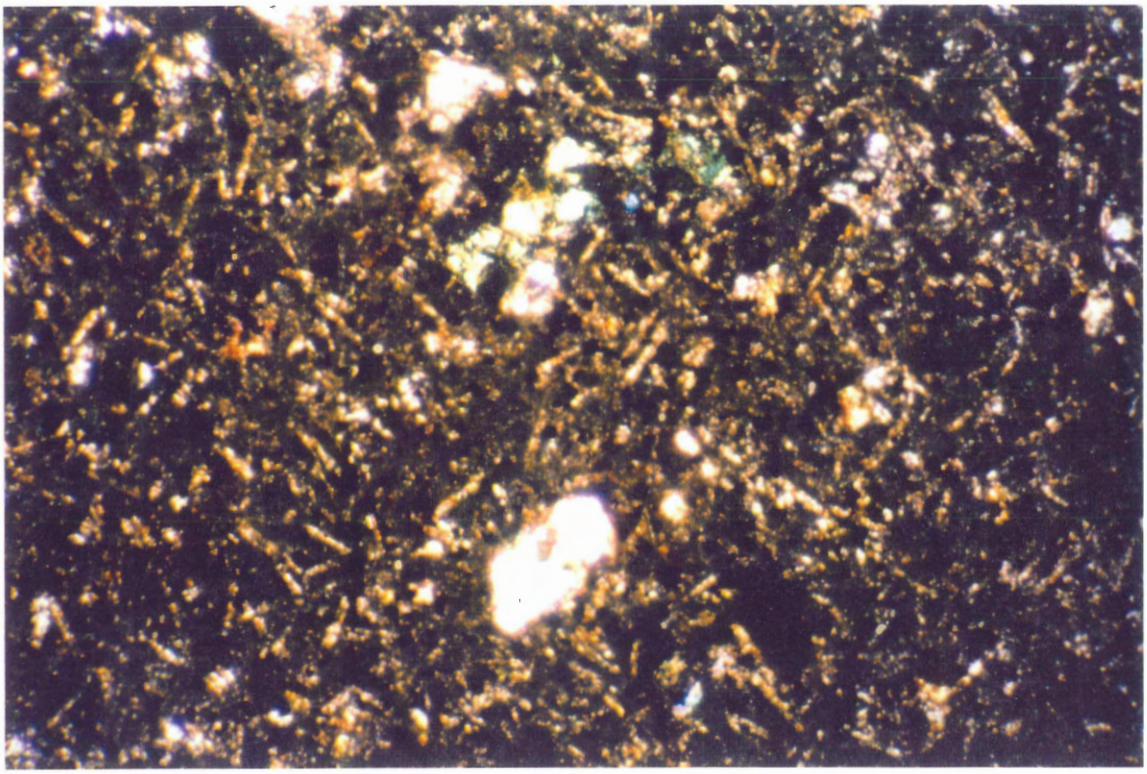

Table 4.3 Representative Pyroxene Analyses

Sample	25-002a	25-002b	26-003	31-002	33-003
SiO2	50.2	48.5	50.9	52.5	51.6
TiO2	0.3	0.3	0.0	0.4	0.0
Al2O3	3.7	2.7	0.6	1.8	0.6
FeO	20.5	28.7	13.5	9.6	13.7
MnO	0.9	1.5	1.0	0.0	0.6
MgO	1.0	7.7	9.7	16.2	10.3
CaO	11.1	5.6	22.5	18.7	22.5
Na2O	0.7	0.8	0.4	0.2	0.2
K2O	0.0	0.0	0.0	0.0	0.0
Total	97.0	95.8	98.6	99.4	99.6
Ca	26.9	14.1	47.7	38.4	46.9
Mg	32.5	26.8	28.4	46.2	29.8
Fe2_Mn	40.6	59.1	23.9	15.4	23.3
WO	27	14	48	38	47
EN	33	27	28	46	30
FS	41	59	24	15	23
WEF	94	93	97	98	98

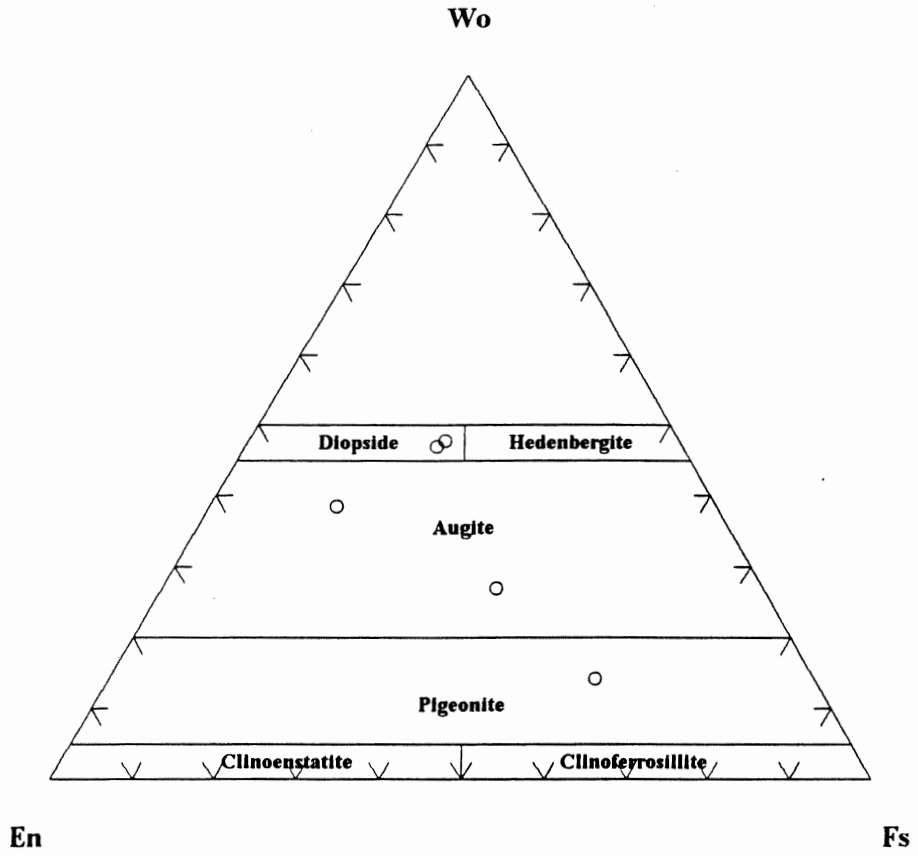

Figure 4.7 Compositional ternary diagram for pyroxene with end-members Enstatite-Ferrosilite-Wollastonite for the samples from this study.

completely altered to chlorite and have rims which consist of very-fine grained opaque oxides.

Opaque oxides occur in all samples. The oxides present are generally subhedral to anhedral and are very fine- to fine-grained primary and secondary minerals.

Chlorite is present as pale to bright green, fine- to medium-grained pseudomorphs, in the microcrystalline groundmass, as mesostasis replacement and as partial alteration of plagioclase grains and in quartz-chlorite vesicle fillings (Fig. 4.8A and 4.8B). Table 4.4 and Figure 4.9 show the representative chlorite compositions from microprobe analysis.

Secondary quartz is present in all samples. Possible primary quartz generally occurs as subhedral to anhedral, very fine- to medium-grained phenocrysts. Secondary quartz is present in the microcrystalline groundmass, as quartz-filled vesicles, and as an alteration product of the mesostasis (Fig. 4.10 A, B, C, and D). Minor calcite, titanite, sulphides, and zeolites (Fig. 4.11) are also present in some of the samples.

4.3.2 Texture

Hydrothermal alteration has caused an overprinting of the original texture changing it from porphyritic and intersertal to intergranular textures. The primary minerals (Section 4.3) are present as small phenocrysts, intergranular and fragmented grains, and microcrystalline groundmass. Secondary/alteration mineral assemblages occur as intergranular grains, grains in the

Figure 4.8 A. Samples 16-003: Chlorite pseudomorphs (light coloured (yellow) equidimensional grains), fresh and altered plagioclase laths, and opaques set in a groundmass of chlorite, chlorite/smectite, quartz ± epidote (?). Magnification 1 cm = 0.2 mm. Plane light.

B. Sample 30-003: Altered plagioclase laths, green, approximately equidimensional chlorite pseudomorphs, small, light coloured quartz grains, and opaques set in a groundmass of chlorite, chlorite/smectite, quartz ± epidote (?). Magnification 1 cm = 0.2 mm. X-nicols.

A

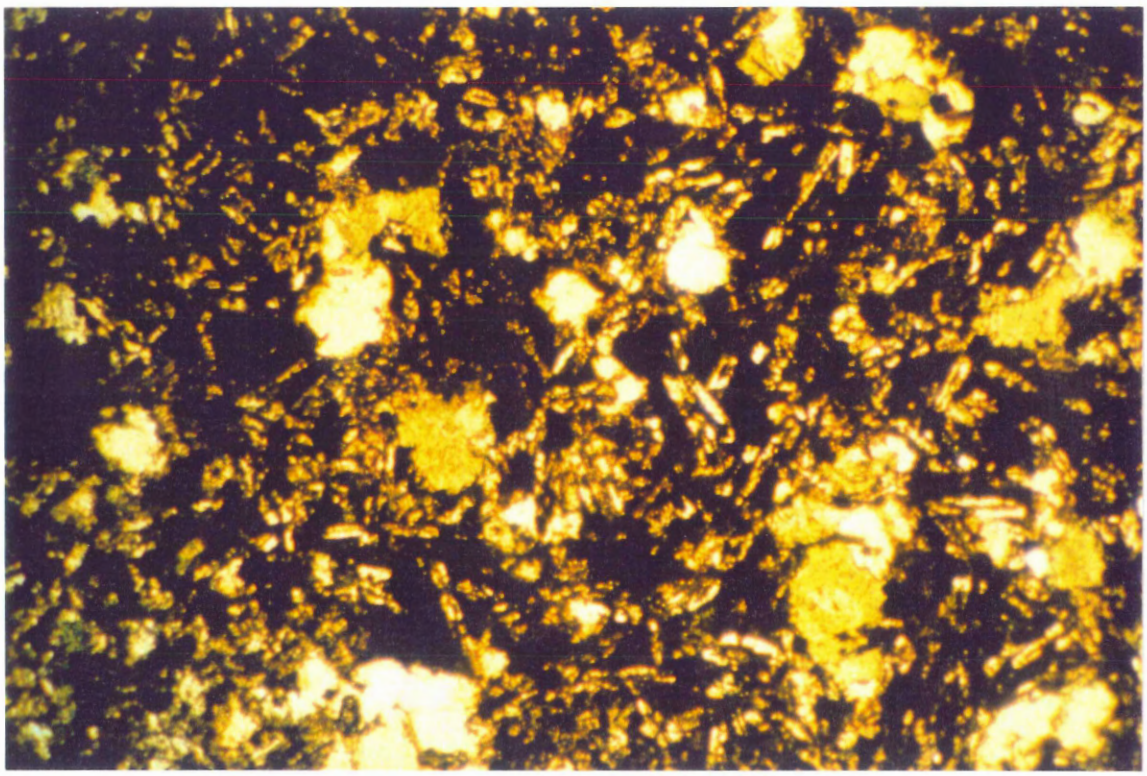

B

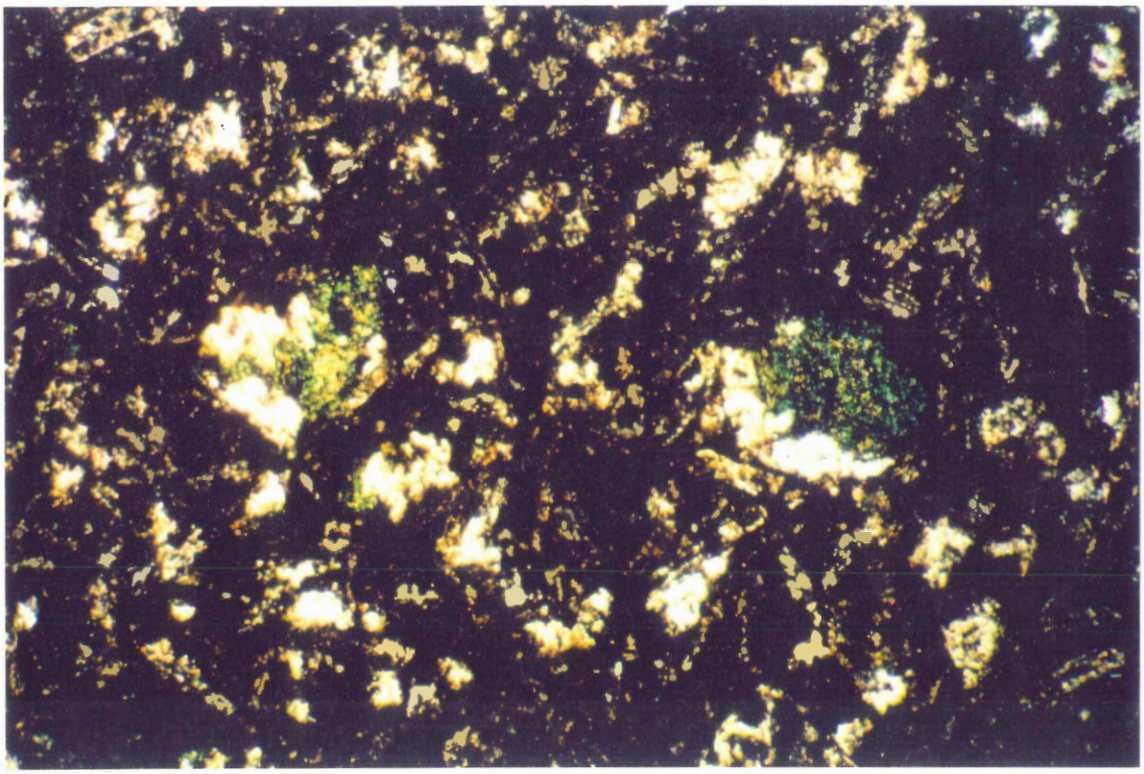

Table 4.4 Representative Chlorite Analyses

Sample	13-007	16-003	23-002	24-003	26-003	32-002
SiO2	27.1	27.2	26.7	26.8	26.6	26.6
TiO2	0.0	0.1	0.0	0.1	0.1	0.1
Al2O3	16.9	18.6	17.4	17.3	17.6	17.8
FeO	25.9	20.5	23.8	25.1	26.5	25.1
MnO	0.8	0.9	1.0	1.2	0.6	0.9
MgO	15.7	19.2	16.6	15.7	14.9	15.7
CaO	0.1	0.0	0.0	0.1	0.1	0.1
Na2O	0.3	0.3	0.3	0.3	0.3	0.3
K2O	0.0	0.1	0.0	0.0	0.0	0.0
Total	86.8	86.8	85.8	86.6	86.7	86.6
O	36.0	36.0	36.0	36.0	36.0	36.0
Fe_FeMg	0.48	0.38	0.44	0.47	0.50	0.47
Mg_FeMg	0.52	0.62	0.56	0.53	0.50	0.53

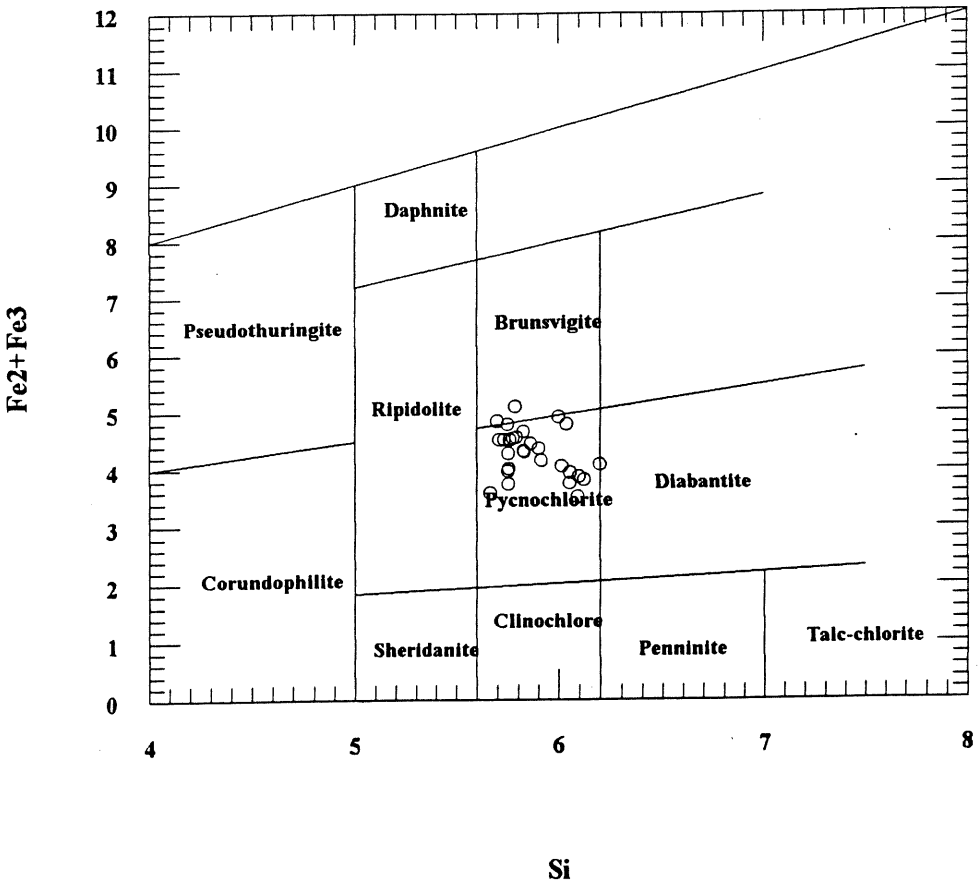

Figure 4.9 Compositional diagram for chlorite for the samples from this study.

Figure 4.10 A. Sample 15-003: Small, light coloured, approximately equidimensional quartz grains, plagioclase laths, opaques, and chlorite pseudomorphs (yellow, approximately equidimensional grains) in a groundmass of chlorite, chlorite/smectite, quartz ± epidote (?). Magnification 1 cm = 0.2 mm. X-nicols.

B. Sample 27-003: Quartz filled vesicle (centre of photo) with chlorite alteration around the rim with opaques around the vesicle, chlorite altered feldspar, opaques, and small quartz grains in a groundmass of chlorite, chlorite/smectite, quartz ± epidote (?). Magnification 1 cm = 0.2 mm. X-nicols.

C. Sample 24-003: Quartz-filled vesicles (upper left corner of photo) with chlorite alteration around the rim, small quartz grains, chlorite altered feldspar laths, chlorite pseudomorphs, and opaques in a very fine-grained groundmass of chlorite, chlorite/smectite, quartz ± epidote (?). Magnification 1 cm = 0.2 mm. Plane light.

D. Sample 24-003: Same as above. Magnification 1 cm = 0.2 mm. X-nicols.

A

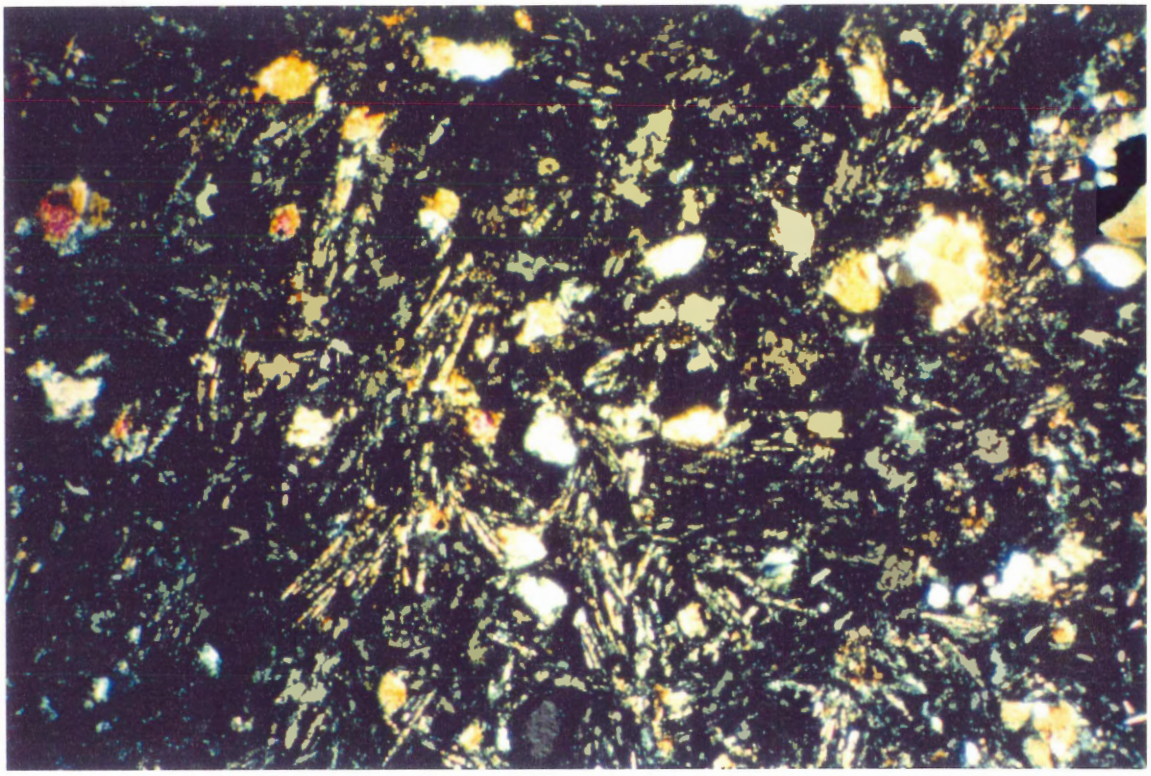

B

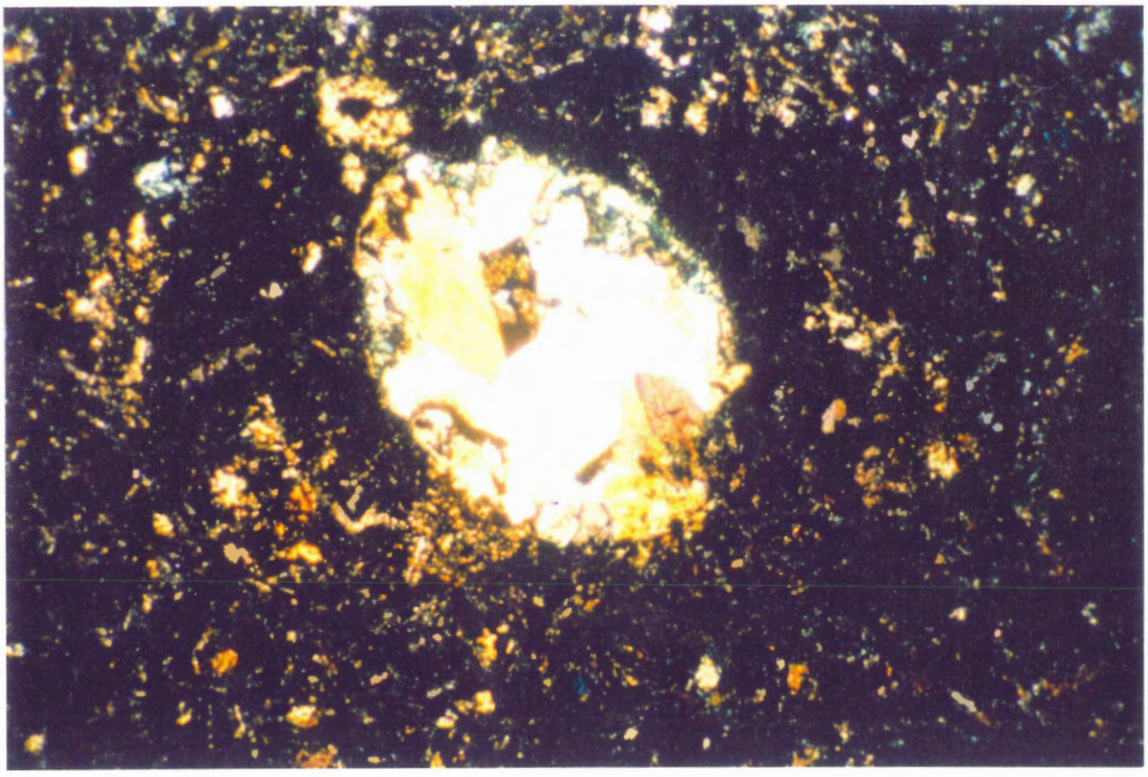

C

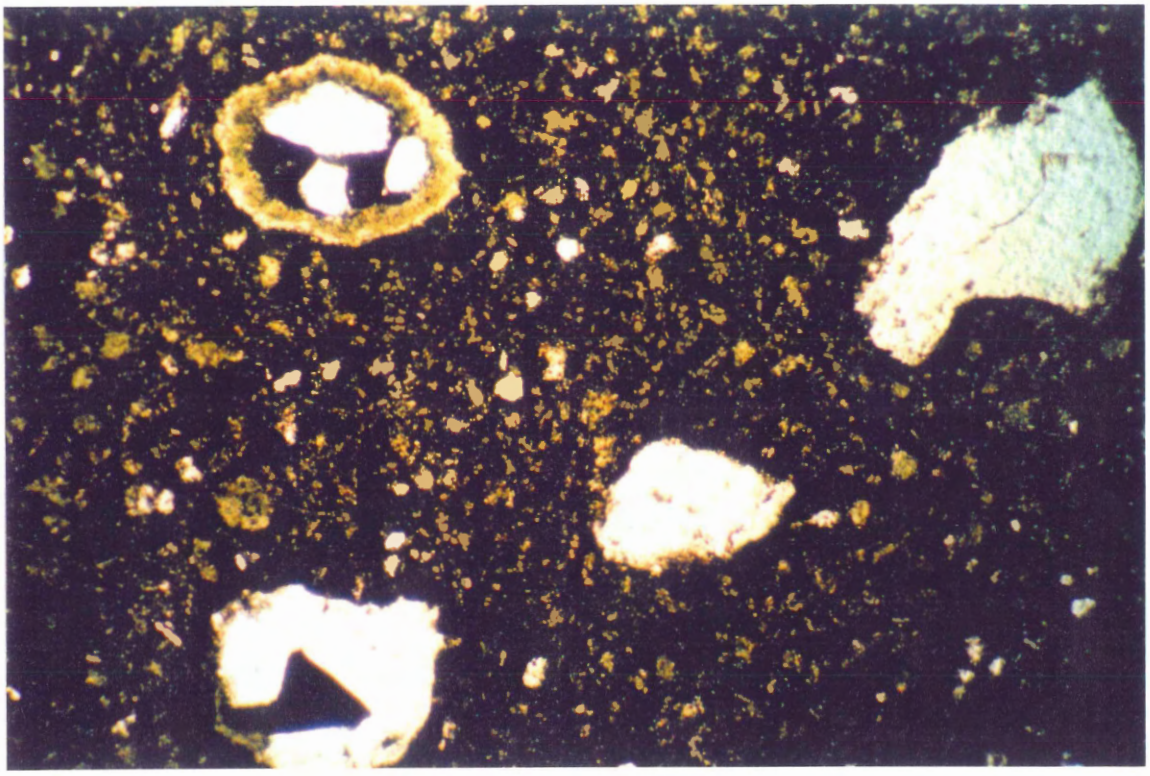

D

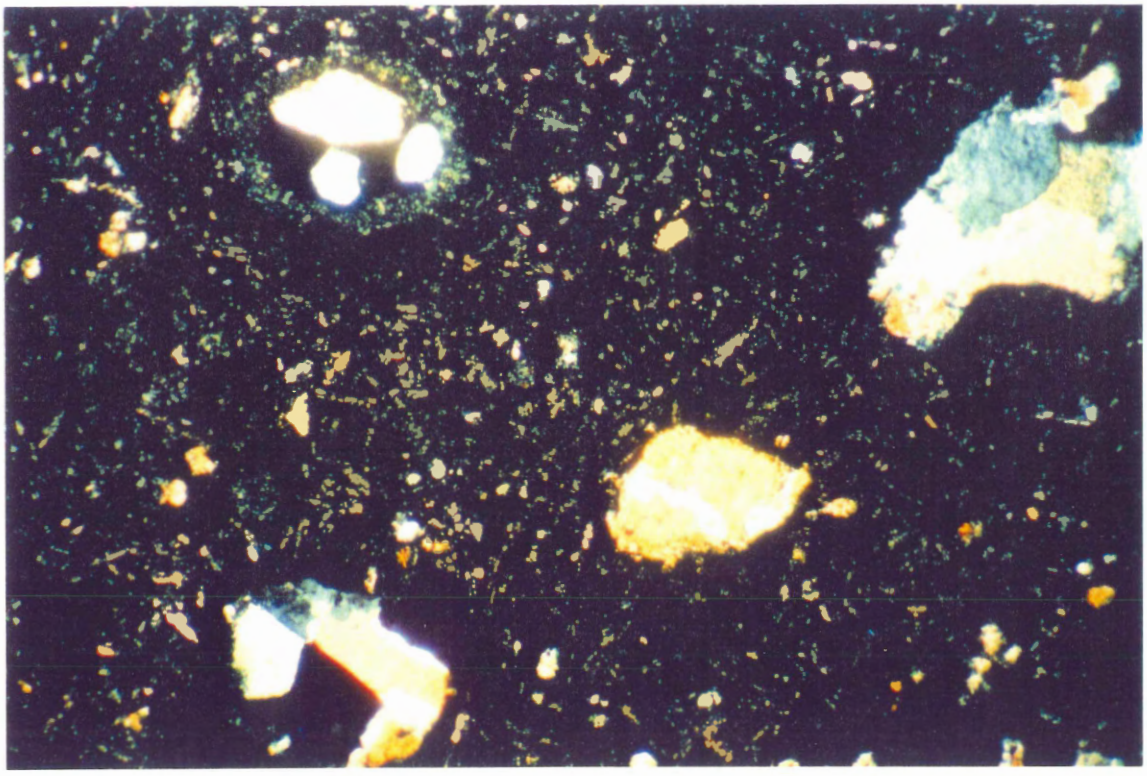

Figure 4.11 Sample 20-004: Zeolite-filled vesicles (centre of photo), probably laumontite, small quartz grains, feldspar laths (intergrown and altered by chlorite), opaques and chlorite pseudomorphs ina groundmass of chlorite, chlorite/smectite, quartz, ± epidote (?). Magnification 1 cm = 0.2 mm. X-nicols.

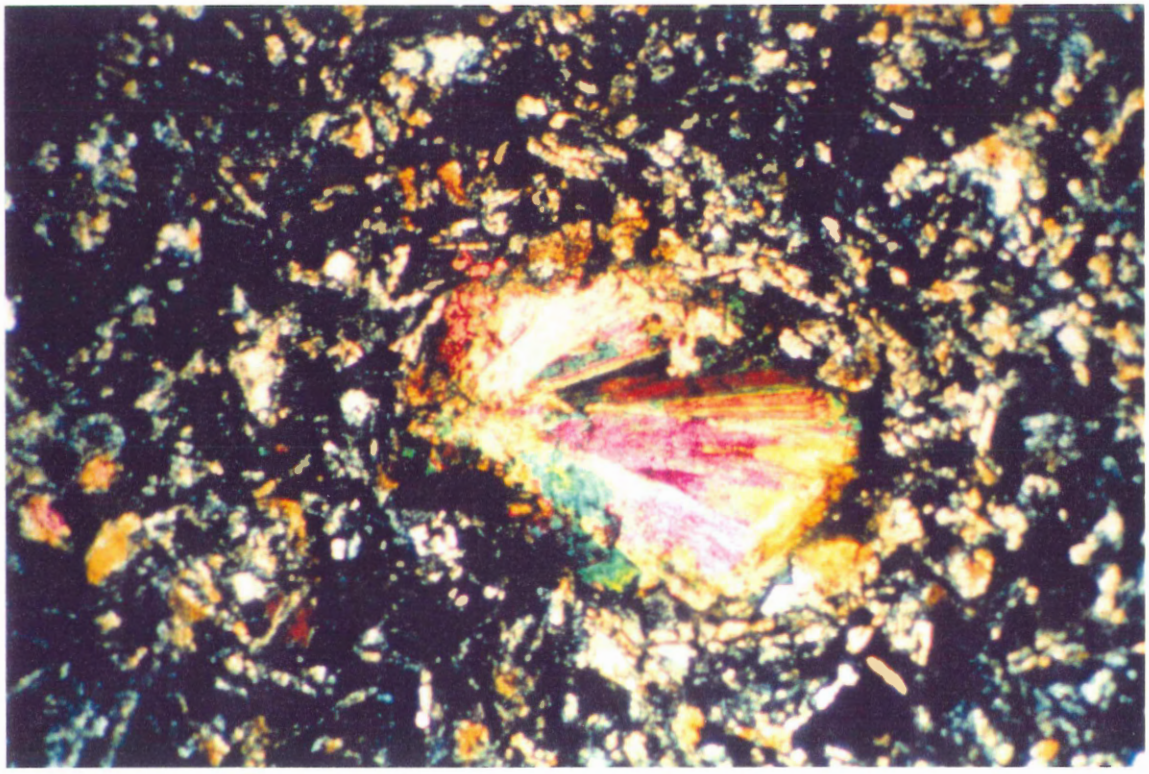

microcrystalline groundmass, and as alteration of the mesostasis.

4.4 Alteration Zones In The Troodos Ophiolite

Gillis (1986) and Gillis and Robinson (1988) defined five alteration zones for the lava screens and the dikes of the Troodos ophiolite on the basis of secondary mineral assemblages and field appearances (Gillis and Robinson 1988): a seafloor weathering zone, a low temperature zone, a transition zone, an upper dike zone, and a mineralized zone (Table 4.5).

Red "oxidized" halos occurring along pillow margins and fractures, pervasive alteration, and an abundance of interpillow sediments characterize the seafloor weathering zone (SWZ). The characteristic mineral alteration is plagioclase replaced by K-feldspar, and olivine by Fe-hydroxides, smectite, and calcite, whereas clinopyroxene remains unaltered (Table 4.5). In general, the rocks preserve an igneous texture, however altered groundmass slightly obscures the igneous texture in some units.

The variable intensity of alteration, and fresh glassy margins adjacent to extensively altered zones, characterize the low temperature zone (LTZ). Assemblages of zeolites and clays fill clay-lined vesicles and fractures. Calcite is locally abundant throughout the zone. K-feldspar replaces plagioclase and the clinopyroxene remains fresh (Table 4.5).

Characteristics of both the overlying LTZ and the underlying upper dyke zone (UDZ) are present in the transition zone (TZ). The appearance of

Table 4.5 Characteristics of the regional alteration zones for the Troodos ophiolite. (after Gillis 1986).

Zone*	Primary Minerals	Groundmass	Glassy Margins	Void filling
SWZ	oliv - goet + calc (T) cpx - smec (F-M) spinel (F)	cpx - smec (S) plag - smec (S-M) plag - K-spar (T) Ti mag - maghem (S-M) mesos - smec, calc (M-T)	smec ± phil (T)	smec + Fe hydro ana, adularia calc paly
LTZ	oliv - goet + calc (T) cpx - smec (F-S) plag - smec, celad (F) spinel (F) Ti mag (F)	cpx - smec (S) plag - smec, celad, calc (F-M) Ti mag - maghem (S-M) mesos - smec, celad, calc (F-M)	smec ± phil (T) ± ana smec ± celad ± clino	smec + celad Na-Ca zeo, qtz, chal calc paly
TZ	cpx - smec, smec/chl (S-M) (S-M) plag - albite (M-T) Ti mag (F)	cpx - smec, smec/chl (S-M) plag - smec, smec/chl (S-M) plag - albite (T) Ti mag (F) mesos - smec, smec/chl, qtz (M-T)	smec ± smec/chl ± laum	smec ± smec/chl ± qtz + pyr laum + qtx ± pyr calc
UDZ	cpx - chl (S-M) plag - albite (T) plag - calc, epi, chl (M-T)	cpx -chl (S-M) plag - albite (T) plag - epi + chl (M-T) Ti mag- titanite (S-M) mesos - chl, qtz, epi, pyr (T)	chl ± qtz ± pyr ± epi	chl ± epi ± qtz ± pyr qtz + pyr calc

NOT F= fresh; S= slightly altered; M= moderately altered; T= totally altered;

oliv= olivine; cpx= clinopyroxene; plag= plagioclase; Ti mag= titanomagnetite; mesos= mesostasis; smec= smectite; smec/chl= mixed-layer smectite/chlorite; celad= celadonite; chl= chlorite; paly= palygorskite; Fe hydro= Fe hydroxides; goet= goethite; maghem= maghemite; calc= calcite ana= analcime; phil= phillipsite; clino= clinoptilolite; laum= laumontite; epi= epidote; chal= chalcedony; qtz= quartz; pyr= pyrite; K-spar= potassium feldspar.

* SWZ= seafloor weathering zone; LTZ= low temperature zone; TZ= transition zone; UDZ= upper dike zone.

laumontite, and smectite/chlorite delineates the upper boundary of this zone, and the presence of chlorite + quartz + pyrite in the groundmass indicates the lower boundary. Variable alteration to smectite, smectite/chlorite, laumontite and quartz occurs at the margins of pillows and massive flows. Quartz, laumontite, calcite, pyrite and/or clay mineral assemblages partly to totally fill ovoid, clay-lined vugs. Partial alteration to clay minerals occurs in plagioclase and clinopyroxene phenocrysts. The mesostasis is uniformly altered to smectite or smectite/chlorite with minor quartz and pyrite. Microlites of plagioclase alter to albite, clay minerals, or rarely K-feldspar (Table 4.5). Igneous textures are well preserved in the rocks of the transition zone.

More extensive alteration is characteristic of the upper dyke zone (UDZ) (Table 4.5). Uniform alteration of the mesostasis and glassy margins to chlorite + pyrite ± epidote occurs. Epidote, pyrite, chlorite, or calcite assemblages fill chlorite-lined, quartz-rimmed vesicles, vugs, and fractures. Although the plagioclase is completely albitized, the clinopyroxene remains relatively fresh, with only minor chloritic alteration. Preservation of the igneous textures occurs, with the exception of small zones of epidosite.

From the mineral assemblages described for this study area, the samples fit into the transition alteration zone defined by Gillis (1986). This placement is based on the occurrence of chlorite and clays together in the same sample (refer to the definition of the alteration zone in Table 4.5).

4.5 Summary

The primary mineral assemblages of the rocks in this study were plagioclase, clinopyroxene, quartz, opaque oxides, mesostasis, and olivine (in some samples). The secondary/alteration minerals are chlorite, albite, alkali-feldspar, quartz, opaque oxides, and minor amounts of calcite, titanite, sulphides, epidote, and zeolites. The rocks from the study area show porphyritic and intersertal to intergranular textures. Alteration in the samples is of the hydrothermal type and everywhere is incomplete. The samples from this study fit into the transition alteration zone as defined by Gillis (1986).

CHAPTER 5 GEOCHEMISTRY

5.1 Introduction

This chapter presents X-ray fluorescence analyses of major and trace elements. For the purpose of comparison, and to establish the context for the samples described in this thesis, I use major and trace element variation diagrams from Mehegan (1988).

5.2 Previous Geochemical Interpretation Of The Troodos Ophiolite

On the basis of major element compositions, Mehegan (1988) separated the lavas from the Extrusive sequence on the northern flank of the ophiolite into Magma Groups A and B. The characteristic major element compositions of the groups are as follows: 1) Magma Group A comprises a tholeiitic sequence of rhyodacites, dacites, andesites, basaltic andesites, and basalts, enriched in TiO_2 and FeO (1 - 1.6 wt% TiO_2 and 10 - 15 wt% FeO); 2) Magma Group B consists of Groups B2 and B1; Group B2 lavas are basaltic andesites and andesites with intermediate TiO_2 concentrations (0.75 - 0.85 wt%) and distinctive trace element characteristics; Group B1 lavas are mildly calc-alkaline.

The division into Group A and B on the basis of major element compositions is substantiated by trace element compositions. The characteristic trace element compositions of the groups are: 1) The andesites and basaltic andesites of Group A generally have greater than 20 ppm Y and

30 ppm Zr, and less than 10 ppm Cr and 20 ppm Ni; Ti and V become more compatible and are rapidly depleted with increasing fractionation in the Group A rocks; 2) Magma group B was subdivided into Groups B2 and B1 using major elements, but their detailed definition involves trace element compositions; Group B2 is defined on Zr/TiO2-Zr, Y/TiO2-Y, and Zr/Y-Zr variation diagrams which illustrate clearly that the Group B2 lavas are intermediate to Group A and Group B1; Group B1 has a Y content of less than 30 ppm and a Zr content of less than 50 ppm, and Cr and Ni concentrations greater than 100 ppm and 40 ppm, respectively.

Lavas of Group A generally extend into the Basal Group of the Extrusive Sequence as pillow and massive screens, forming the oldest volcanic sequence. The younger and progressively more depleted lavas of Group B2 overlie those of Group A. Group B2 lavas are followed upward by the Group B1 lavas.

The variation and discrimination diagrams from Mehegan (1988) are used in this thesis as a comparison tool and as a means of deciding the magma group to which the lava screens and dikes from this study belong.

Baragar et al. (1990) concluded that the compositional range and trends of the dike units of the Sheeted Complex, which underlies the Transition Zone of the Extrusive Sequence, match those of the lavas of the Extrusive Sequence, but do not show the distinct geochemical discontinuity that occurs between Magma Groups A and B in the Extrusive Sequence.

5.3 Major And Trace Element Whole-Rock Geochemistry

Table 5.1 presents whole-rock XRF measurements of major and trace elements for the samples from the study.

5.3.1 Major element analysis

Figures 5.1 and 5.2 show the major element compositions of the samples from this study. The samples of this study represent a tholeiitic sequence of rocks (Fig. 5.1), from basalt-basaltic andesite-andesite (Fig. 5.2).

The question arises as to whether the mobility of SiO_2 during hydrothermal alteration has offset or distorted the true primary range of compositions. This possibility has been investigated through testing the relationship between SiO_2 and Zr. Zirconium, an immobile element, increases with differentiation which is also expressed by an increase in SiO_2 content, thus a linear relationship between SiO_2 and Zr would imply that little change in primary silica content is likely to have occurred as a result of alteration. Figure 5.3 shows a strong linear component to the relationship and this result supports an original basalt-basaltic andesite-andesite range for the composition of the samples from this study. The small departures for individual samples from the overall linear trend suggest minor changes in SiO_2. However, none of these departures is large enough , nor are the alkalis likely to affect the magnetic results, so as to invalidate the conclusion.

Variation diagrams (Figs. 5.4A to 5.10A) show whole-rock major element compositions of the samples from this study. Figures 5.4B to 5.10B

Table 5.1 X–Ray Fluoresence Major and Trace Element Data

Sample	13–007	14–015	15–003	16–003	18–001	19–008	20–004	21–003	22–008	23–002	24–003	25–002	26–003	27–003	28–002	29–002	30–002	31–002	32–001	33–003
Majors																				
SiO2	52.92	58.64	58.76	55.08	49.74	51.61	59.63	53.14	61.50	60.13	52.39	61.60	54.64	53.64	53.37	53.67	53.04	53.93	46.41	53.90
Al2O3	15.02	15.20	14.76	14.47	14.43	15.03	14.43	15.11	14.52	14.58	15.68	14.05	14.37	14.95	13.73	14.42	14.45	15.13	15.25	14.76
Fe2O3	12.06	10.07	11.97	11.62	12.99	11.59	9.97	12.69	9.23	10.21	13.99	10.19	13.31	12.26	13.92	10.34	13.71	12.20	9.60	13.00
MgO	5.67	5.56	3.50	5.06	4.54	7.21	3.32	5.23	2.91	3.87	5.86	2.33	4.76	5.15	5.76	6.85	5.46	4.72	5.85	4.87
CaO	6.39	3.45	4.77	6.14	5.39	5.15	5.46	6.86	4.71	4.64	5.01	5.03	6.53	6.05	5.32	6.26	5.25	6.33	12.61	6.70
Na2O	2.10	1.96	2.84	2.22	2.53	1.59	3.17	2.27	3.53	3.14	3.16	4.15	2.90	3.56	3.45	2.36	3.54	3.71	2.90	2.95
K2O	0.09	0.81	0.56	0.76	0.42	1.28	0.22	0.59	0.15	0.10	0.11	0.07	0.18	0.16	0.39	0.98	0.64	0.27	0.33	0.31
TiO2	1.21	0.86	1.26	1.25	1.40	0.92	1.09	1.27	0.99	1.18	1.22	1.13	1.32	1.24	1.39	0.73	1.33	1.33	1.67	1.39
MnO	0.35	0.31	0.24	0.29	0.24	0.33	0.35	0.39	0.28	0.29	0.35	0.21	0.21	0.21	0.23	0.23	0.25	0.22	0.16	0.24
P2O5	0.09	0.12	0.14	0.09	0.07	0.07	0.16	0.09	0.17	0.14	0.08	0.24	0.10	0.08	0.08	0.05	0.09	0.09	0.16	0.09
L.O.I.	4.40	4.00	2.00	3.00	6.80	5.00	2.30	3.50	2.10	2.40	2.60	1.40	2.50	3.10	3.20	4.20	3.30	2.10	3.70	2.60
Trace																				
Ba	51	12	37	18	22	25	14	30	31	20	20	30	43	31	27	17	11	25	31	31
Rb	<5	<5	<5	<5	<5	5	<5	<5	<5	<5	<5	<5	<5	<5	<5	<5	<5	<5	<5	<5
Sr	89	81	119	86	100	74	126	94	127	111	109	117	92	102	100	78	91	106	91	94
Y	32	37	44	33	26	26	42	36	50	43	29	53	36	32	33	21	29	34	32	35
Zr	72	90	100	69	71	51	104	72	110	92	58	117	74	69	66	41	68	75	65	75
Nb	<5	<5	<5	<5	<5	<5	<5	<5	<5	<5	<5	<5	<5	<5	<5	<5	<5	<5	<5	<5
Th	<10	<10	<10	<10	<10	<10	<10	<10	<10	<10	<10	<10	<10	<10	<10	<10	<10	<10	<10	<10
Pb	<10	<10	<10	<10	<10	<10	<10	<10	<10	<10	<10	<10	<10	<10	<10	<10	<10	11	<10	<10
Ga	19	18	18	17	21	18	19	22	18	21	20	19	19	19	18	15	18	18	19	17
Zn	191	248	158	194	196	170	142	212	162	222	245	76	88	83	142	119	199	103	164	116
Cu	34	33	121	20	20	16	107	71	8	8	105	15	24	33	9	141	21	27	47	67
Ni	14	13	<5	19	16	17	8	17	<5	6	22	<5	15	9	10	18	<5	15	9	9
V	385	235	196	490	379	382	128	444	100	182	620	66	456	458	5	360	469	453	491	449
Cr	15	9	<5	<5	9	9	8	12	6	<5	<5	<5	<5	<5	<5	11	<5	8	<5	<5

NOTE: Major elements – All values in weight percent
Total iron determined as Fe2O3 (assuming iron is converted to Fe 3+ during L.O.I.)
Loss on Ignition (L.O.I.) determined after heating sample at 1050 C

Trace elements – All values in parts per million (ppm)
Detection limit is 5 ppm, except Th & Pb (10 ppm)

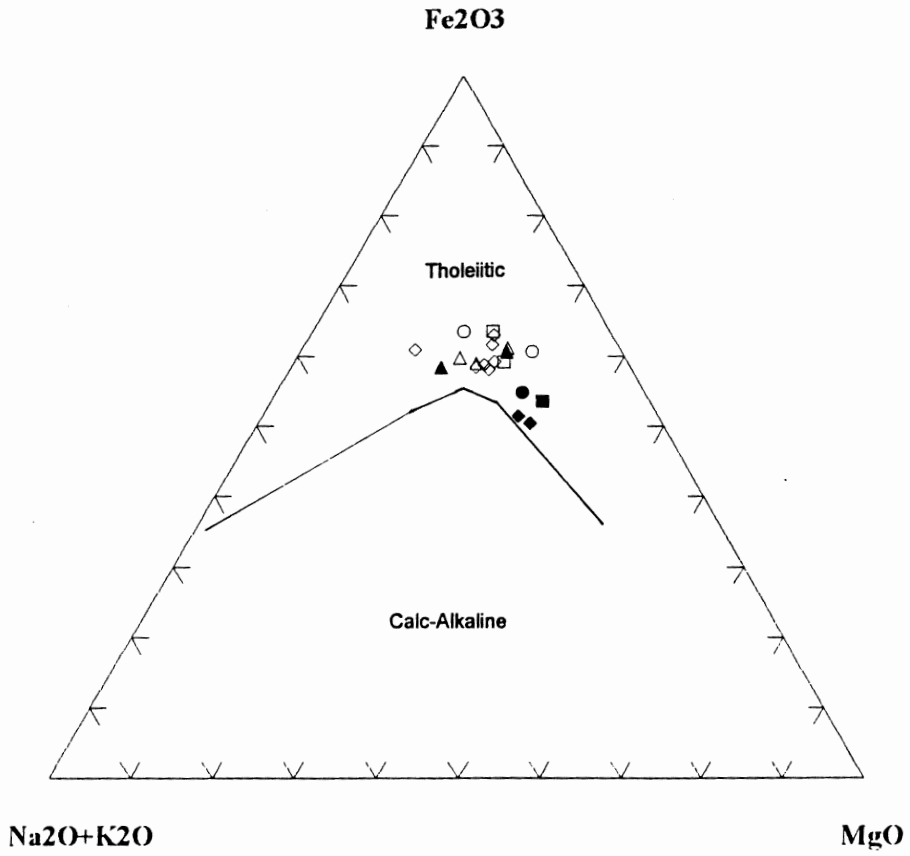

Figure 5.1 AMF (Na_2O + K_2O, MgO, Fe_2O_3) diagram showing the composition of the samples from the study (values in wt%). All of the dikes and screens lie in the "Tholeiitic" field of the diagram(after Irvine and Baragar 1971). Symbols are as follows: open symbols - dike units; closed symbols - screen units; Section 1 - ○ ; Section 2 - □ ; Section 3 - △ ; Section 4 - ◇ .

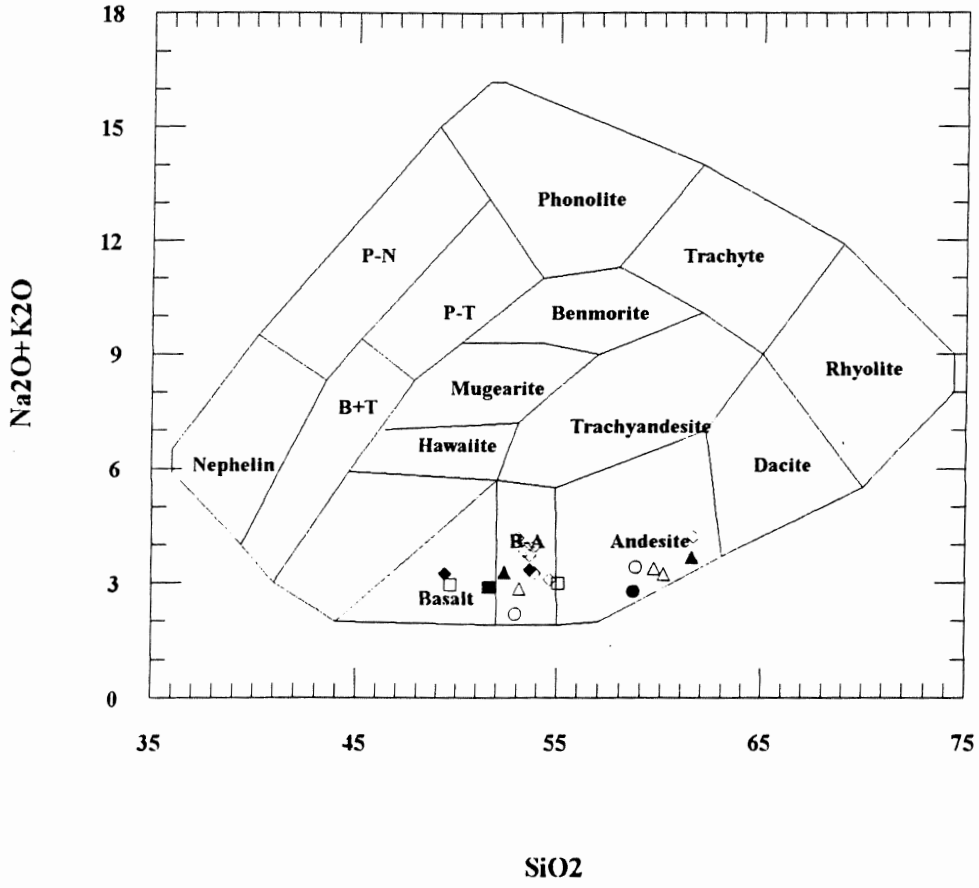

Figure 5.2 Major element classification diagram for the samples from this study (values in wt%). Samples fall into the Basalt-Basaltic Andesite-Andesite zone (after Cox et al. 1979). Symbols are as follows: open symbols - dike units; closed symbols - screen units; Section1-○ ; Section 2 - □ ; Section 3 - △ ; Section 4 - ◇.

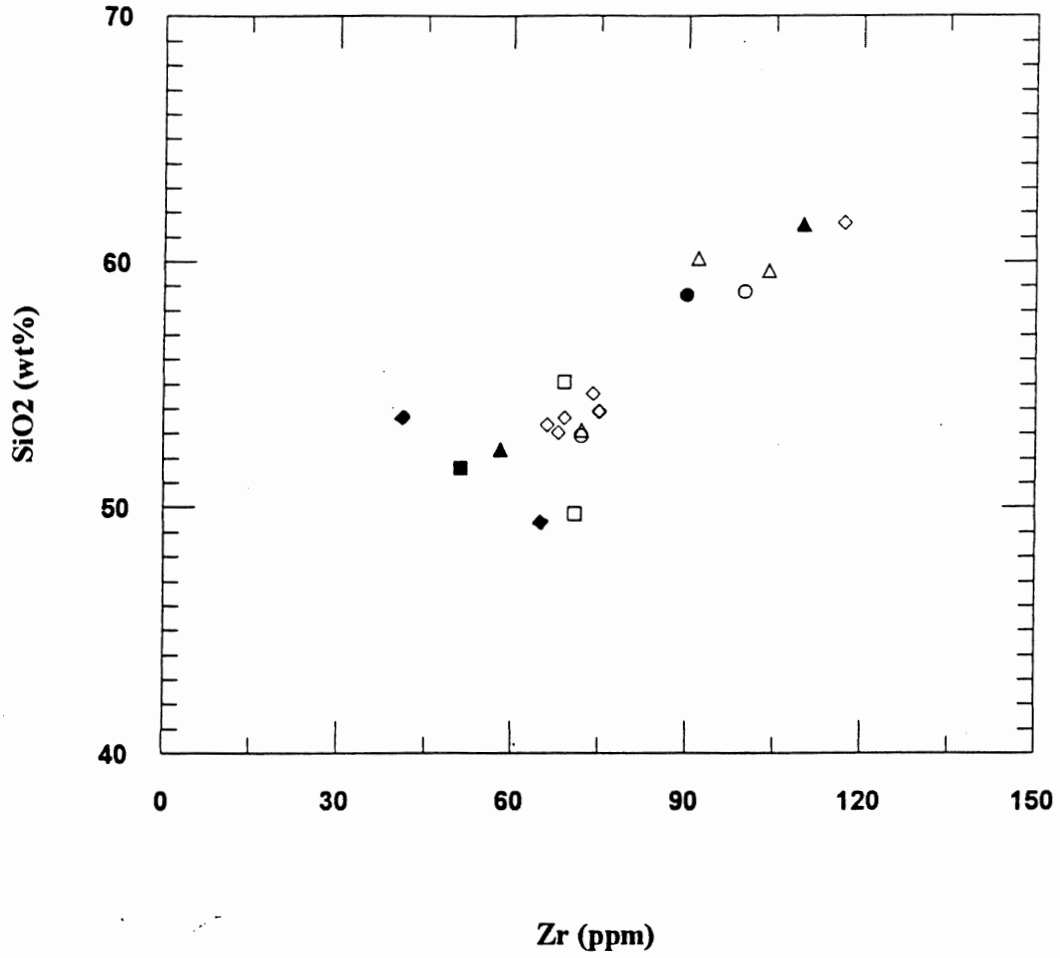

Figure 5.3 SiO_2 - Zr variation diagram for samples from the Argaki tou Ayiou Onouphriou river, Troodos ophiolite (values of SiO_2 in wt% and Zr in ppm). Symbols the same as in Figure 5.1.

show the corresponding major element plots of Mehegan (1988). The major element analyses for the samples of this study correspond closely to the Group A magmas as defined by Mehegan (1988).

5.3.2 Trace element analysis

Trace element analysis is used here to further characterize the samples of this study. Table 5.1 shows the XRF trace element analysis measurements Figures 5.11-5.13 show the ratios of the incompatible and relatively immobile alteration-resistant trace elements Y, Zr, and TiO_2. These elements are useful in further determining the appropriate magma group of Mehegan (1988) to which the samples belong because the elements are incompatible with major crystallizing phases. Figures 5.14-5.17 show the trends of the compatible transition elements Cr, Ni, V, and Zn versus Zr, and Figures 5.18-5.20 show Sr versus Zr, Ba versus Sr, and Rb versus Sr, respectively.

The Y/TiO_2 versus Y plot (Fig. 5.11A), shows that the values of Y range from 30 to 50ppm and Y/TiO_2 from 20 to 50. A linear trend is apparent; as Y increases so does Y/TiO_2. Screen units 19, 24, and 29 lie at the lower end of the distribution and screen units 14 and 22 are at the high end. Screen unit 32 falls among the group of dikes shown at about Y from 30 to 37ppm and Y/TiO_2 from 20 to 30. The distribution of values falls within the Magma Group A range defined in Mehegan (1988) (Fig. 5.11B).

In the Zr/TiO_2 versus Zr plot, (Fig. 5.12A), the values of Zr range from 40 to 117ppm and from 38 to 112 for Zr/TiO_2. The Zr-Zr/TiO_2 ratio distribution

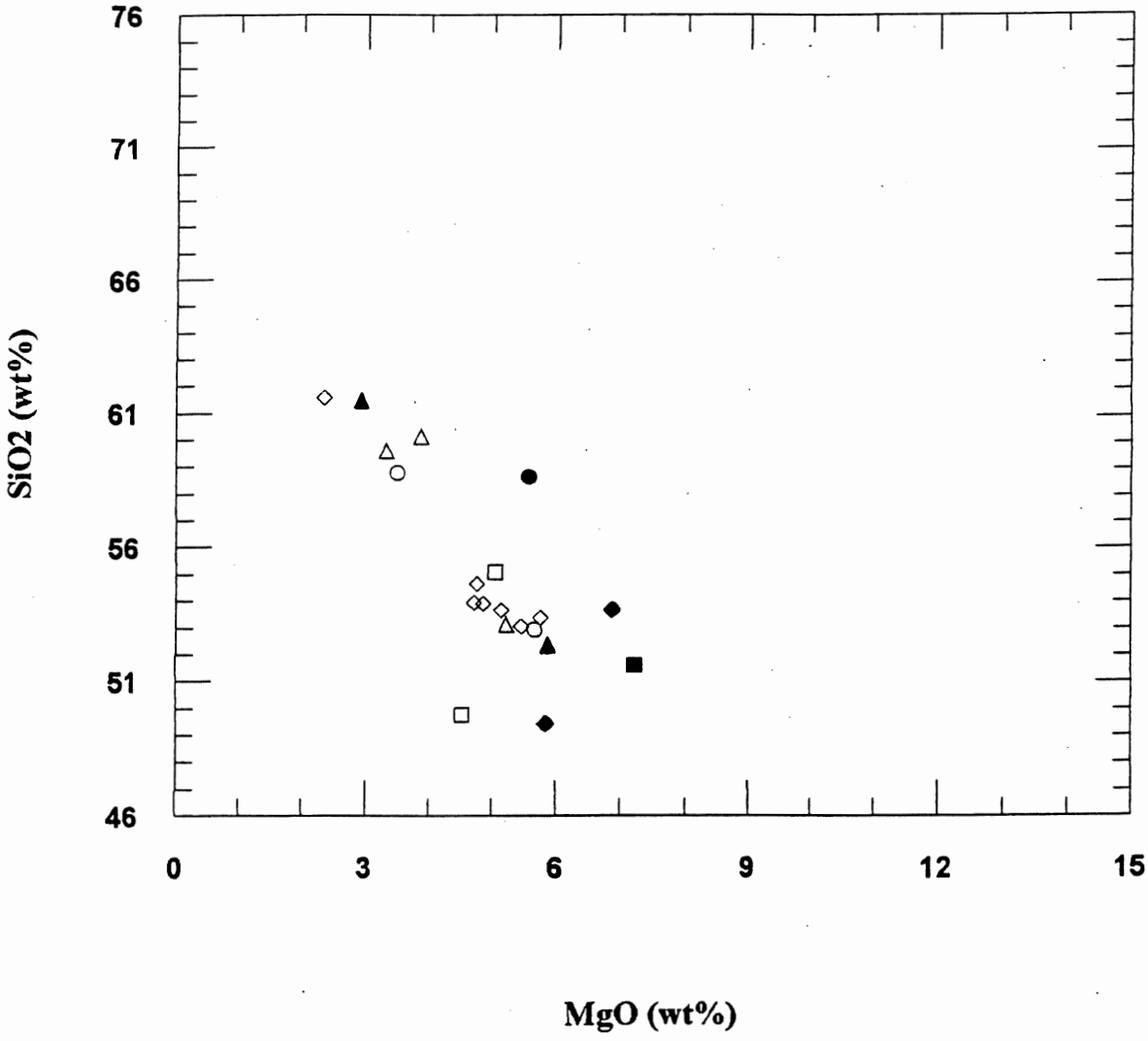

Figure 5.4A. SiO_2 - MgO variation diagram.
Samples from this study. Symbols as in Figure 5.1.

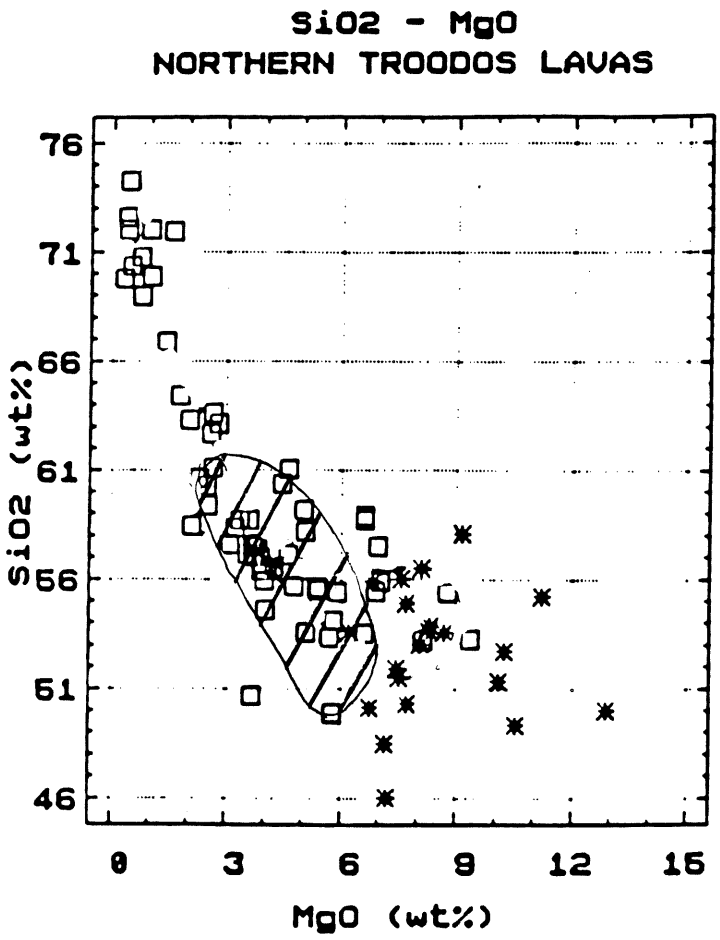

Figure 5.4B. SiO_2 - MgO variation diagram.
Group A and Group B samples from Mehegan (1988). Open boxes - Group A; stars - Group B. Glass composition fields: solid lines - Group A; dash lines - Group B; Hatched area represents the range of samples from this study.

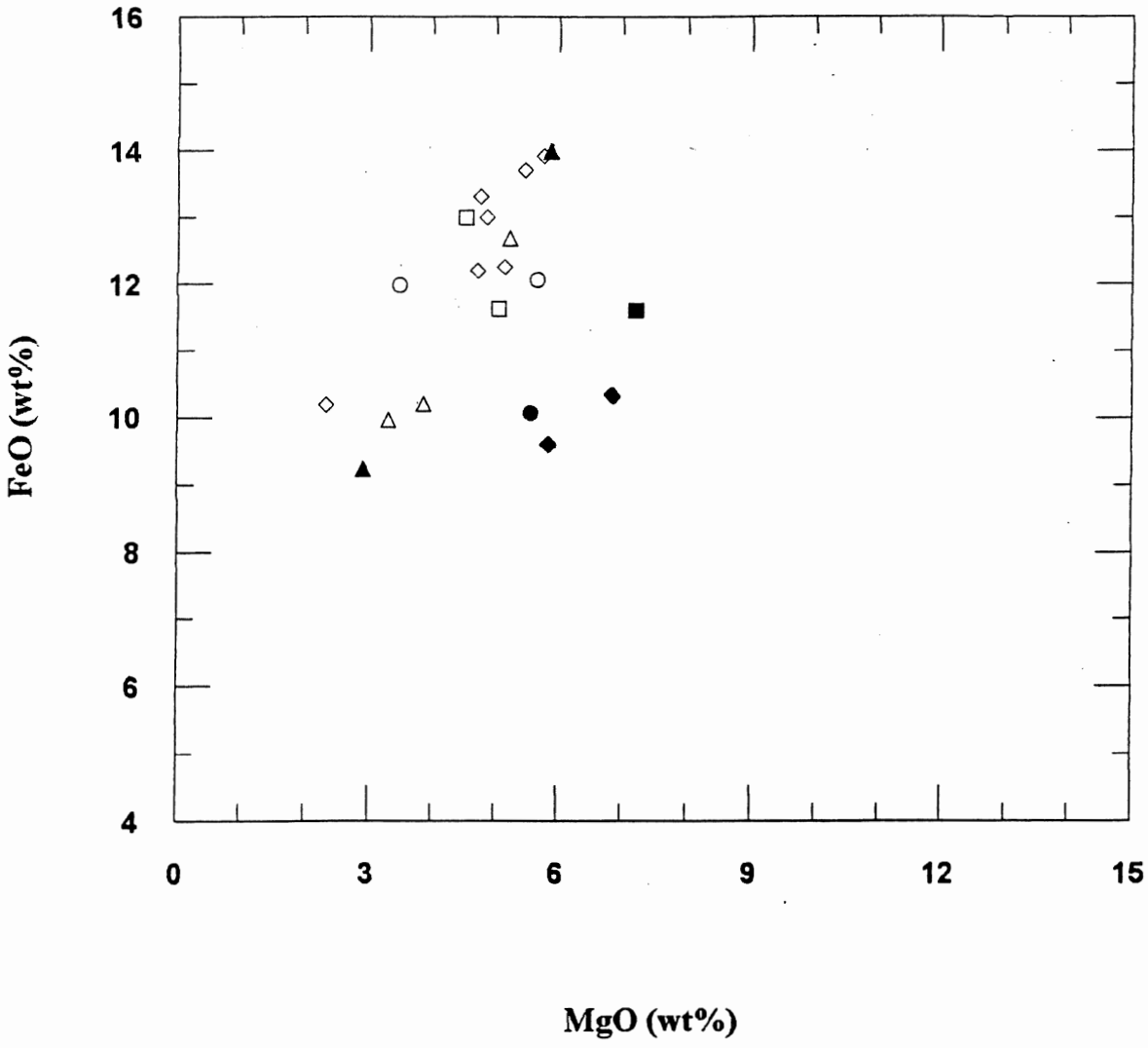

Figure 5.5A. Fe_2O_3 - MgO variation diagram.
Samples from this study. Symbols as in Figure 5.1.

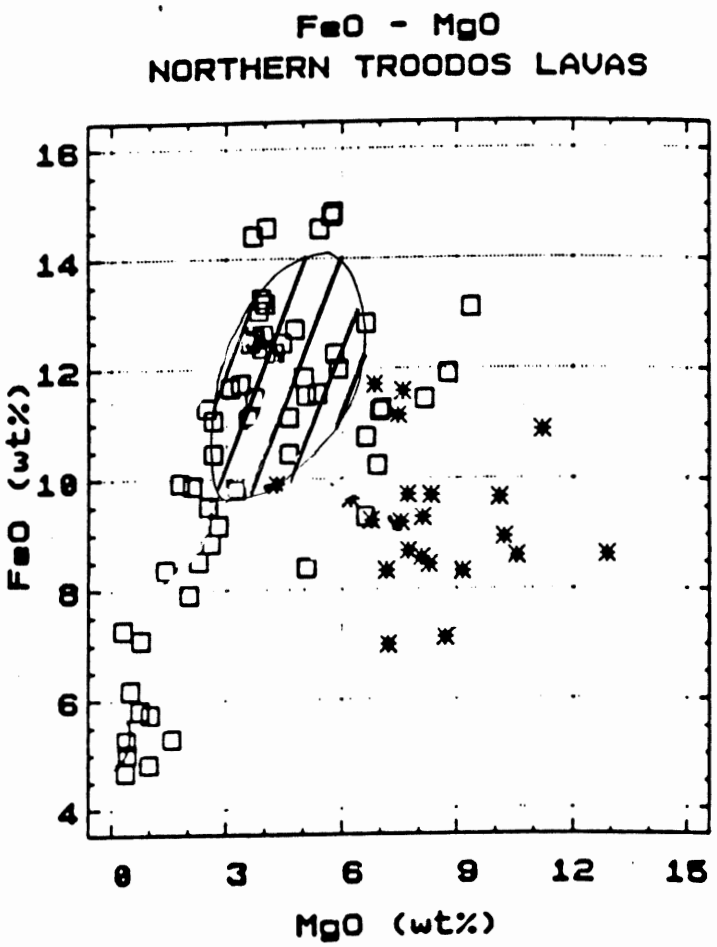

Figure 5.5B. Fe_2O_3 - MgO variation diagram
Group A and Group B samples from Mehegan (1988). Symbols as in Figure 5.4B.
Hatched area represents the range of values for this study.

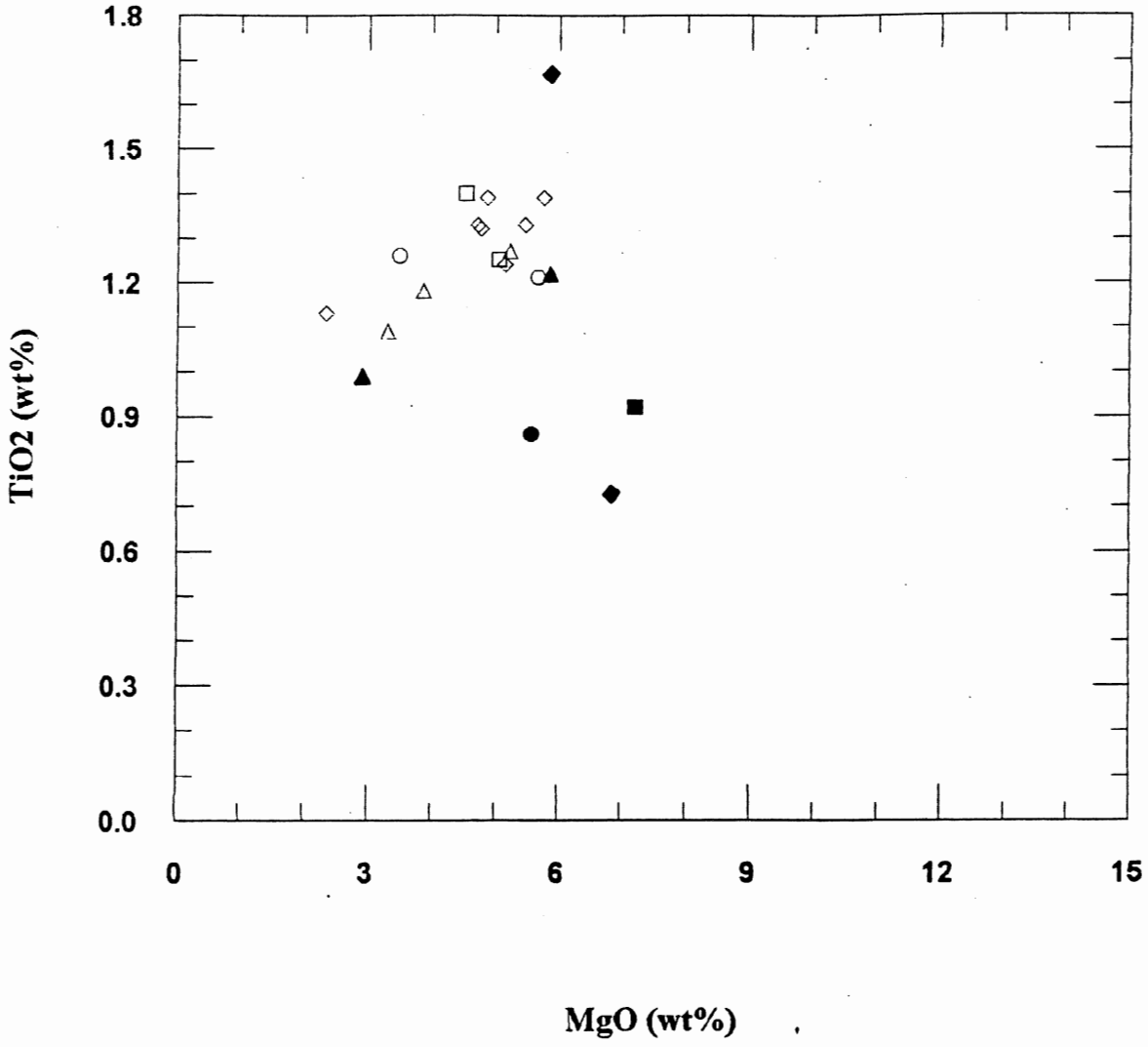

Figure 5.6A. TiO_2 - MgO variation diagram.
Samples from this study. Symbols as in Figrue 5.1.

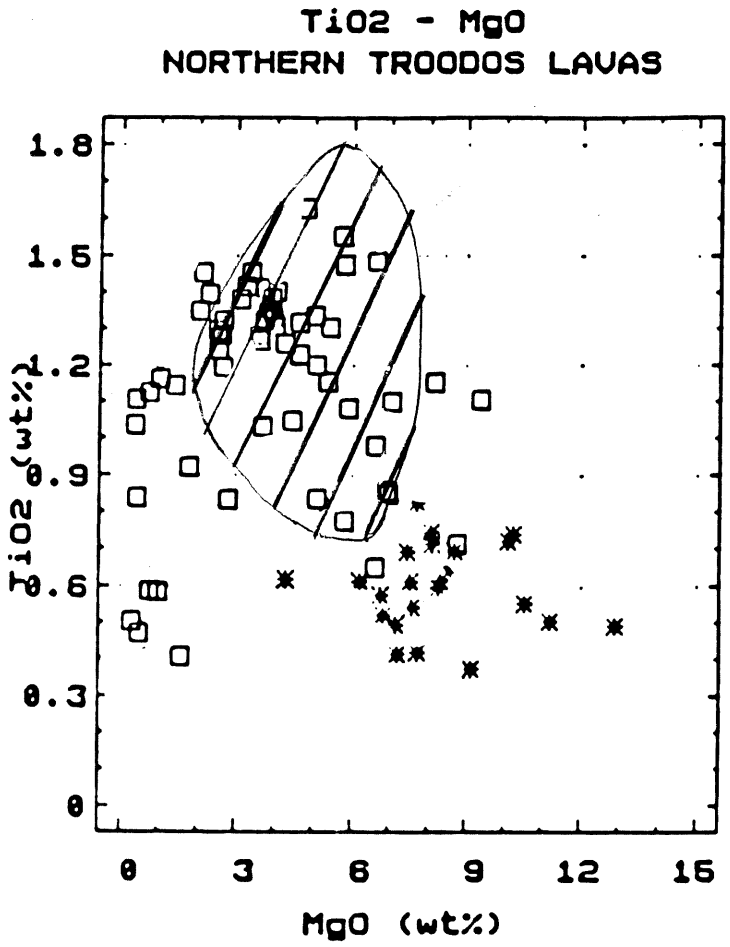

Figure 5.6B. TiO_2 - MgO variation diagram.
Group A and Group B samples from Mehegan (1988). Symbols as in Figure 5.4B.
Hatched area represents the range of values for this study.

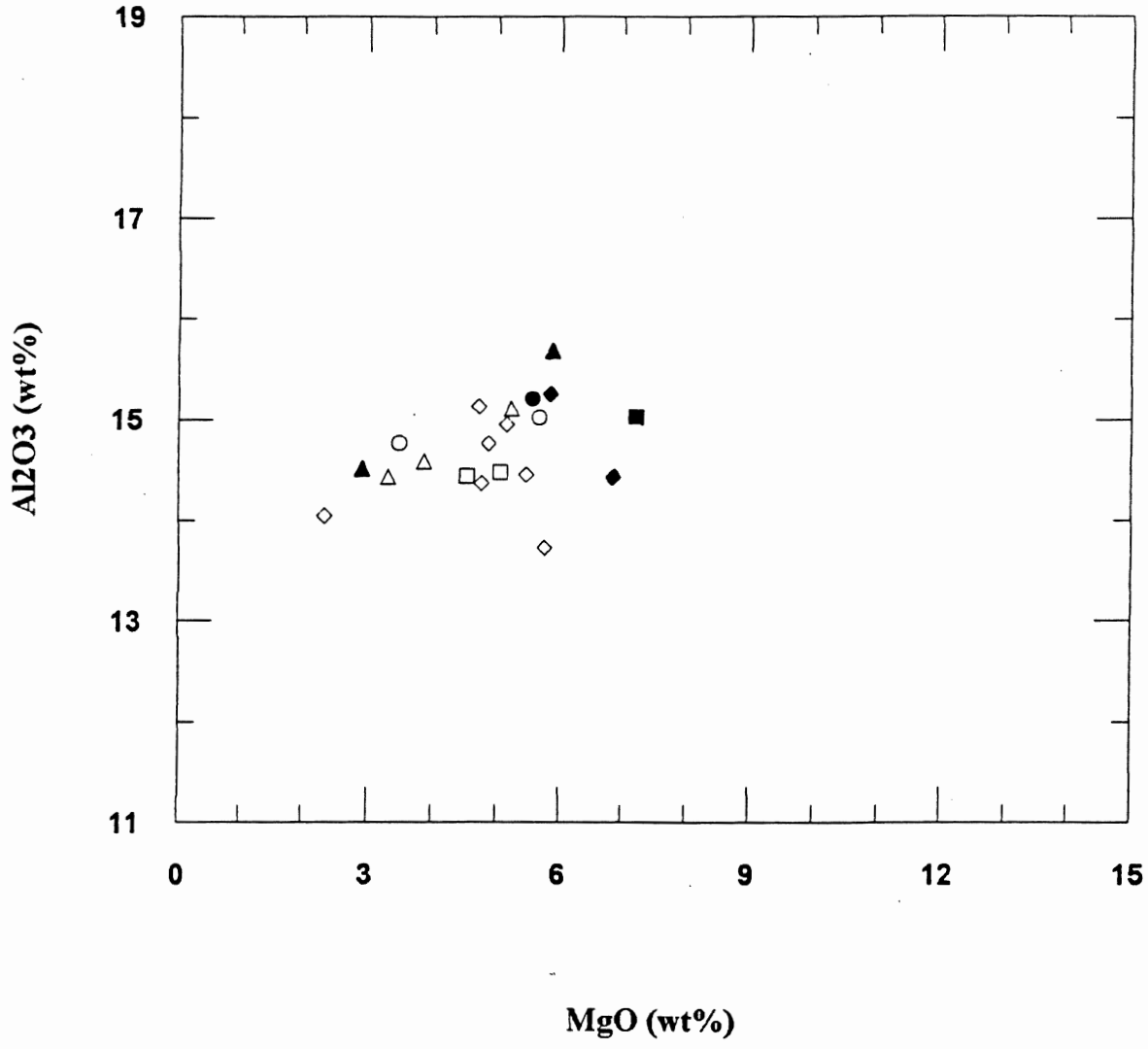

Figure 5.7A. Al_2O_3 - MgO variation diagram.
Samples from this study. Symbols as in Figure 5.1.

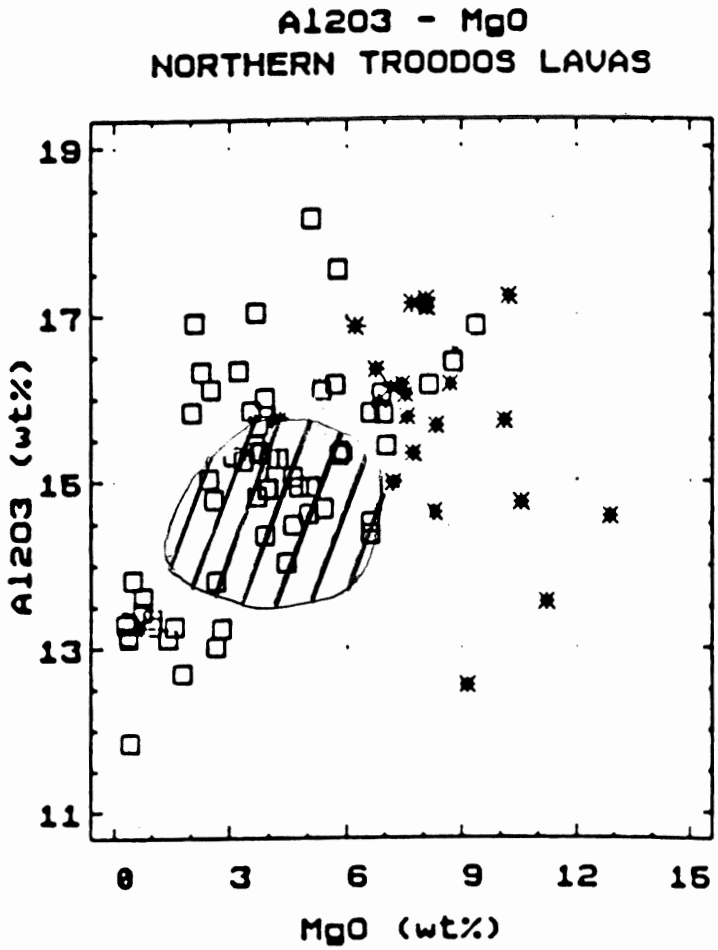

Figure 5.7B. Al_2O_3 - MgO variation diagram.
Group A and Group B samples from Mehegan (1988). Symbols as in Figure 5.4B.
Hatched area represents the range of values for this study.

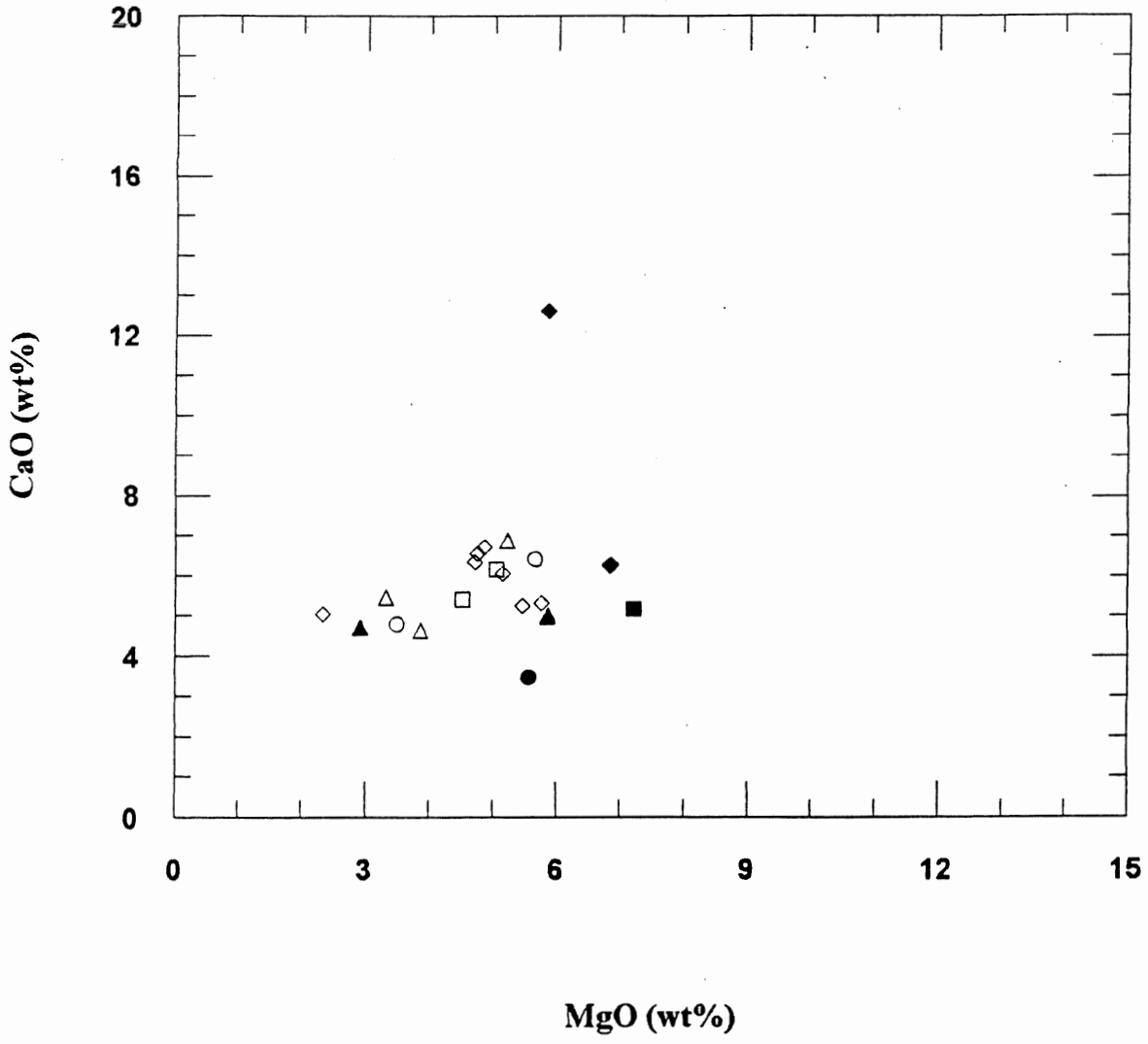

Figure 5.8A. CaO -MgO variation diagram.
Samples from this study. Symbols as in Figure 5.1.

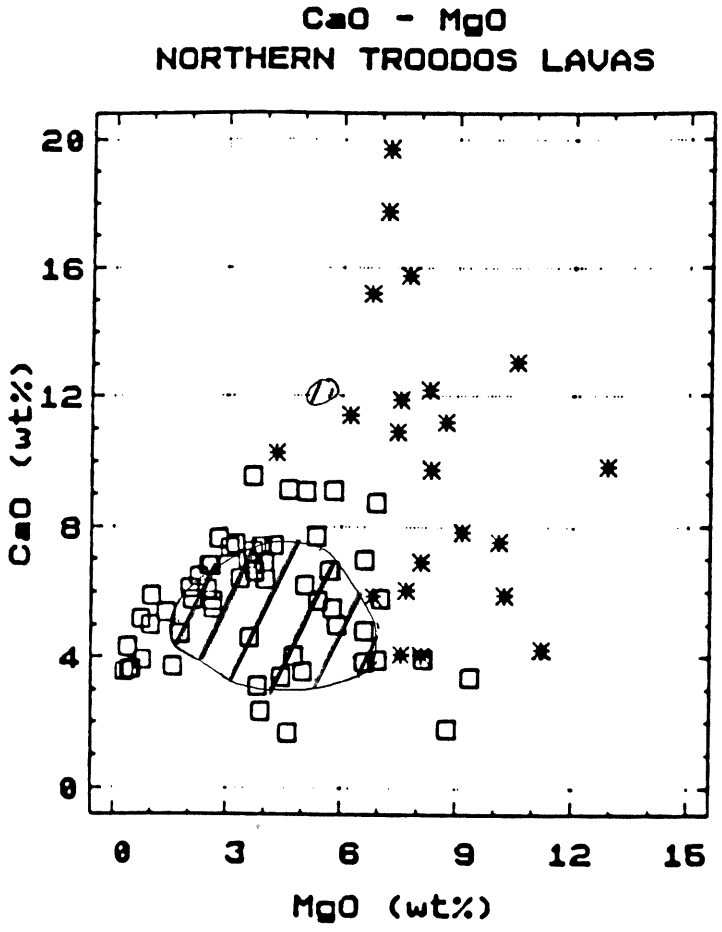

Figure 5.8B. CaO -MgO variation diagram.
Group A and Group B samples from Mehegan (1988). Open boxes - Group A; stars - Group B. Hatched area represents the range of values for this study.

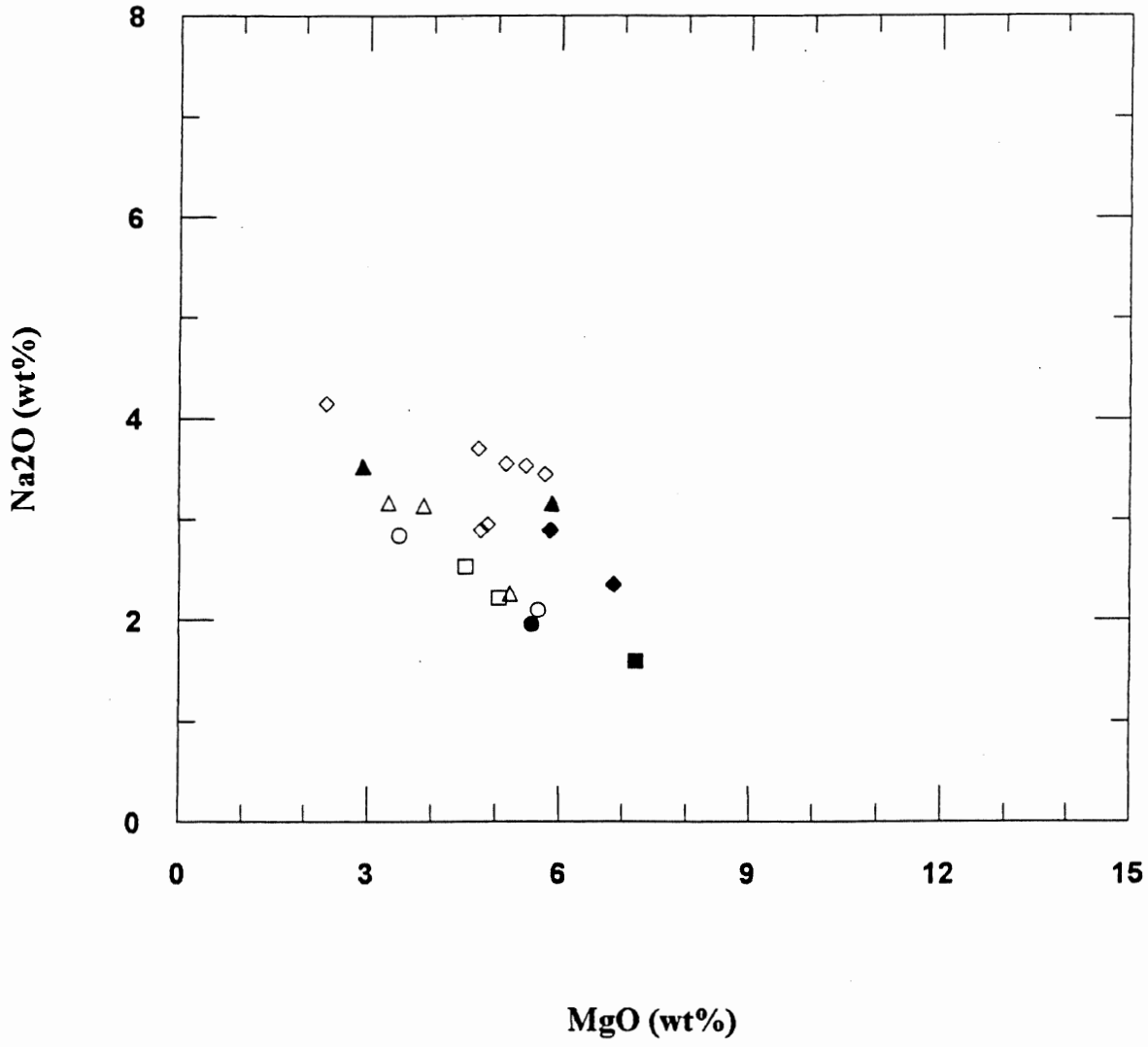

Figure 5.9A. Na_2O - MgO variation diagram.
Samples from this study. Symbols as in Figure 5.1.

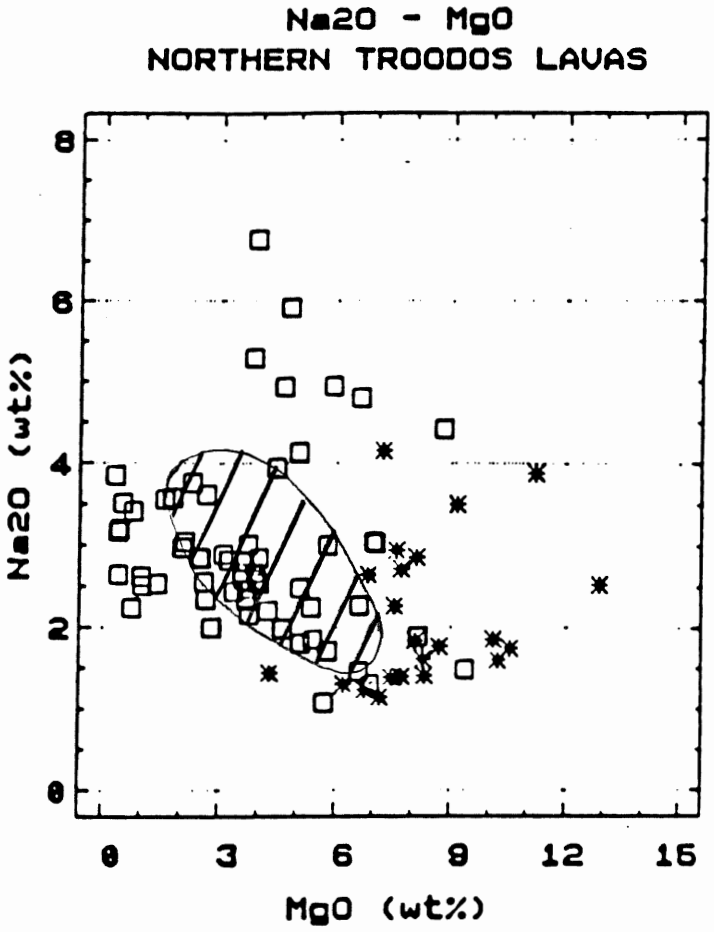

Figure 5.9B. Na_2O - MgO variation diagram.
Group A and Group B samples from Mehegan (1988). Symbols as in Figure 5.8B.
Hatched area represents the range of values for this study.

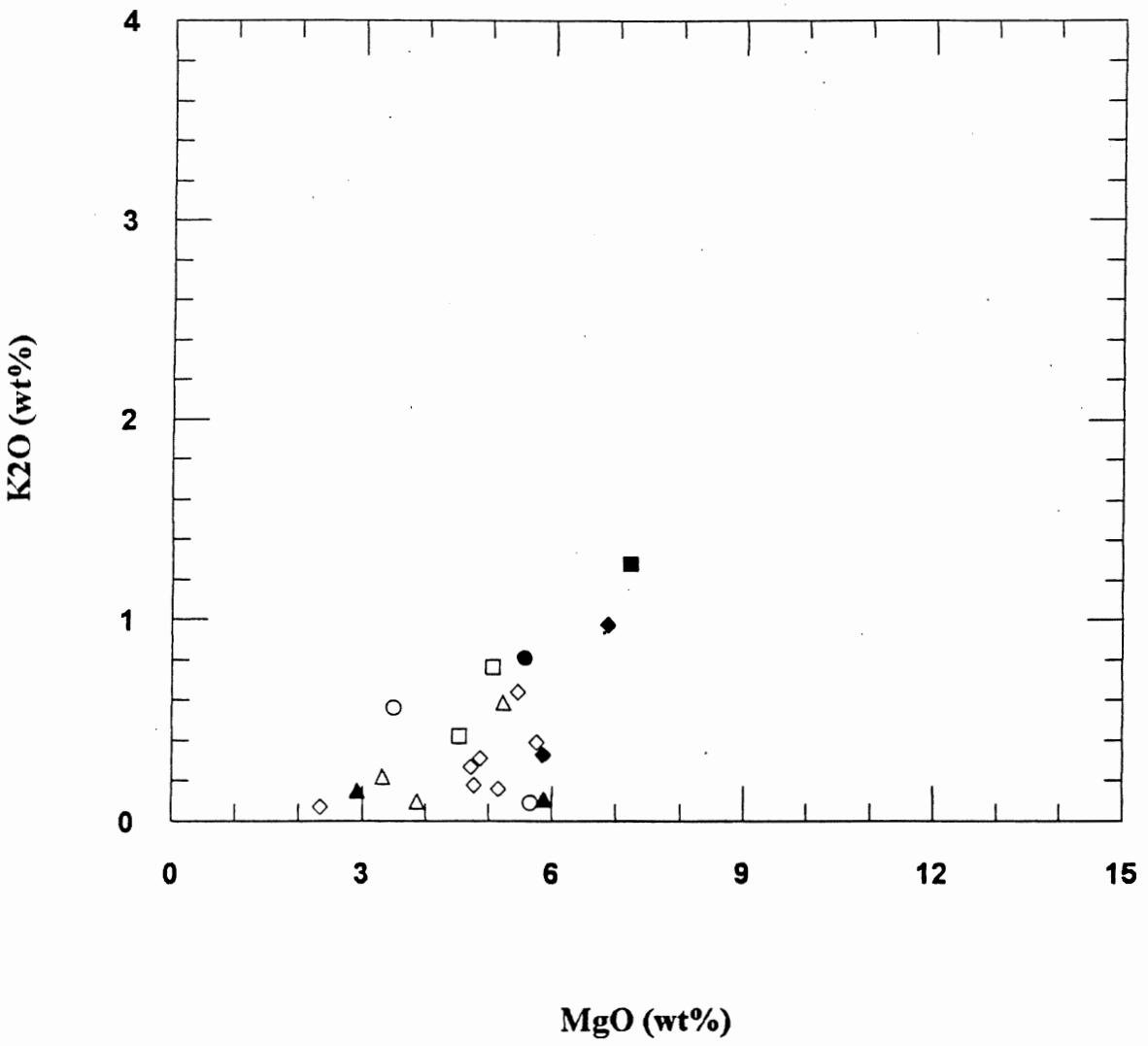

Figure 5.10A. K_2O - MgO variation diagram.
Samples from this study. Symbols as in Figure 5.1.

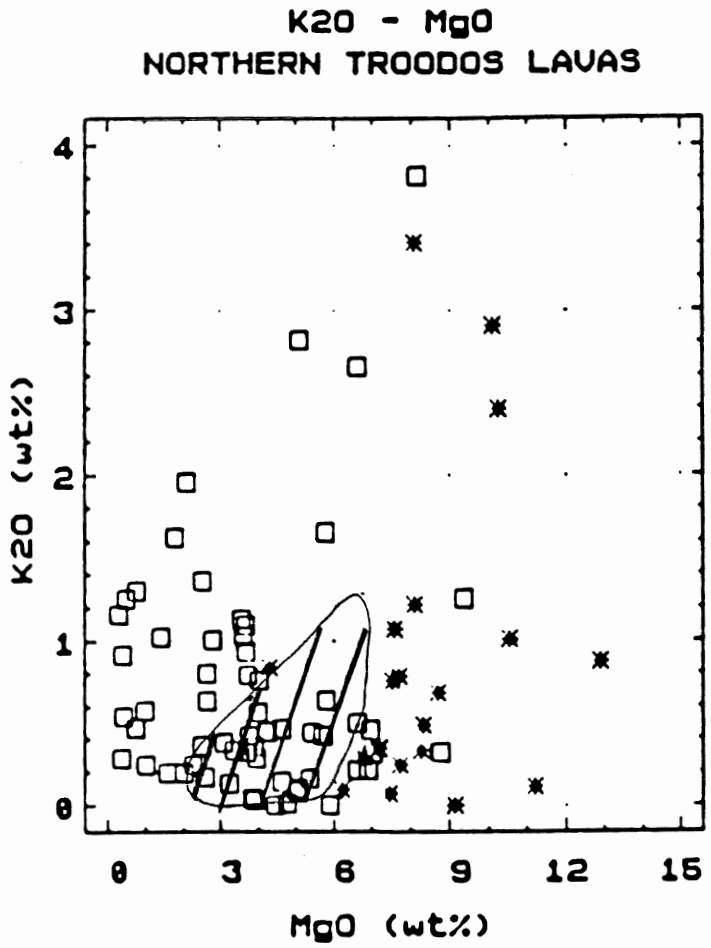

Figure 5.10B. K_2O - MgO variation diagram.
Group A and Group B samples from Mehegan (1988). Symbols as in Figure 5.8B.
Hatched area represents the range of values for this study.

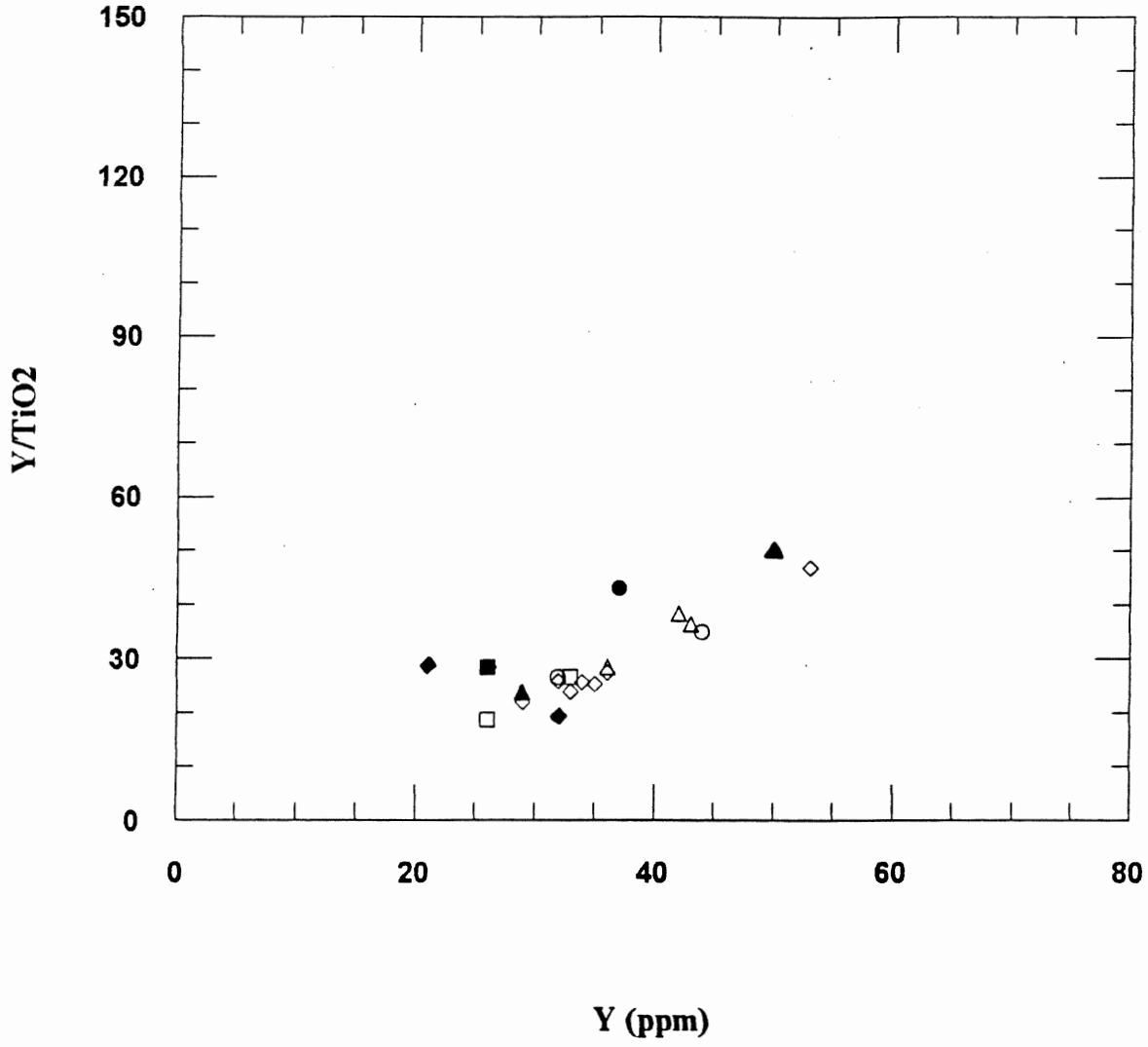

Figure 5.11A. Y/TiO_2 - Y variation diagram.
Samples from this study. Symbols are as follows: open symbols - dike units; closed symbols - screen units; Section 1 - ○ ; Section 2 - □ ; Section 3 - △ ; Section 4 - ◇.

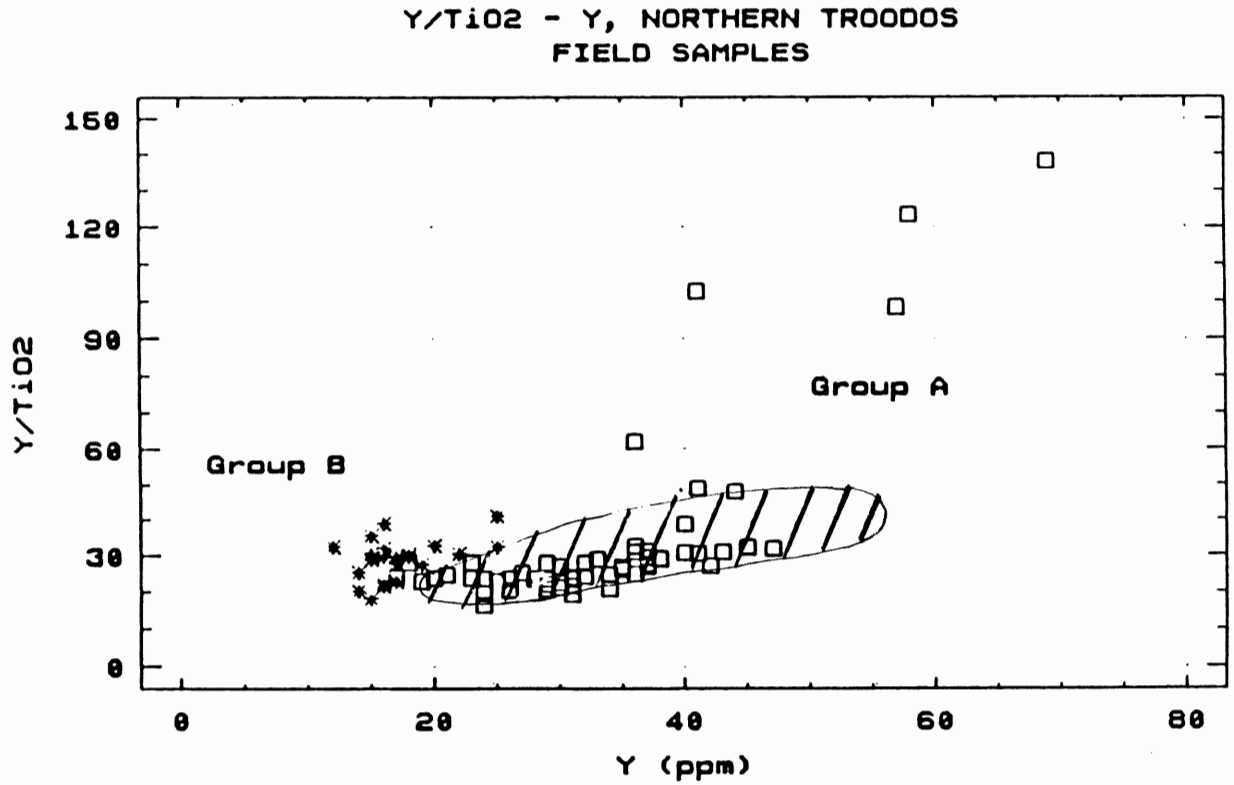

Figure 5.11B. Y/TiO_2 - Y variation diagram.
Group A and Group B samples from Mehegan (1988). Open boxes - Group A; stars - Group B. Hatched area represents the range of samples from this study.

defines a positive linear trend. Screen units 19, 24, 29, and 32 are at the lower end of the distribution and screen units 14 and 22 at the upper end. A group of dike units occurs between values of Zr from 65 to 75 ppm and of Zr/TiO_2 from 48 to 65. The trend of the values closely follows that described by Mehegan (1988) for the Magma Group A samples (Fig. 5.12B).

The Zr/Y versus Zr plot, (Fig. 5.13A), shows that the values of Zr range from 40 to 117ppm and Zr/Y from 2 to 2.7. The parameters show a positive correlation. Screen units 19, 24, and 29 lie at the lower end, and 14 and 22 at the upper end of the distribution. Screen unit 32 occurs within the dike unit group with Zr from 65 to 75 ppm and Zr/Y from 2 to 2.5. The range of values falls in the upper part of the Magma Group A range of Mehegan (1988) (Fig. 5.13B).

The compatible transition elements, Cr, Ni, V, and Zn, show a variety of relationships with Zr. On a Zr versus Cr plot values fall in the range of Zr 40 to 117 ppm and of Cr from <5 to 15 ppm (Fig. 5.14A). Values are scattered throughout this range, with the majority restricted to the low Cr end. Screen units 19, 24, and 29 are at the lower end of the Cr distribution, and units 14 and 22 are at the upper end. Screen unit 32 is situated within the dike unit group noted earlier. The Cr-Zr range follows and spans the trend found by Mehegan (1988) for the North Troodos Group A lavas (Fig. 5.14B).

On a Ni-Zr plot,(Fig. 5.15A) the values fall in the range of Zr from 40 to 117 ppm and of Ni from <5 to 23 ppm. A linear relationship with negative slope

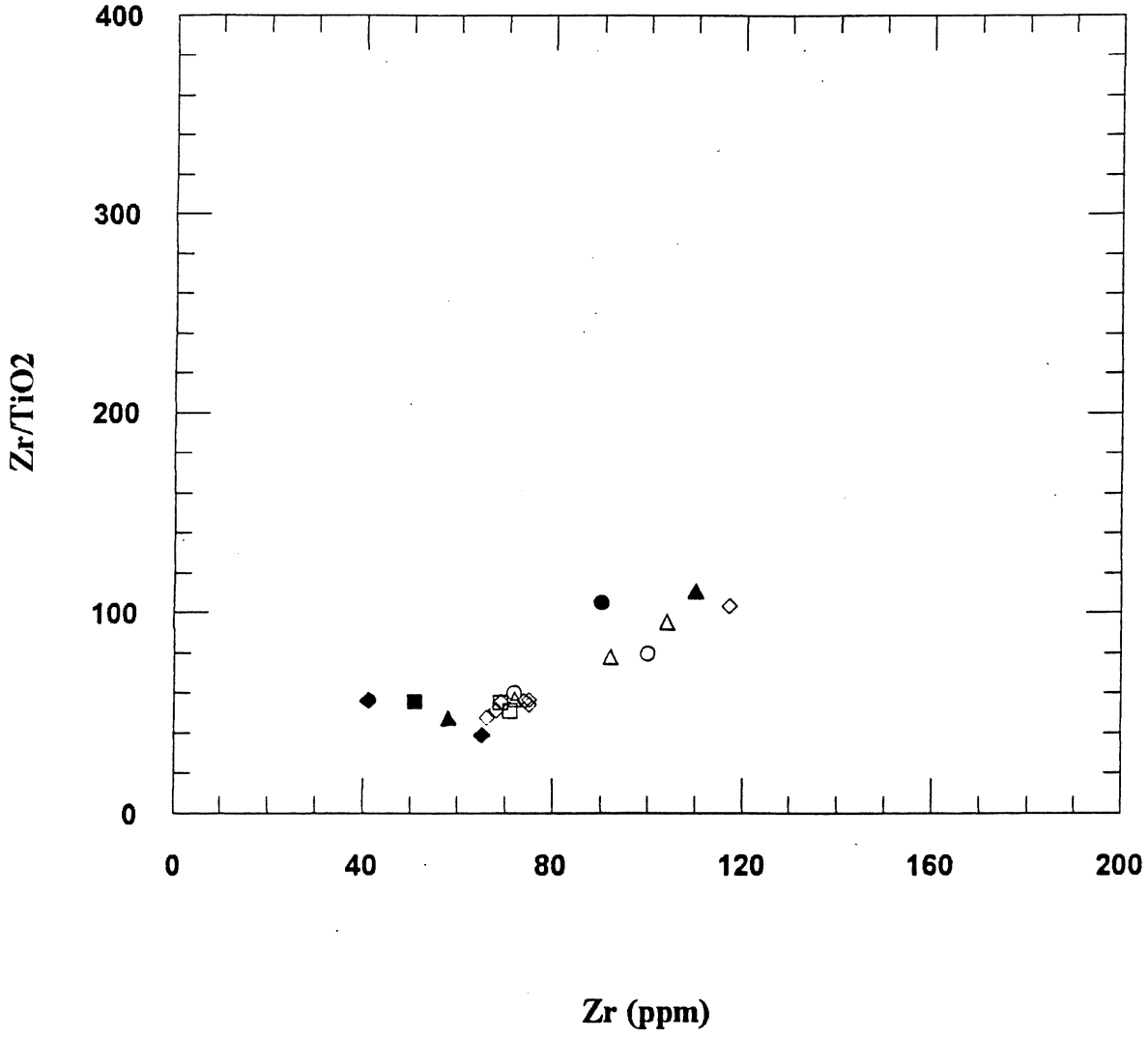

Figure 5.12A. Zr/TiO_2 - Zr variation diagram.
Samples from this study. Symbols are as in Figure 5.11A.

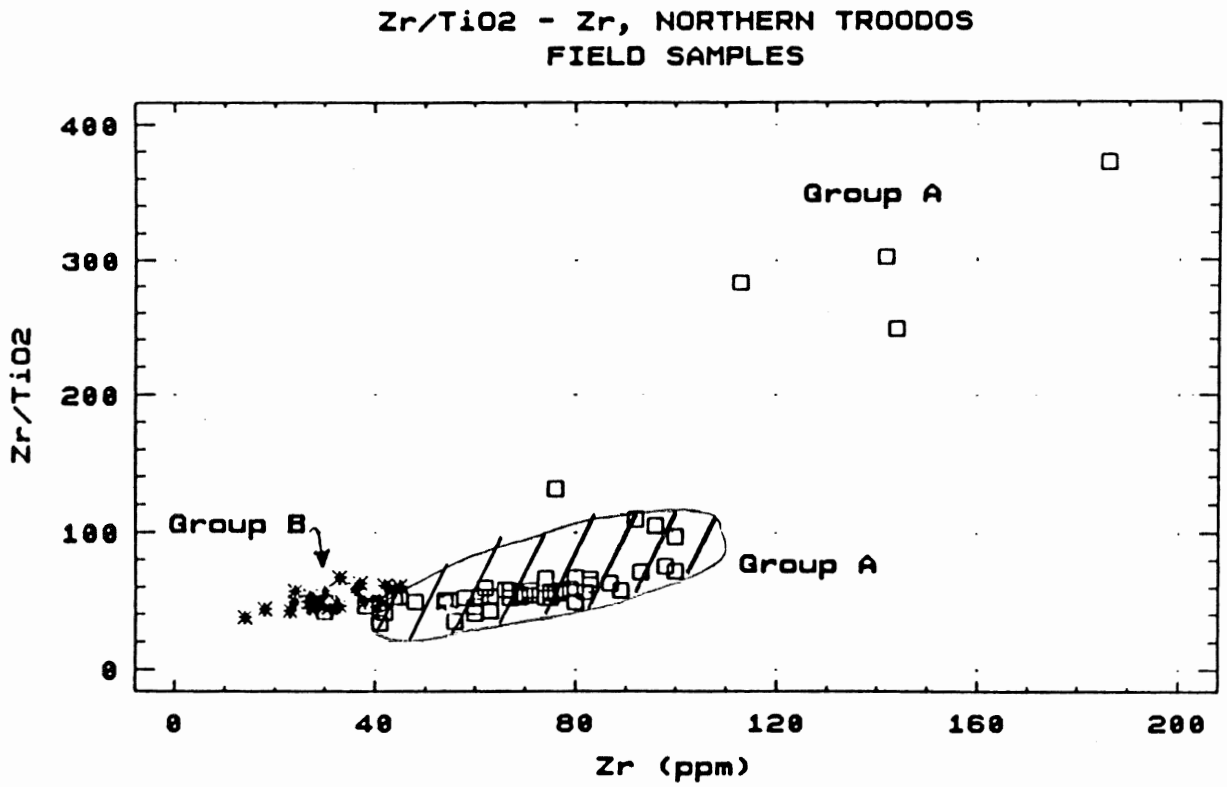

Figure 5.12B. Zr/TiO_2 - Zr variation diagram.
Group A and Group B samples from Mehegan (1988). Open boxes - Group A; stars - Group B. Hatched area represents the range of samples from this study.

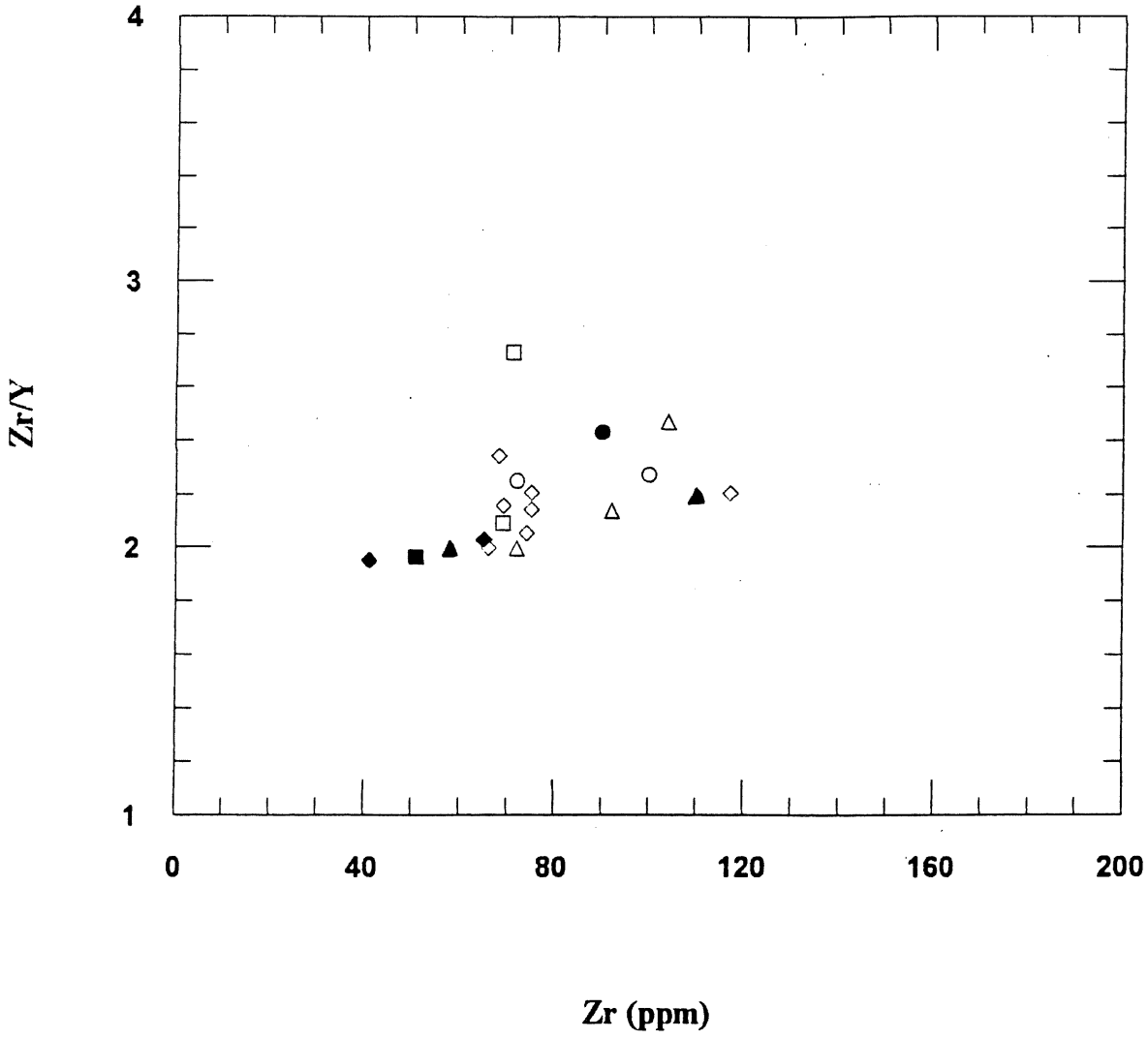

Figure 5.13A. Zr/Y - Zr variation diagram.
Samples from this study. Symbols as in Figure 5.11A.

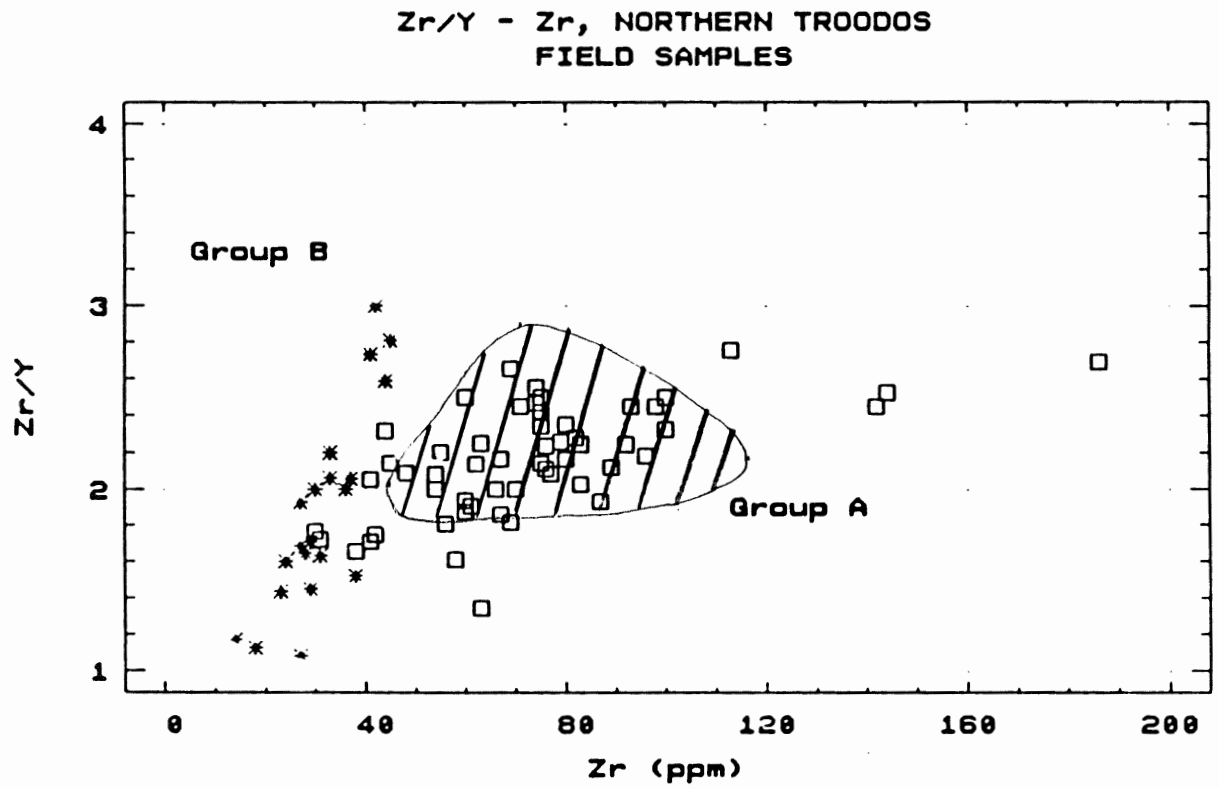

Figure 5.13B. Zr/Y - Zr variation diagram.
Group A and Group B samples from Mehegan (1988). Open boxes - Group A; stars - Group B. Hatched area represents the range of samples from this study.

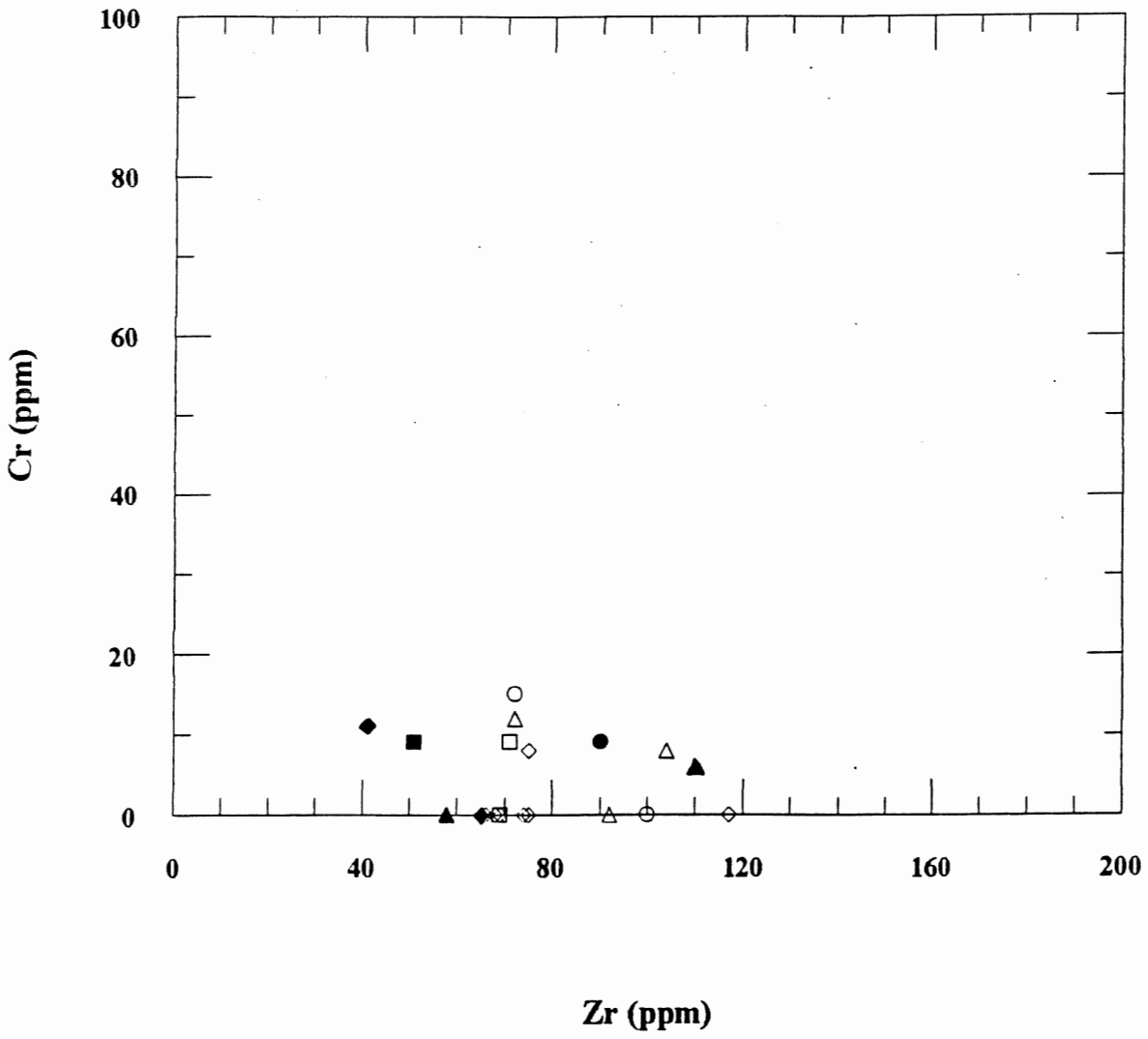

Figure 5.14A. Cr - Zr variation diagram.
Samples from this study. Symbols as in Figure 5.11A.

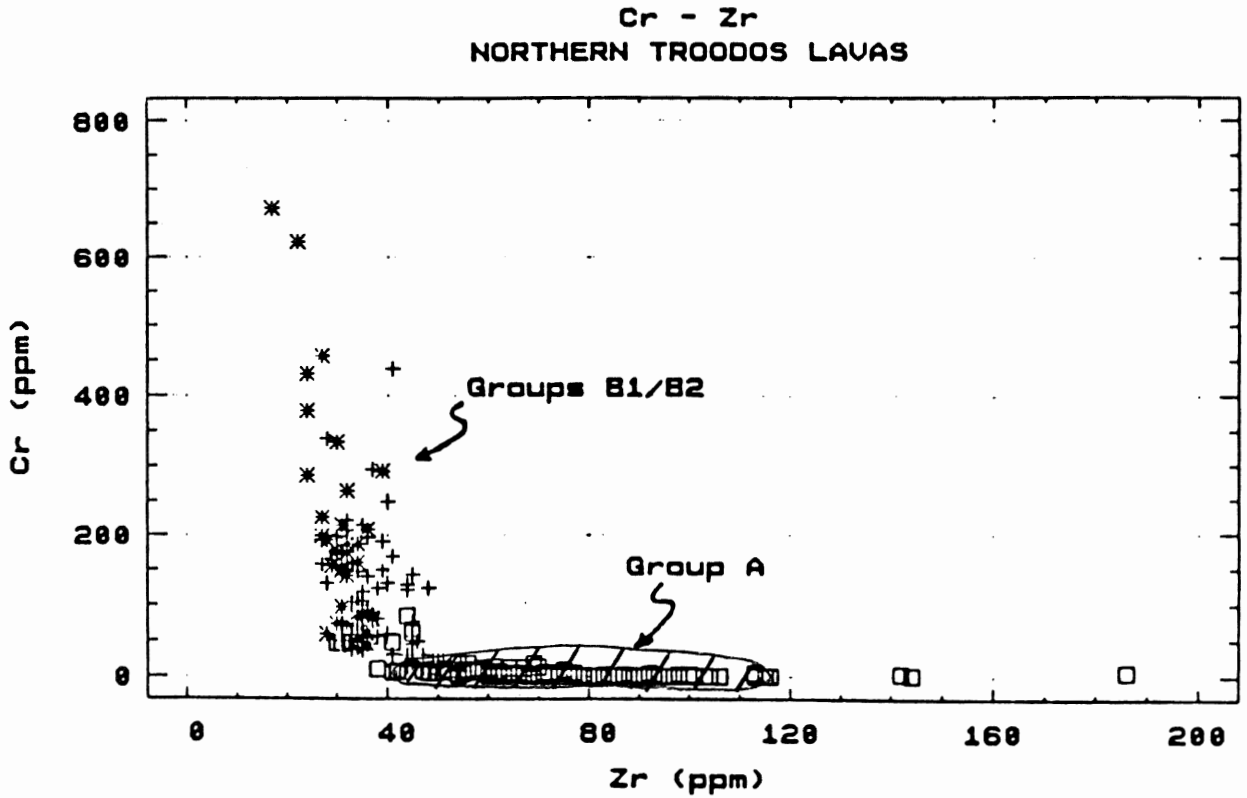

Figure 5.14B. Cr - Zr variation diagram.
Group A and Group B samples from Mehegan (1988). Open boxes - Group A; stars and crosses - Group B1/B2. Hatched area represents the range of samples from this study.

is evident. Screen units 19, 24, and 29 are at the high end of the distribution and screen unit 22 is at the low end. This trend follows and spans the range for the North Troodos Group A lavas (Fig. 5.15B) defined by Mehegan (1988).

On a V versus Zr plot (Fig. 5.16A), values span a range of Zr from 40 to 117 ppm and of V from 75 to 640 ppm. A linear relationship with negative slope is again evident. Screen units 19, 24, and 29 lie at the upper end of the distribution and screen units 14 and 22 are at the lower end. Screen unit 32 is located in the dike unit group defined by Zr from 65 to 75 ppm and V from 375 to 550 ppm. Using the V-Zr relationship, Mehegan (1988) defined a fractionation trend for the Magma Group A lavas. This trend is followed very closely by the samples from this study (Fig. 5.16B).

On a Zn-Zr plot the values of Zr range from 40 to 117 ppm and of Zn from 75 to 250 ppm (Fig. 5.17A). Values are scattered throughout the range, with samples from Section 4 (units 25-33) tending to have lower Zn values. With the exception of unit 32, values for the screen units are located on the periphery of the distribution. The pattern shown in Figure 5.17A falls within the higher part of the range for Magma Group A of Mehegan (1988) (Fig. 5.17B). The higher values of Zn for the screens may be related to their macroscopically visible sulphide mineralization (Fig. 4.3A).

On a Sr-Zr plot values of Zr range from 40 to 117 ppm and of Sr from 70 to 130 ppm. A linear relationship with positive slope is evident in Figure 5.18A. With the exception of unit 32, the screen units lie on the periphery of

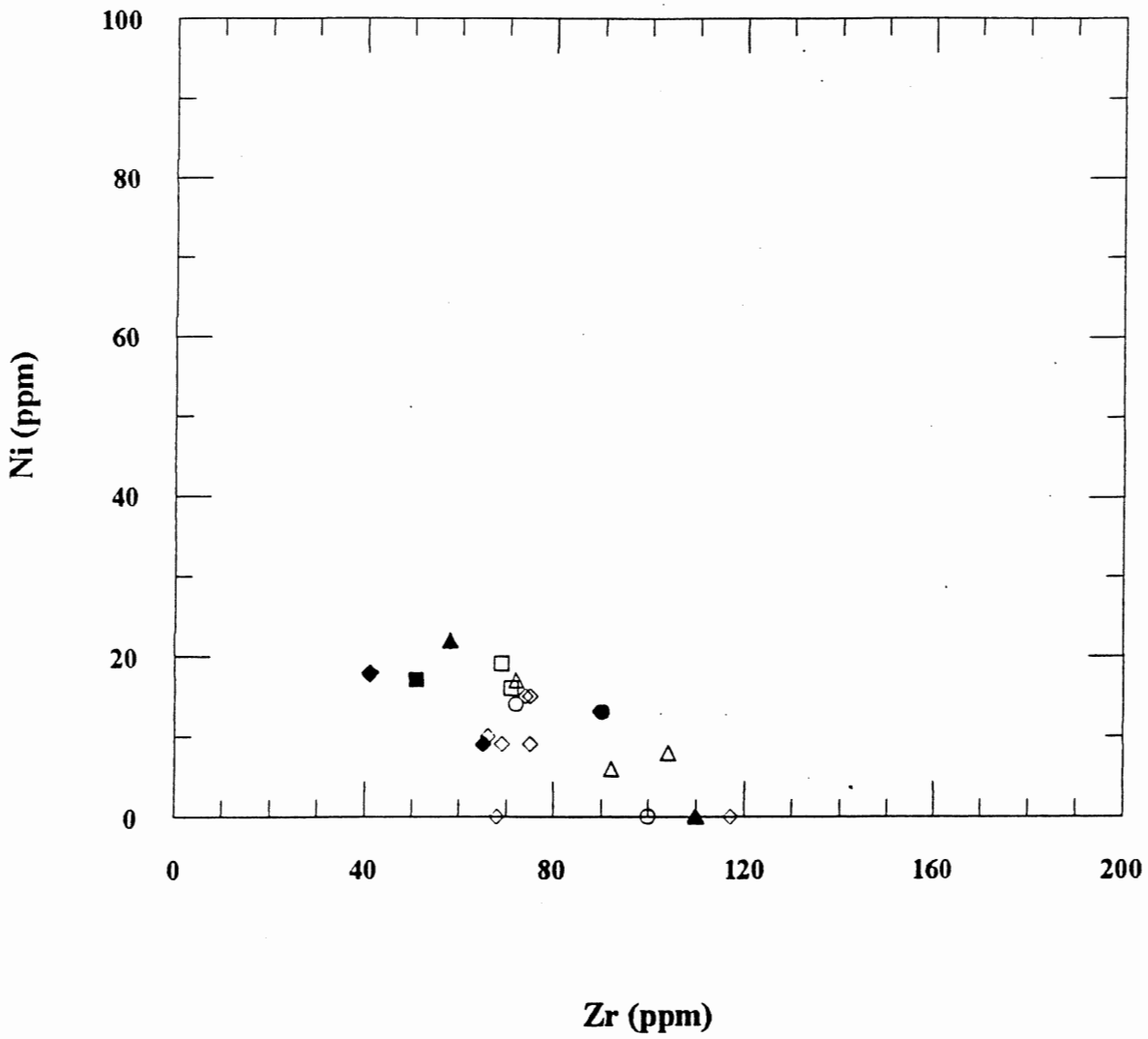

Figure 5.15A. Ni - Zr variation diagram.
Samples from this study. Symbols as in Figure 5.11A.

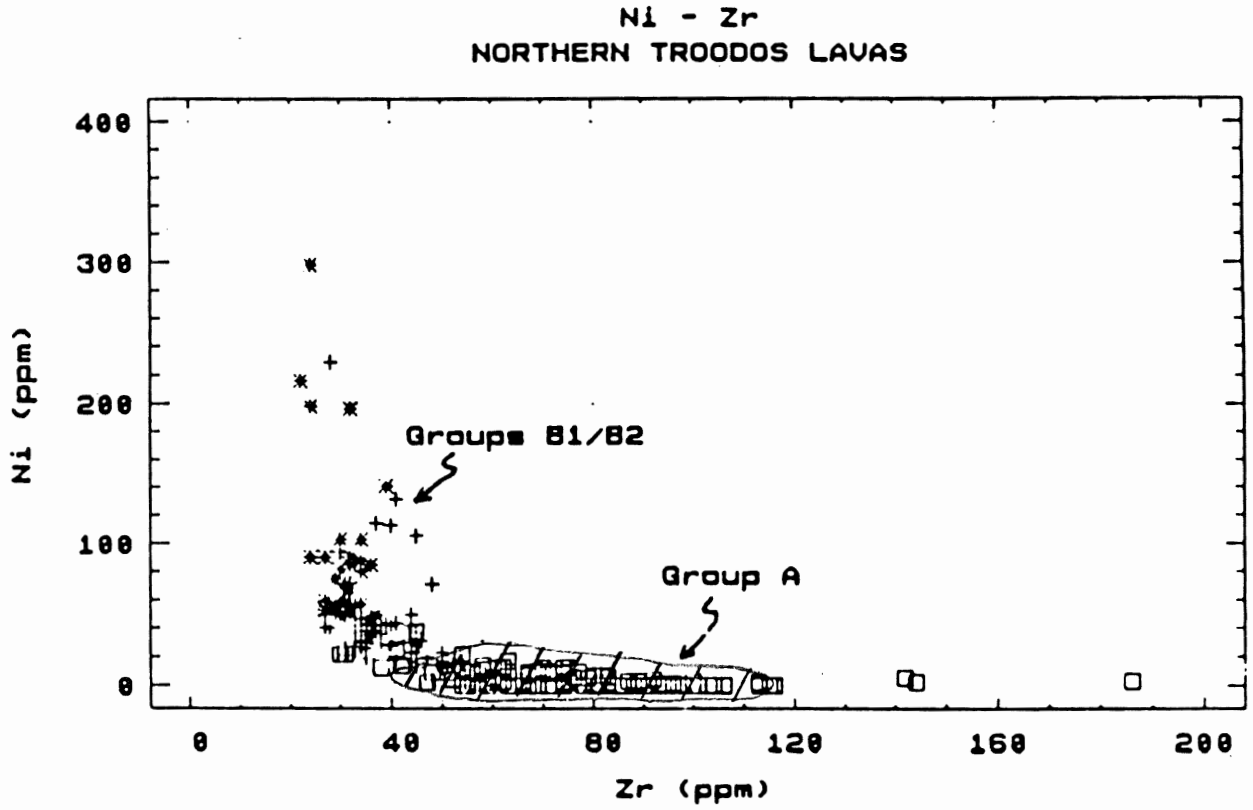

Figure 5.15B. Ni - Zr variation diagram.
Group A and Group B samples from Mehegan (1988). Symbols as in Figure 5.14B.
Hatched area represents the range of samples from this study.

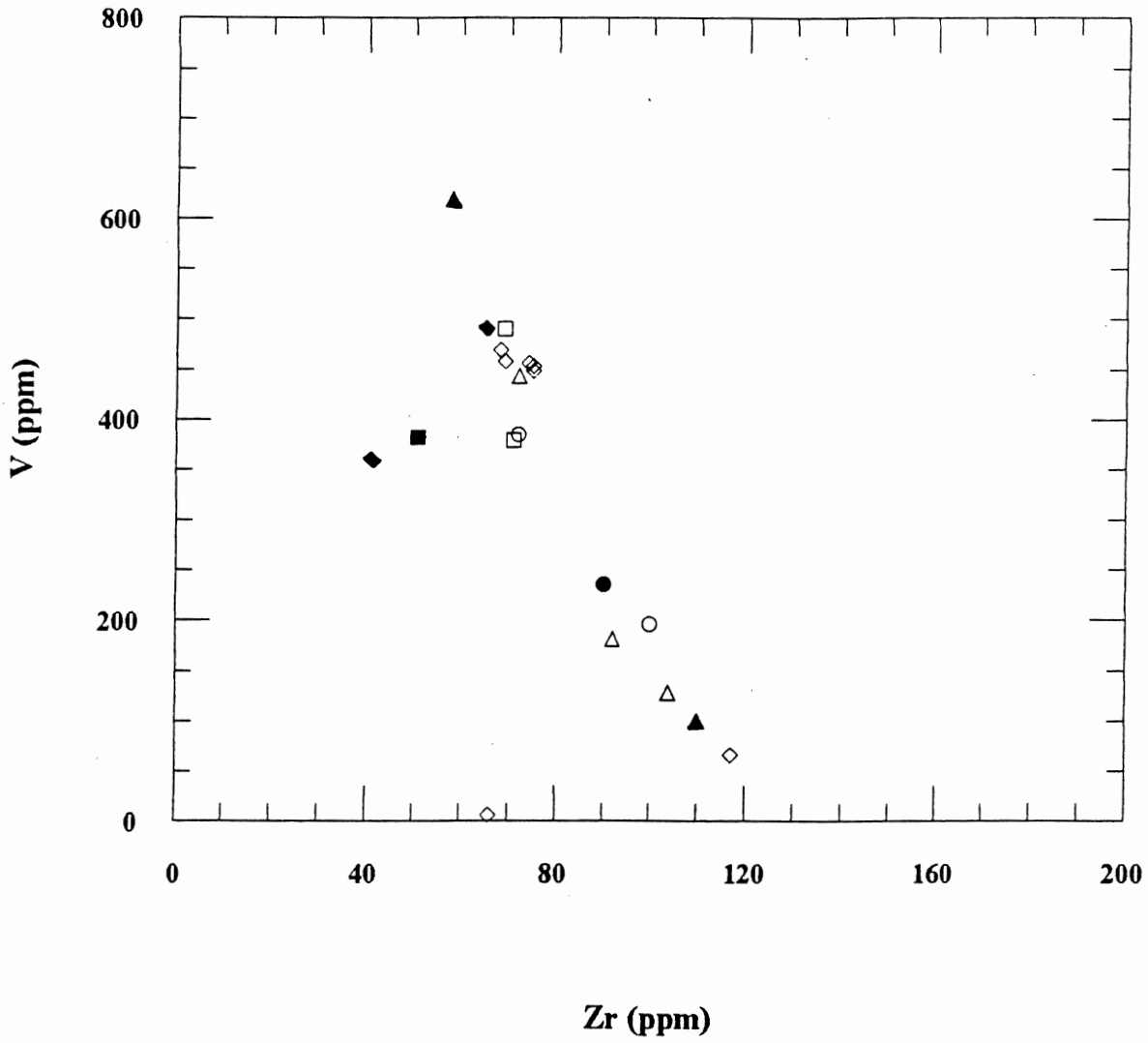

Figure 5.16A. V - Zr variation diagram.
Samples from this study. Symbols as in Figure 5.11A.

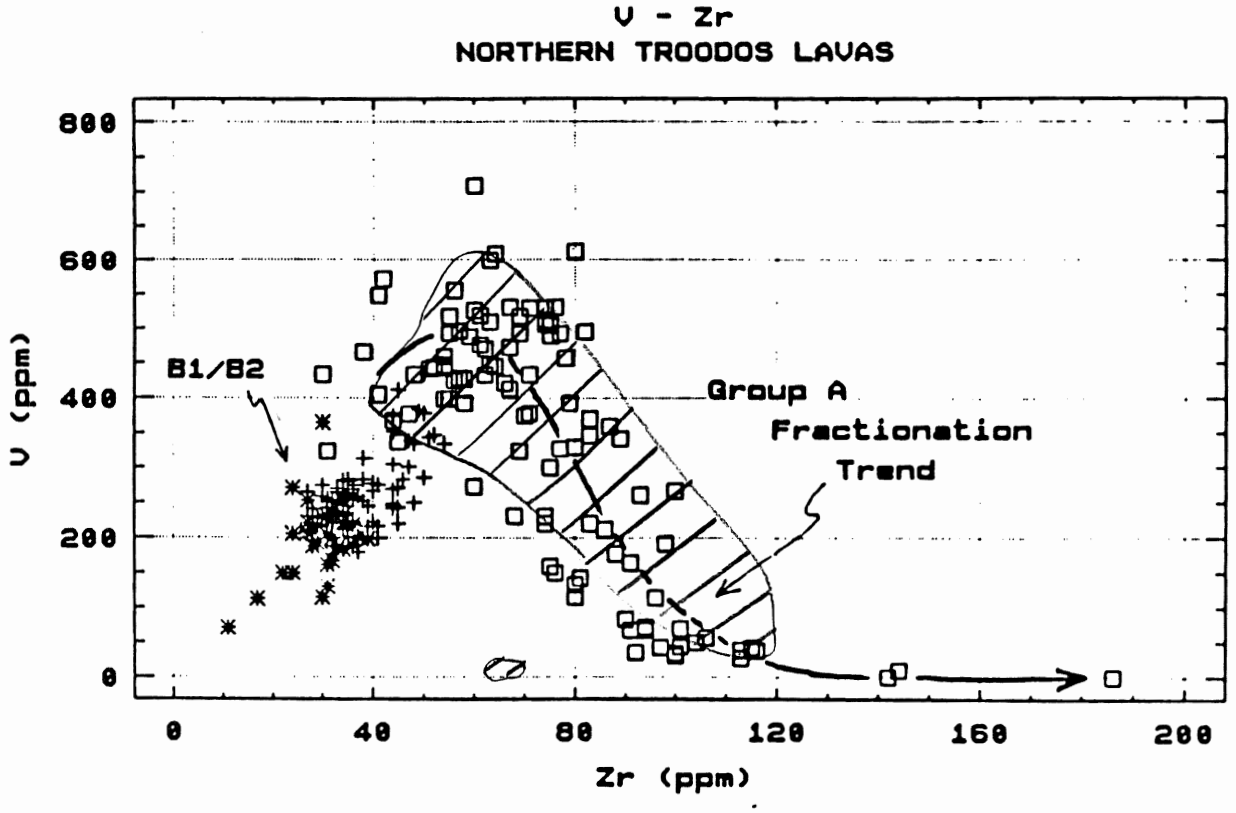

Figure 5.16B. V - Zr variation diagram.
Group A and Group B samples from Mehegan (1988). Symbols as in Figure 5.14B.
Hatched area represents the range of samples from this study.

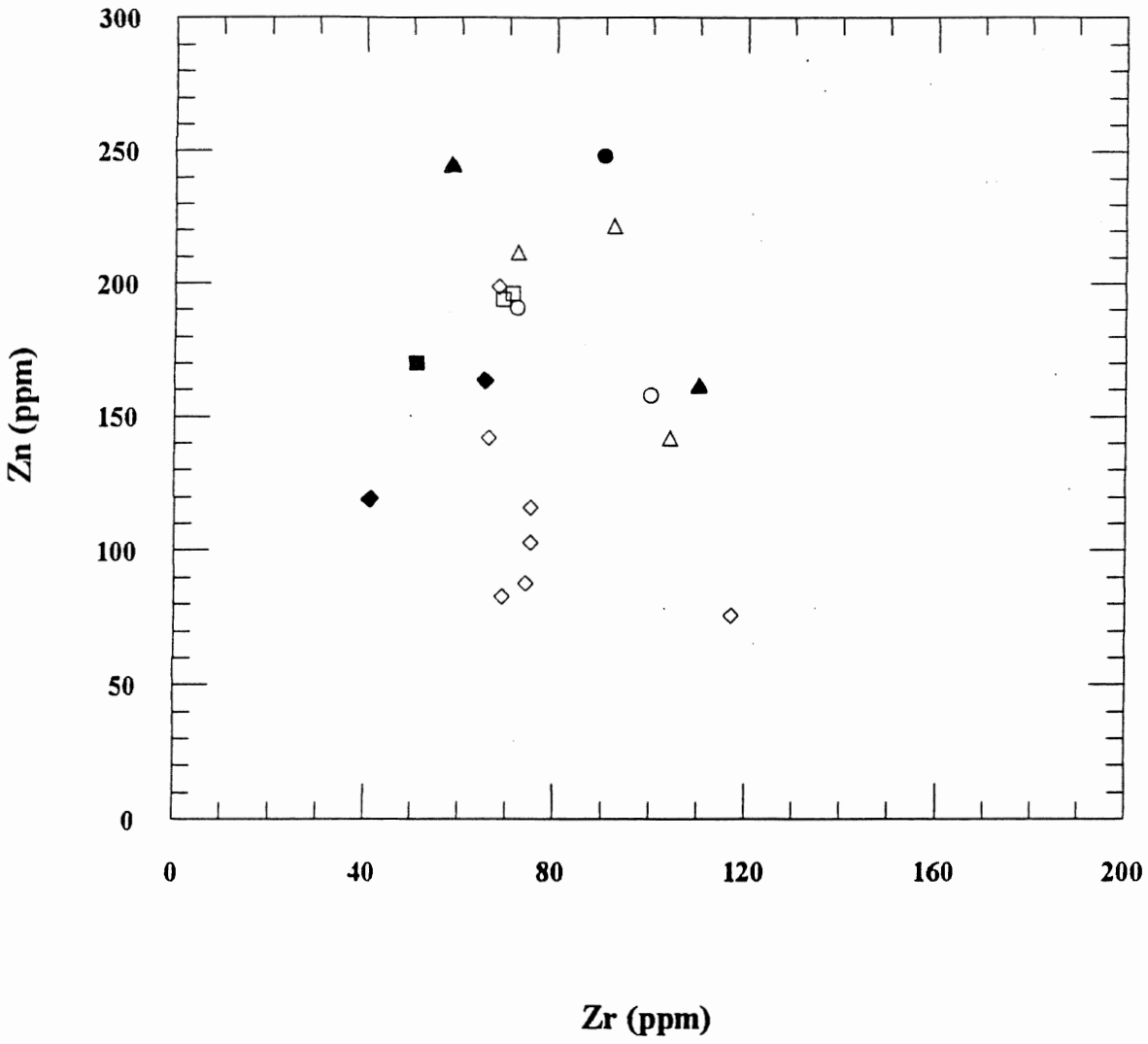

Figure 5.17A. Zn - Zr variation diagram.
Samples from this study. Symbols as in Figure 5.11A.

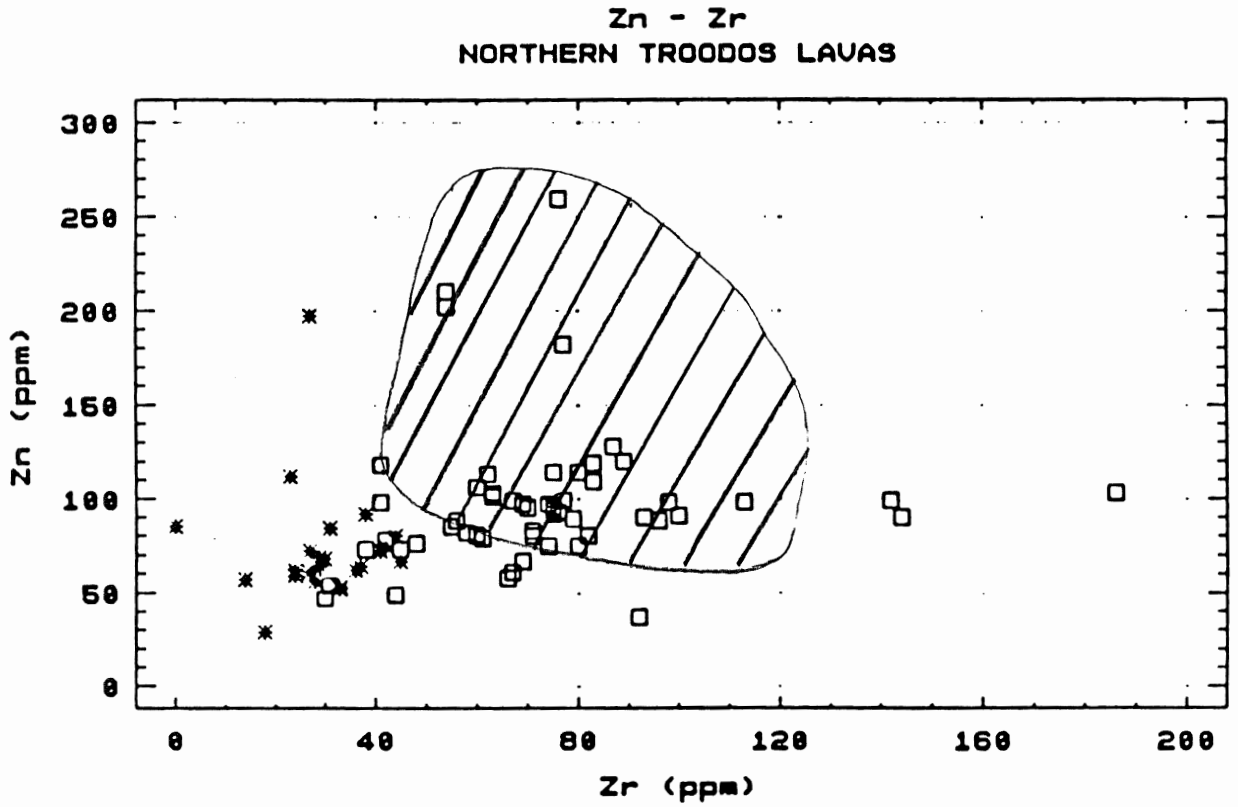

Figure 5.17B. Zn - Zr variation diagram.
Group A and Group B samples from Mehegan (1988). Open boxes - Group A; stars - Group B. Hatched area represents the range of samples from this study.

the field. Values follow closely the trend shown in Figure 5.18B for Magma Group A established by Mehegan (1988).

Values of Sr and Ba are scattered within a range of Sr from 70 to 130 ppm and of Ba from 10 to 50 ppm (Fig. 5.19A). Although the values are scattered there is an increase of Ba with Sr. Screen units 14, 19, and 29 lie at the lowest end of the distribution, with screen 22 at the highest end. Screen units 24 and 32 are intermediate in the distribution as are the dike units. The distribution of values corresponds closely with that of Magma Group A by Mehegan (1988) (Fig. 5.19B).

The values plotted for Rb-Sr lie along the Rb <5 interval in a Sr range from 70 to 130 ppm (Fig. 5.20A). The values from this study correspond to the lower values for Mehegan's Group A shown in Figure 5.20B. The low Rb values from this study are possibly the result of hydrothermal alteration.

5.4 Summary

With the use of major element whole-rock geochemistry, the samples from the Argaki canyon fall in Group A, a tholeiitic sequence defined by Mehegan (1988). Group A forms a continuous sequence of basalt-basaltic andesite-andesite-dacite-rhyodacite. Although the samples fit into the Group A sequence, they only occupy the basalt-basaltic andesite-andesite portion of the sequence with no apparent discontinuity in their distribution over this interval.

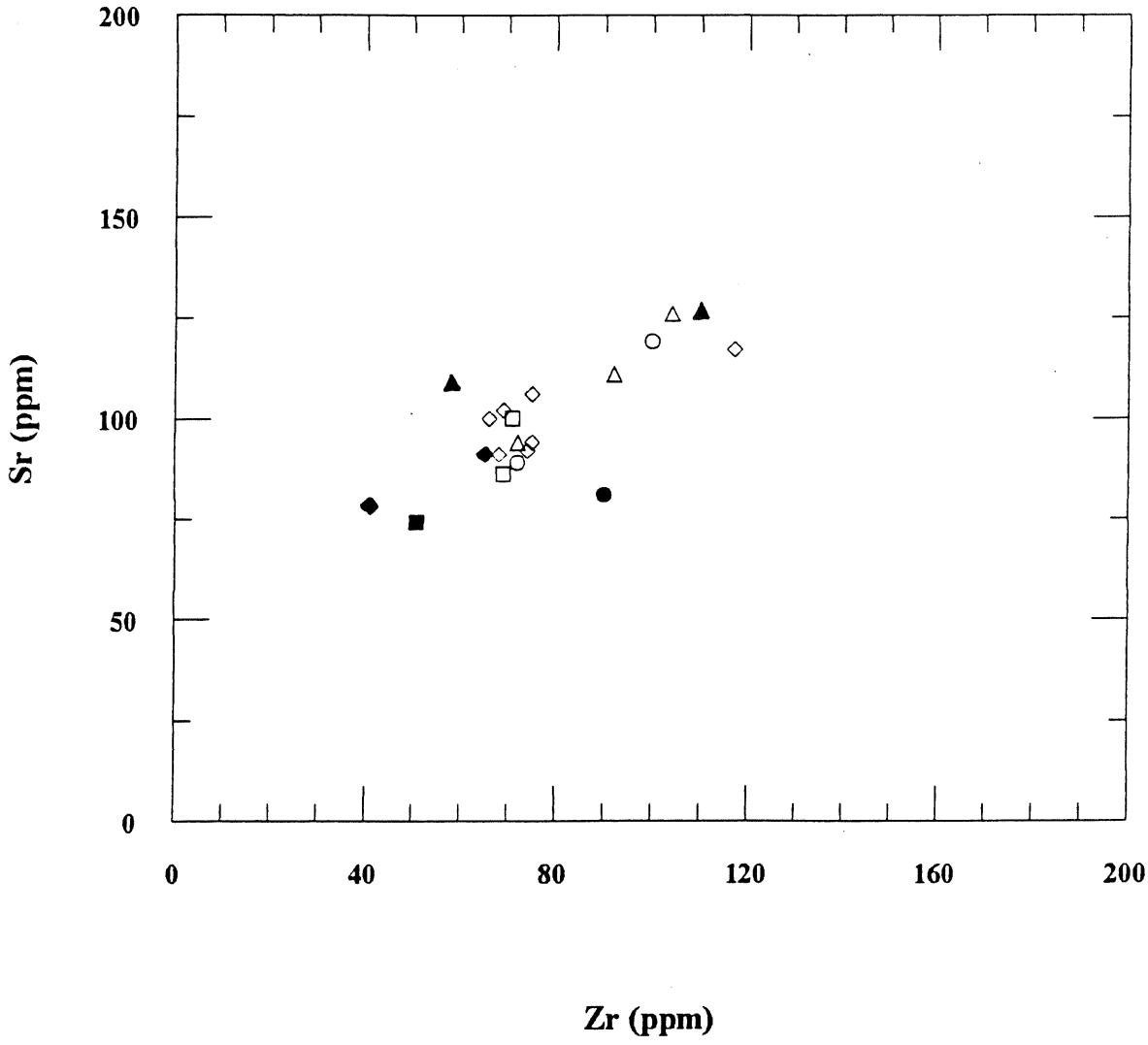

Figure 5.18A. Sr - Zr variation diagram.
Samples from this study. Symbols as in Figure 5.11A.

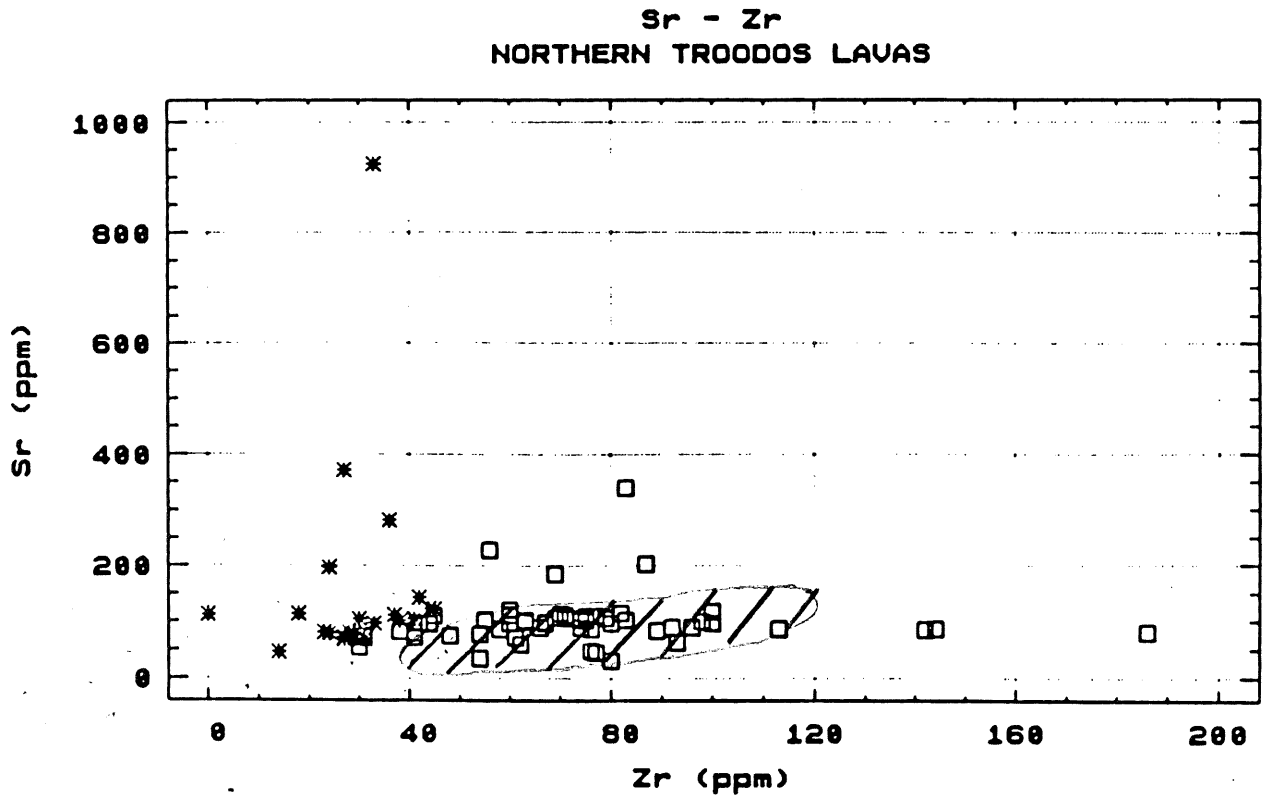

Figure 5.18B. Sr - Zr variation diagram.
Group A and Group B samples from Mehegan (1988). Symbols as in Figure 5.17B.
Hatched area represents the range of samples from this study.

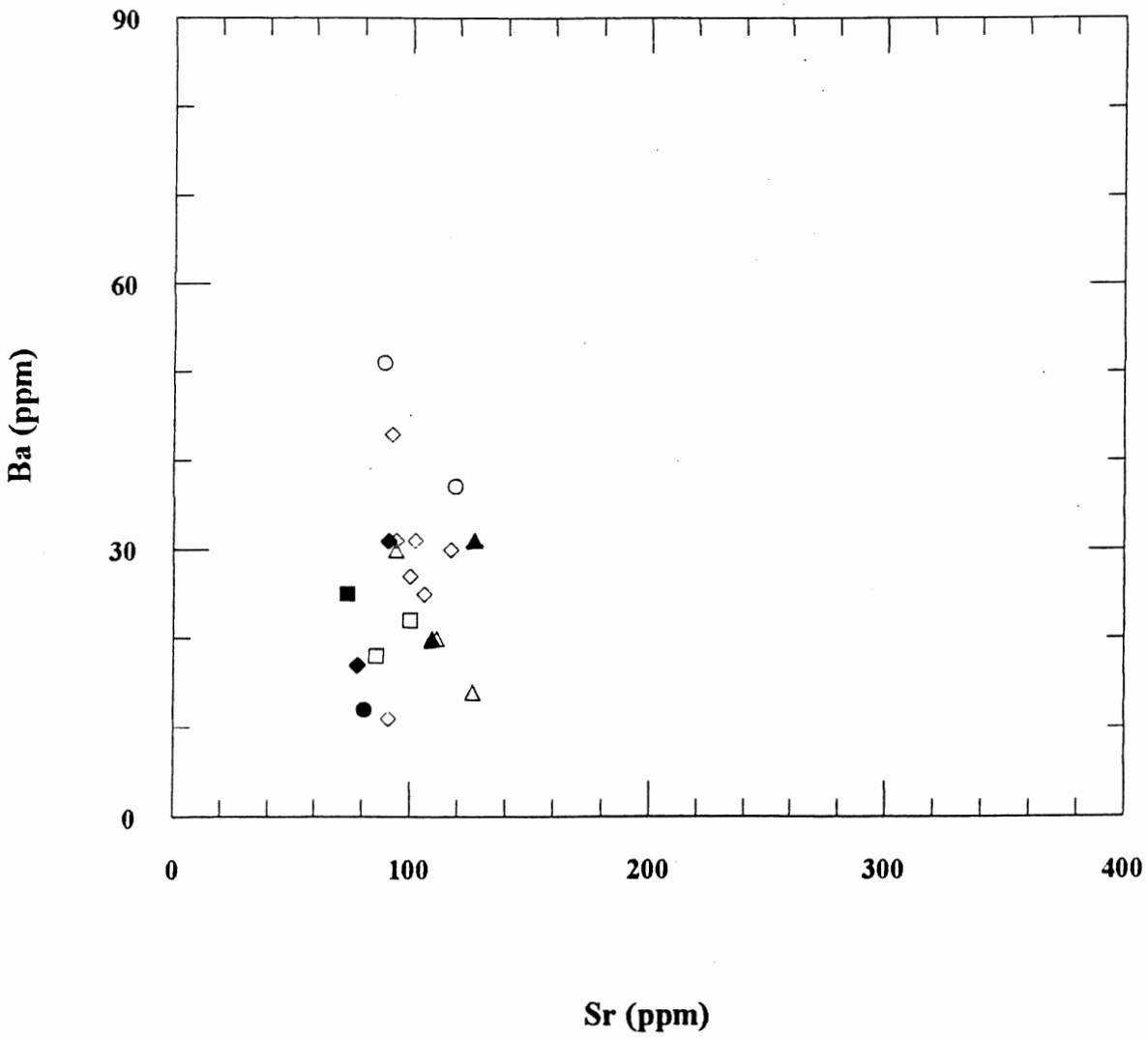

Figure 5.19A. Ba - Sr variation diagram.
Samples from this study. Symbols as in Figure 5.11A.

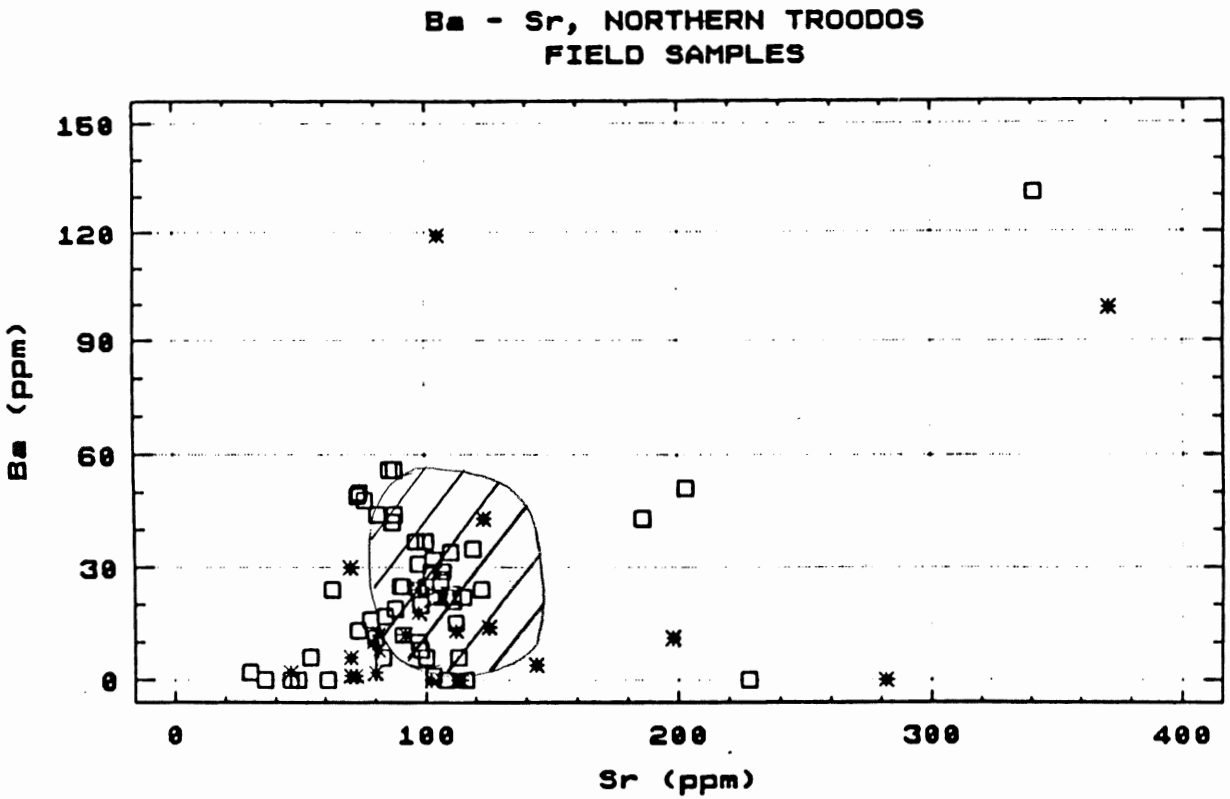

Figure 5.19B. Ba - Sr variation diagram.
Group A and Group B samples from Mehegan (1988). Symbols as in Figure 5.17B.
Hatched area represents the range of samples from this study.

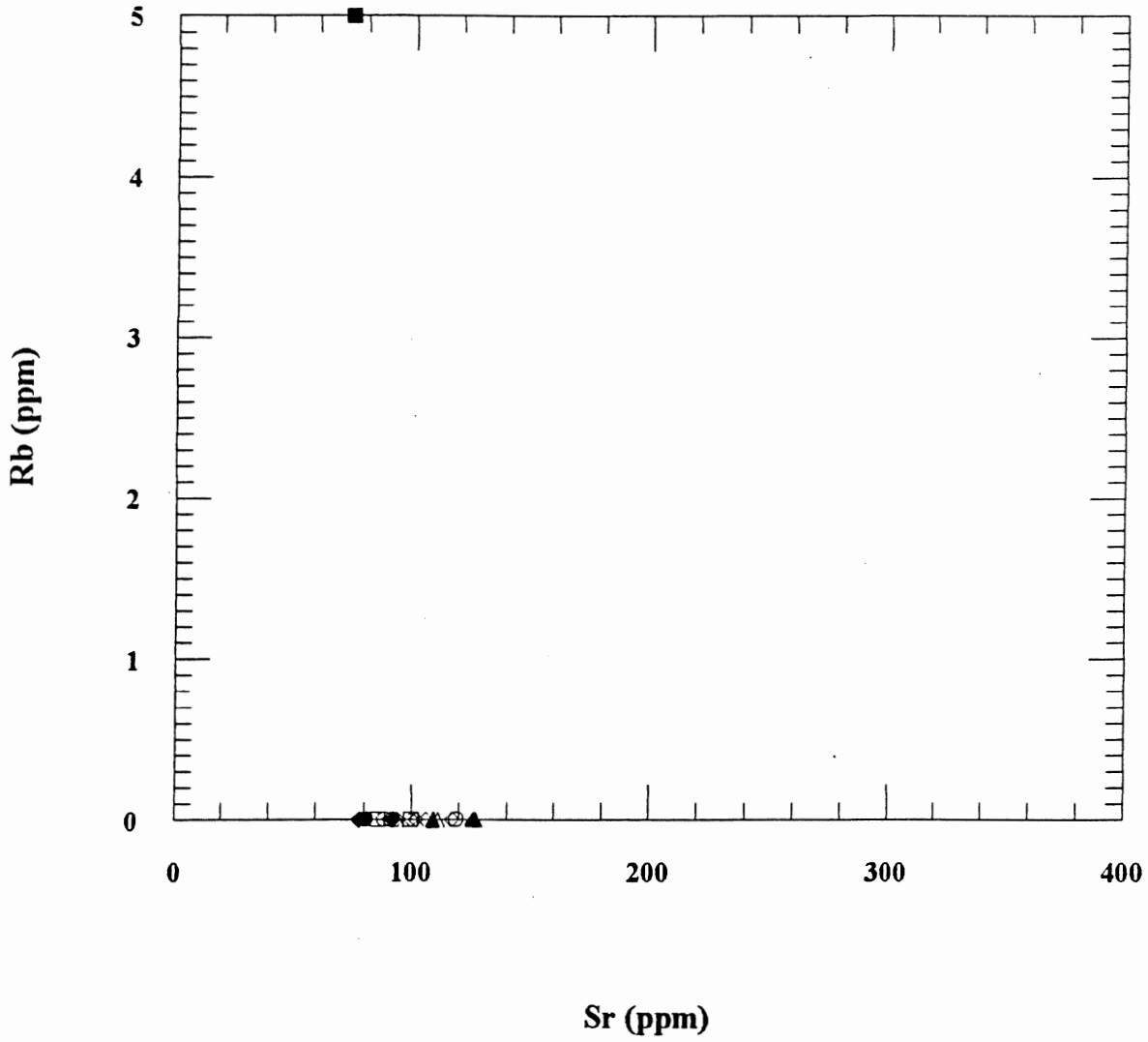

Figure 5.20A. Rb - Sr variation diagram.
Samples from this study. Symbols as in Figure 5.11A. Value at zero really <5 because 5ppm is the detection limit.

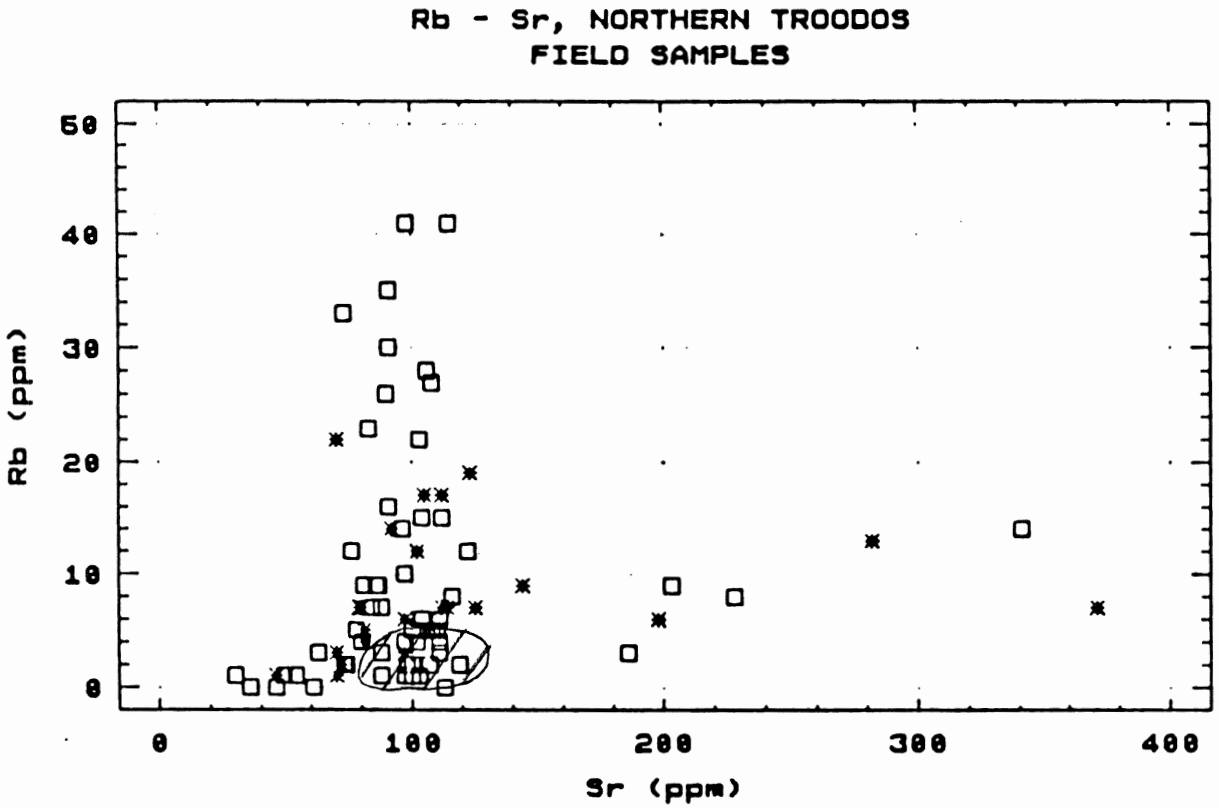

Figure 5.20B. Rb - Sr variation diagram.
Group A and Group B samples from Mehegan (1988). Symbols as in Figure 5.17B.
Hatched area represents the range of samples from this study.

The close agreement of the trace element values for this study with those found by Mehegan for Magma Group A also lead to the conclusion that the samples from this study occur in one magma series.

CHAPTER 6 DISCUSSION AND CONCLUSIONS

6.1 Summary

Interleaved screen and dike units in the Transition Zone from Extrusives to Sheeted Dikes in the Troodos ophiolite yield the following results:

1) Primary mineralogies are defined as plagioclase and opaque oxides in all of the samples, with clinopyroxene, quartz, olivine, and mesostasis occurring in some samples;

2) Hydrothermal alteration is widespread but never complete. A ubiquitous secondary phase is chlorite. Other secondary phases are albite, alkali feldspar, quartz, epidote, calcite, titanite, sulphides, epidote, and zeolites;

3) Secondary minerals show that the units have experienced hydrothermal alteration corresponding to the lower part of the Transition and/or upper part of the greenschist zone defined by Gillis (1986); and

4) Geochemical results show that the samples from this study are restricted to the Basalt-Basaltic Andesite-Andesite interval of Mehegan's (1988) Magma Group A series.

6.2 Discussion and Conclusions

The results obtained provide some clear answers to the problems posed in the introduction to this thesis, namely whether differences in magnetization of the dike and screen units could be accounted for by differences in primary composition or by differences in secondary alteration.

Marked differences in the magnetization of the dike and screen units has led to further study of the relationship between the magnetization and the nature of the rocks. The results from this investigation show that the differences in magnetization can not be explained by the primary composition of the samples, thus secondary alteration is likely to explain the differences in magnetization of the dike and screen units. However, the possibility of a link between secondary alteration and magnetization has not been demonstrated directly in this thesis. This question could be addressed further through obtaining quantitative information on degree of replacement of primary phases by secondary phases (especially regarding the Fe-Ti oxides) in the dike and screen units.

The main result obtained from the investigation addressed in the thesis implies that the results of the parallel magnetic study are likely to be relevant to the interpretation of the lithological section presented at DSDP/ODP Hole 504B. Both the Troodos ophiolite sequence and DSDP/ODP Hole 504B sequence contain units within restricted and overlapping compositional ranges and have similar alteration styles. In these circumstances, magnetic variations in both sequences are likely to reflect variations of alteration.

6.3 Recommendations for future work

A more detailed investigation into the secondary phases of the samples from the Transition Zone is needed in order to further the investigation of the

magnetic differences. A physical approach (e.g. effective size of parts of units that are in contact with hydrothermal fluids) needs to be taken in investigating the origin of the relationship between alteration and magnetization.

REFERENCES

Alt, J. C., Anderson, T. F., and Bonnell, L. 1989. The geochemistry of sulfur in a 1.3 km section of hydrothermally altered oceanic crust, DSDP Hole 504B. Geochimica et Cosmochimica Acta, 53: 1011-1023.

Alt, J. C., Honnorez, J., Laverne, C., and Emmerman, R. 1986. Hydrothermal Alteration of a 1 km section through the upper oceanic crust, Deep Sea Drilling Project Hole 504B: Mineralogy, chemistry, and evolution of seawater-basalt interactions. Journal of Geophysical Research, 91: 10309-10335.

Alt, J. C., Laverne, C., and Muehlenbachs, K. 1985. Alteration of the upper oceanic crust: Mineralogy and processes in Deep Sea Drilling Project Hole 504B, leg 83. Initial Report of Deep Sea Drilling Project, 83: 217-241.

Bagnall, P. S. 1960. The geology and mineral resources of the Pano Lefkara-Larnaca area. Geological Survey Deptartment Cyprus Memoir 5, 116 pp.

Baragar, W. R. A., Lambert, M. B., Baglow, N., and Gibson, I. L. 1990. The sheeted dike zone in the Troodos ophiolite. In: Malpas, J., Moores, E., Panayiotou, A., and Xenophontos, C., (eds.), Ophiolites, Oceanic Crustal Analogues, Proceedings of the Symposium "Troodos 1987", Cyprus, p. 37-52.

Baroz, F. 1977. Observation nouvelles sur l'Eocene de la Chaine de Kyrenia (Chypre). Bulletin de la Societe Geologique de France, 18: 429-437

Baroz, F., Desmet, A., and LaPierre, H. 1976. Les traits dominants de la geologie de Chypre. Bulletin de la Societe Geologique de France, 18: 429-437.

Baroz, F., Desmet, A., and LaPierre, H. 1975. Trois familles volcaniques pre-orogeniques a Chypre: Comparison et discussion geotectonique. 3e. Reunion annual Scientifique de la Terre, Monpellier, 126 pp.

Bear, L. M. 1960. The geology and mineral resources of the Akaki Lythrodonda area. Geological Survey Department Cyprus, Memoir 3, 122pp.

Becker, K. et al. 1989. Drilling Deep into the Young Oceanic Crust, Hole 504B, Costa Rica Rift. Reviews of Geophysics, 27: 79-102.

Biju-Duval, B., LaPierre, H., and Letouzey, J. 1976. Is the Troodos Massif (Cyprus) allochthonous? Bulletin de la Societe Geologique de France, 18: 1347-1356.

Carr, J. M. and Bear, L. M. 1960. The geology and mineral resources of the Peristerona-Lagoudhera area. Geological Syrvey Department Cyprus, Memoir 2, 79 pp.

Constantinou, G. 1980. Metallogenesis associated with the Troodos ophiolite. In: Panayiotou, A., (ed.), Ophiolites, Proceedings, International Ophiolite Symposium, Cyprus 1979. Ministry of Agriculture and Natural Resources, Geological Survey Department, p. 663-674.

Constantinou, G. 1976. Genesis of the conglomerate structure, porosity and collomorphic textures of the massive sulphide ores of Cyprus. In: Strong, D. J., (ed.), Metallogeny and Plate Tectonics, Geological Association of Canada Special Paper, 14: 187-210.

Cox, K.G., Bell, J. D., and Pankhurst, R. J. 1979. The Interpretation of Igneous Rocks. London: George, Allen and Unwin.

Desmons, J., Delaloye, M., Desmet, A., Gagny, C., Rocci, G., and Voldet, P. 1980. Trace and rare earth element abundances in Troodos lavas and sheeted dikes, Cyprus. Ofioliti, 5: 35-56.

Dilek, Y., Thy, P., Moores, E. M., and Ramsden, T. W. 1990. Tectonic evolution of the Troodos Ophiolite within Tethyan framework. Tectonics, 9: 811-823.

Gass, I. G. 1960. The geology and mineral resources of the Dhali area. Geological Survey Department Cyprus, Memoir 4, 116 pp.

Gass, I. G. 1980. The Troodos Massif: Its role in the unravelling of the understanding of constructive plate margin processes. In: Panayiotou, A., (ed.), Ophiolites, Proceedings, International Ophiolite Symposium, Cyprus 1979. Ministry of Agriculture and Natural Resources, Geolological Survey Department, p. 23-35.

Gass, I. and Smewing, J. D. 1973. Intrusion, extrusion and metamorphism at constructive margins: Evidence from the Troodos Massif, Cyprus. Nature 242: 26-29.

Gillis, K. M. 1986. Multistage alteration of the extrusive sequence, Troodos Ophiolite, Cyprus. Unpublished Ph.D. Thesis, Dalhousie University, Halifax, Nova Scotia, Canada, 387 pp.

Gillis, K. M. and Robinson, P. T. 1988. Distribution of alteration zones in the upper oceanic crust. Geology, 16: 262-266.

Gillis, K. M. and Robinson, P. T. 1990. Multistage alteration in the extrusive sequence of the Troodos ophiolite, Cyprus. In: Malpas, J., Moores, E., Panayiotou, A., and Xenophontos, C., (eds.), Ophiolites, Oceanic Crustal Analogues, Proceedings of the Symposium "Troodos 1987", Cyprus, p 655-664.

Govett, G. J. S. and Pantazis T. M. 1971. Distribution of Cu, Zn, Ni, and Co in the Troodos Pillow Lava series, Cyprus. Transactions of the Institute of Mining and Metallurgy, (section B), 80: 285-308.

Hall, J. M., Walls, C. C., Yang, J., Hall, S. L., & Bakor, A. R. 1991. The magnetization of oceanic crust: contribution to knowledge from the Troodos, Cyprus, ophiolite. Canadian Journal of Earth Science, 28: 1812-1826.

Honnorez, J., Laverne, C., Hubberten, H.-W., Emmerman, R., and Muehlenbachs, K. 1983. Alteration processes in layer 2 basalts from Deep Sea Drilling Project hole 504B, Costa Rica Rift. Initial Report of Deep Sea Drilling Project, 69: 509-546.

Irvine, T. N., and Baragar, W. R. 1971. A guide to the chemical classification of the common volcanic rocks. Canadian Journal of Earth Science, 8: 523-548.

LaPierre, H. 1975. Les formations sedimentaires et eruptive des nappes de Mamonia et leurs relations avec le Massif de Troodos (Chypre occidentale). Memoir de la Societe Geologique de France, 123: 132pp.

Leg 140 Shipboard Scientific Party. 1992. ODP Drills Deepest Hole in Oceanic Crust. EOS (American Geophysical Union), 73: 537 & 539-540.

Malpas, J. and Langdon, G. 1984. Petrology of the upper pillow lava suite, Troodos ophiolite, Cyprus. In: Gass, I. G., Lippard, S. J., and Shelton, A. W., (eds.), Ophiolites and oceanic lithosphere. Blackwell Scientific Publications, Oxford, p. 155-167.

Malpas, J., Brace, T., and Dunsworth, S. M. 1989. Structural and petrologic relationships of the CY-4 drill hole of the Cyprus Crustal Study Project. In: Gibson, I. L., Malpas, J., Robinson, P. T., and Xenophontos, C., (eds.), Cyprus Crustal Study Project: Initial Report, Kole Cy-4, Geological Survey of Canada, Paper 88-9: 39-67.

Mehegan, J. 1988. Temporal, spatial, and chemical evolution of the Troodos Ophiolite lavas, Cyprus: Supra-subduction zone volcanism in the Tethys Sea. Unpublished Ph.D. Thesis. Dalhousie University, Halifax, Nova Scotia, Canada. 700 pp.

Mehegan, J. and Robinson, P. T. 1985. Lava compositions of the Troodos Ophiolite, Cyprus. EOS (American Geophysical Union Transactions), 66: 1123.

Moores, E. M., Robinson, P. T., Malpas, J., and Xenophonotos, C. 1984. Model for the origin of the Troodos massif, Cyprus, and other mideast ophiolites. Geology, 12: 500-503

Morin, R. H., Anderson, R. N., and Barton, C. A. 1989. Analysis and interpretation of the borehole televiewer log: Information on the state of stress and the lithostratigraphy at Hole 504B. In: Becker, K., Sakai, H., et al. 1989. Proceedings: ODP, Science Results, 111. College Station, Texas (Ocean Drilling Program). p. 109-118.

Mukasa, S. and Ludden, J. 1987. Uranium-lead isotopic ages of plagiogranites from the Troodos ophiolite, Cyprus, and their tectonic significance. Geology, 15: 825-828.

Nicolas, A. 1989. Structures of Ophiolites and Dynamics of Oceanic Lithosphere. Kluwer Academic Publishing.

Panayiotou, A. 1979. Ophiolites, Proceedings, International Ophiolite Symposium, Cyprus 1979. Ministry of Agriculture and Natural Resources, Geological Survey Department, p. 23-35.

Pantazis, T. M. 1967. The geology and mineral resources of the Pharmakas-Kalavasos area. Geological Survey Department Cyprus, Memoir 8, 190 pp.

Robertson, A. H. F. 1977. Tertiary uplift history of the Troodos massif, Cyprus. Geological Society of America Bulletin, 88: 1763-1772.

Robertson, A. H. and Woodcock, N. 1980. Tectonic setting of the Troodos massif in the east Mediterranean. In: Panayiotou, A., (ed.), Ophiolites, Proceedings, International Ophiolite Symposium, Cyprus 1979. Ministry of Agriculture and Natural Resources, Geological Survey Department, 36-49.

Robinson, P. T., Melson, W. G., O'Hearn, T., and Schmincke, H. -U. 1983. Volcanic glass composition of the Troodos Ophiolite, Cyprus. Geology, 11: 400-404.

Schmincke, H.U., Rautenschlein, M., Robinson, P. T., and Mehegan, J. M. 1983. Troodos extrusive series of Cyprus: A comparison with oceanic crust. Geology, 11: 405-409.

Searle, D. L. and Panayiotou, A. 1980. Structural implications in the evolution of the Troodos massif, Cyprus. In: Panayiotou, A., (ed.), Ophiolites, Proceedings, International Ophiolite Symposium, Cyprus 1979. Ministry of Agriculture and Natural Resources, Geological Survey Department.

Shipboard Scientific Crew. 1983. Sites 501 and 504: Sediments and ocean crust in an area of high heat flow on the southern flank of the Costa Rica Rift. In: Cann, J. R., Langseth, M. G., Honnorez, J., Von Herzen, R. P., White, S. M., et al., Initial Reports DSDP, 69: Washington (U.S. Govt. Printing Office), p. 31-176.

Shipboard Scientific Party. 1988. Site 504. Proc. Ocean Drill. Prog. Initial Rep., Part A, 111, p. 35-251, Ocean Drilling Program, College Station, Texas.

Shipboard Scientific Party. 1992. Site 504. In: Dick, H. J. B., Erzinger, J., Stokking, L. B., et al., Proceedings of the Ocean Drilling Program, Initial Reports 140: College Station, Texas (Ocean Drilling Program) p. 37-200.

Shipboard Scientific Party. 1993. Site 504B, Part 2. In: Alt, J.C., Kinoshita, H., and Stokking, L.B., et al., Proceedings of the Ocean Drilling Program. Intitial Reports 148: College Station, Texas (Ocean Drilling Program) p. 27-84.

Simonian, K. O. and Gass, I. G. 1978. Arakapas fault belt, Cyprus, a fossil transform fault. Geological Society of America Bulletin, 89: 1220-1230.

Smewing, J. 1975. Metamorphism of the Troodos Massif, Cyprus. Unpublished Ph.D. thesis, Open University, U.K. 132 pp.

Smith, G. C. and Vine, F. J. 1991. The physical properties of basalts from CCSP Drillholes CY-1 and CY-1A, Akaki Canyon, Cyprus. In: Gibson, I. L., Malpas, J., Robinson, P. T., and Xenophontos, C. (eds.). 1991. Cyprus Crustal Study Project: Initial Reports, Holes Cy-1 and 1A. Geological Survey of Canada, Paper 90-20, p. 217-232.

Swarbrick, R. E. 1980. The Mamonia Complex of southwest Cyprus: A Mesozoic continental margin and its relationship to the Troodos complex. In: Panayiotou, A., (ed.), Ophiolites, Proceedings, International Ophiolite

Symposium, Cyprus 1979. Ministry of Agriculture and Natural Resources, Geological Survey Department, 86-92.

Thy, P. 1987. Petrogenetic implications of mineral crystallization trends of Troodos cumulates, Cyprus. Geological Magazine, 124: 1-11.

Thy, P., Brooks, C. K., and Walsh, J. N. 1985. Tectonic and petrogenetic implications of major and rare earth element chemistry of Troodos glasses, Cyprus. Lithos, 18: 165-178.

Yang, J. 1992. Constructional and Alteration Features and their Relationships to Sulphide Deposits in the Upper Part of the Troodos Ophiolite, Cyprus. Unpublished Ph.D. Thesis, Dalhousie University, Halifax, Nova Scotia, Canada, 415pp.

Appendix A
Field Notes
Cyprus, 1993 and 1994

Note: Field notes describe all sample locations. Representative samples were used for this study (i.e., one sample from each dike or screen unit).

Re-occupation of Stations 25-33 of 1993:June 23,1994

Geological - Magnetic Comments

Station 25(Dike) - (70.75,122.04)

25-1: -approximately in the centre of the dike
-uniform dark rock
-no special comments

25-2: -as for 25-1, grain size appears similar

25-3: -as for 25-1, grain size appears similar

25-4: -as for 25-1 grain size appears similar
-grain size decrease towards chilled margin starts visibly about a further 0.05m. towards the contact
-dike is pitted/vesicular locally in the central region and shows banded differential erosion towards the upper contact
-this includes the location of samples 25-3 and 25-4
-discontinuous narrow screens occur locally between dikes 25 and 26
-these have the weathering characteristics of massive lava, but could be earlier dike material

Station 26(Dike) - (70.75,122.04)
-some banded differential weathering especially in the lower 0.2m.
-pustular sub-aerial weathering in the central zone

26-1: -in massive medium grained rock

26-2: -in massive slightly finer grained material

26-3: -in massive finer-again material

26-4: -in massive finer grained material near the contact

Station 27(Dike) - (70.75,122.04)
-exhibits columnar cross jointing from contact to contact

27-1: -in coarsest grainsize massive material near the centre of the dike

27-2: -appears to be in slightly finer grained massive material

27-3: -as for 27-2

27-4: -in distinctly finer grained material in the grain size transition to the upper contact
-dikes 27 and 28 are separated locally by thin screens of probably massive lava.

Station 28(Dike) - (70.75,122.04)
-uniform gray-green rock not well cross-jointed and locally small white-filled vesicles.

28-1: -in massive material with the maximum grain size near the centre of the dike

28-2: -material that resembles 28-1

28-3: -in finer material near the upper contact
-the contact between dike 28 and screen 29 is complex with a 0.05m. dikelet probably branching from 28 being located about 0.2m. into the screen, and roughly parallel to the contact.

Station 29(Screen) - (70.75,122.04)
-consists of pillows, pillow fragments, and slightly more massive material
-the pillow margins now show a distinctive darker grey-green colour with abundant rounded white inclusions that were originally varioles
-the pillow interiors and more massive material are now a paler grey-green sometimes with small white filled vesicles
-the size of pillow sections varies from 0.1m. up to 0.5m.

29-1: -in pillow interior 0.02m. from a variolitic zone

29-2: -either in the interior of a more massive pillow or a tongue of massive lava
-thickness of more massive material is at least 0.3m., and the sample is 0.07m. from the weathered edge of the interval

29-3: -in the centre of a 0.1m. diameter probable pillow section

29-4: -appears possibly to be material between two pillows
-0.05m. outside of the variolitic zone of a large pillow

29-5: -in the centre of a 0.15m. section through a pillow

29-6: -just within the variolitic margin of a 0.3m. or greater section of a pillow

-the variolitic zone is 0.02m. wide and the sample is 0.05m. from the outer edge of the zone

29-7: -in a 0.5m. section through a pillow with a 0.02m. thick variolitic margin
-the sample is 0.09m. from the outer edge of the margin

29-8: -in or just within variolitic material in a largely buried pillow

29-9: -in or just within the variolitic margin of an elongated pillow section 0.2m. by 0.12m.

29-10: -in or near variolitic material in a pillow section 0.55m. by 0.25m.
-a less than 0.01m. dikelet is 0.05m. from the sample

29-11: -in or near the variolitic zone of a 0.1m. diameter section of a largely buried pillow

Note: -29-12 and 29-13 are both within a tongue of pillowed material with a 0.02m. thick variolitic margin

29-12: -0.07m. from the outer margin of the pillow

29-13: -an uncertain distance from the outer margin

29-14: -in an interval near the contact of dike 30
-probably in the pillow interior material of the pillow in which 29-12 and 29-13 are located

Station 30(Dike) - (70.75,122.04)
-a massive poorly jointed light grey-green dike which is cut of dike 31
-the contact with screen 29 is rather broken and rust-stained

30-1: -from this broken and rust-stained interval

30-2: -in uniform massive material with maximum grain size near the centre of the dike

30-3: -in similar material

30-4: -similar or slightly finer grained material
-in the vicinity of 30-5, the dike is slightly pustular.
-the dike is everywhere slightly vesicular with white-filled vesicles of up to 0.01m. in diameter.

30-5: -in fairly coarse-grained material near the contact with dike 31

Station 31(Dike) - (70.75,122.04)
-blue-grey rather than the grey-green of dike 30
-chills against both dike 30 and screen 32
-the fine grained margins are noticably darker, slatey and blue-gray than the interior

31-1: -in the middle of the grain size transition to the lower contact

31-2: -at the beginning of this transition

31-3: -coarsest grain interval, central 0.2m. of the dike

31-4 and 31-5:
-in identical adjacent positions in the finest grained material near the upper contact of the dike

Station 32(Screen) - (70.75,122.04)
-closely resembles screen 29 in colour and in construction with the exception that the lowest 0.4m. is massive and not pillowed
-several dikelets of up to 0.1m. in thickness run through the lowest 0.5m. of the screen
Note: -a 0.05m. dikelet also cuts the upper contact of dike 31orthoganally

32-1: -massive lava
-the nearest dike to it is the upper contact of 31 at 0.13m. distance

32-2: -massive lava
-0.25m. above the upper contact of dike 31
-0.15m. below a 0.05m. dikelet that parallels the upper contact of dike 31

32-3: -within and just below the 0.02m. thick variolitic exterior of a 0.12m. or more diameter pillow section

32-4: -in the interior material of a largely buried pillow section

32-5: -in and just below the variolitic exterior of a flattened pillow section of 0.23m. by at least 0.35m.

32-6: -in a pillow interior material of a pillow at least 0.12m. in diameter

32-7 and 32-8:
-in the same pillow
-both in pillow interior material with pillow dimension 0.35m. by at least 0.2m.
-the pillow has a 0.02m. variolitic margin

32-7: -0.05m. on the outer part of this margin

32-8: -0.08m. from this margin

32-9: -in the variolitic and adjacent material in the outer part of a pillow with dimensions 0.3m. by at least 0.4m.

32-10: -in a large flattened pillow 0.85m. long by at least 0.4m. high
-the pillow has a 0.02m. thick variolitic margin
-the sample is in the pillow interior material 0.1m. from the outer margin of the pillow

32-11: -a triangular pillow section 0.36m. by 0.36m.
-the pillow has a variolitic margin and the sample is 0.07m. from the outer part of this margin

32-12: -probably in the same pillow as 32-11, but the pillow is rather broken near the dike contact with dike 33
-in pillow interior material

Station 33(Dike) - (70.75,122.04)
-a massive poorly cross-jointed mid-grey dike
-chills against screen 32
-separated from the next dike above by thin, up to 0.3m. thick, continuous screens of probable pillow lava
-other pillowed screens occur above the dikes just above dike 33

33-1: -in visibly fine grained material near the lower contact of the dike

33-2: -also in the grain-size transition to the lower contact

33-3, 33-5, and 33-6:
-in massive material in the maximum grain size interval in the centre of the dike

Re-occupation of Stations 13-15 of 1993:June 27,1994

Geological and Magnetic Comments

Station 13(Dike) - (71.30,122.37)
-an irregularly cross-jointed dike
-the coarse-grained interior is a medium grey-green, and the fine grained margins are a slatey blue-grey
-shows no internal banding or vesicularity

13-1: -in a fine grained upper band of 0.2m. approximate thickness
-this might represent a separate dike, but is more likely to be the fine grained marginal zone of dike 13
-above the contact of dike 13 is a mineralized and shattered screen possibly of pillow lavas

13-2: -still in the finer margin of the dike, but is observed to be closer to the coarser interior than it is to the contact

13-3: -within the coarser interior of the dike

13-4: -as for sample 13-3

13-5: -as for sample 13-3

13-6: -at the beginning of the transition from the coarse interior to the finer margin

13-7: -similar to 13-6

13-8: -distinctly finer and closer to the contact

13-9: -finer again and closest to the lower contact of the dike

Station 14(Screen) - (71.30,122.37)
-appears to consist of variably fractured and mineralized massive lava
-fresh medium to pale blue-grey-green massive rock with rusty coloured cracks
-this is how it is seen in outcrop where it has experienced subaqueous erosion
-where it has experienced subaerial weathering, which is most of the outcrop, the surface is seen to consist of olive-grey blocks of rather massive material from a few cm's to a few tens of cm's in dimension separated by broad rusty partings of softer mineralized material

-sulfides are abundant especially in these partings where they sometimes line cavities up to several cm's in diameter
-in addition to the rusty-stained partings there are extensive areas covered with white (?)sulfate materials
-general appearance of screen is at least locally of low-grade gossan material

14-1: -subaqueous weathering
-in the centre of a large joint block showing little alteration
-0.2m. from the nearest major joint

14-2: -near the edge of a joint-block
-closest joint is 0.07m.
-subaqueous weathering

14-3: -the centre of a medium joint block at the boundary of subaqueous and subaerial weathering
-0.09m. from the nearest major joint

14-4: -in the centre of a small joint block
-nearest major joint is 0.06m.
-subaerial weathering

14-5: -centre of a small joint block
-0.05m. to the nearest major joint
-subaerial weathering

14-6: -appears to be in the centre of a larger joint block
-just in the subaqueous weathering zone
-0.08m. from the nearest major joint

14-7: -in the centre of a large joint block 0.12m. from the nearest joint
-subaqueous weathering

14-8: -subaqueous weathering zone 0.013m. from the nearest major joint

14-9: -subaqueous weathering zone
-nearest major joint is 0.07m.

14-10: -subaqeous weathering zone
-nearest major joint is a few cm's

14-11: -subaqueous weathering zone
-nearest major joint uncertain

14-12: -subaerial weathering zone in the centre of a rectangular joint block 0.05m. from each of the three major joints

14-13: -subaerial weathering zone in the centre of a joint block probably only a few cm. from a major joint

14-14: -subaqueous weathering zone
-0.07m. from the nearest major joint

14-15: -subaerial weathering zone in the centre of a major joint block
-nearest major joint block is 0.08m.

14-16: -in the centre of joint block, subaerial weathering zone 0.07m. from the nearest major joint

Footnote: After examination of all the samples, the alteration of the screen appears to vary from place to place even when allowance is made for the differences in subaqueous and subaerial weathering. Thus, samples from 14,15 and 16 are in a less altered area of the screen.

Station 15(Dike) - (71.30,122.37)
-irregularly cross-jointed dike underlain by a massive lava screen and overlain by screen 14
-where sampled the weathered surface is a uniformly coloured medium to dark blue-grey with a some what pitted subaqueous erosion surface
-all four samples are probably in the grain-sized transition to the upper contact against screen 14
-both the position and the blue rather than the medium grey colour suggest this

Note: It is approximately 340 paces from the middle of section 13-15 to the middle of the bridge. Pictures of Dike 13 and Screen 14 were also taken.

Re-occupation of Stations 16-19of 1993:June 30,1993

Geological and Magnetic Comments

Station 16(Dike) - (71.60,122.50)
-rather uniform regularly cross-jointed dike
-the dike is exposed subaerially
-the weathered joint surfaces are rusty
-fresher surfaces are sulfate stained probably by drainage from mineralized overlying lava screens
-fresh surface of dike material is a light blue-grey
-grain size noticeably decreases towards the contacts where low grade sulfide banding is apparent

16-1: -near the inner edge of the grain size transition towards the upper contact

16-2,16-3, and 16-4:
-in internal zone of rather uniform grain size

Station 17 and 18(Dike) - (71.60,122.50)
-blue-grey where fresh with some sulfide patches
-separate from dike 16, where sampled, by a 0.5m. lava screen
-subaerial surface similar to that of dike 16, however, this dike is much less regularly jointed, and may be somewhat fractured internally

17-1 and 17-2:
-not far from the upper contact of 17, but appear to be in relatively coarse grained dike interior material

18-1: -just in the grain size transition to the lower contact

18-2: -also in relatively coarse grained interior material

Station 19(Screen) - (71.60,122.50)
-consists of a variety of lava morphologies in a variety of states of alteration
-these morphologies consist of massive lava, large pillows, and smaller pillows
-the alteration state varies from relatively fresh appearance massive lava to quite gossanized zones
-the samples from the screen are naturally divided into several groups of which the first is samples 1-3 which are located on the east side of the

stream below dike 17-18 and the thinner dike
-all samples are from the subaqueous weathering zone

19-1 and 19-2:
-from a small pillow section in a rather fractured interval
-the size of the pillow section is 0.3m.(hor.) by 0.2m.(ver.)

19-1: -approximately 0.07m. from the outside of the pillow fragment

19-2: -same as 19-1

19-3: -from a rather obscure fractured zone
-we cannot determine the lava morphological type
(The interval for 19-1 to 19-3 is very fractured.)

NOte: -the next group of samples from 19-4 to 19-7 are from the west bank of the stream across and immediately downstream of 19-1 to 19-3
-this section consists of massive lava with some large pillows near the base
-in the upper part the massive lava has white-filled vesicles
-discrete veins of sulfide are widely scattered, and individual sulfide grains are present in the lava

19-4: -located within a large pillow section
-the section is 0.8m. long by 0.35m. high
-the interior of the pillow section is relatively little cracked and altered, and resembles in freshness the massive lava immediately above the pillow
-however, 19-4 is clearly finer grained than the overlying massive lava
-the sample is in the middle of the pillow horizontally, and is 0.12m. from the lower edge of the pillow
-a little jasper-like material occurs near the centre of the pillow

19-5: -uniform massive lava of fresh appearance well away from any large mineralized fractures

19-6: -in massive somewhat vesicular lava near the base of the exposed section
-well away from any large mineralized fractures

19-7: -within a large pillow section near the base of the exposure
-the pillow is 0.5m.(hor.) by 0.35m.(ver.)
-the sample is in the middle horizontally and is 0.1m. from the upper part of the pillow

-the pillow material is a light grey-blue similar to the rest of the flow
-it is a little fractured and has no variolitic zone (same as for the pillow in which 19-4 is located)
-the pillow material differs only from the centre of the massive interval by being finer grained

Note: -the next group of samples is 19-8,19-9 and 19-10
-these occur over a horizontal interval of 2.5m. some 7.0m. below 19-4 to 19-7 on the west bank of the stream

19-8: -occurs in an interval of massive fresh somewhat vesicular lava

19-9: -occurs in what looks like a fractured pillow fragment close to the mineralized zone in which 19-10 occurs
-this may be an interval of pillow breccia
-the sample occurs in the vesicular fragment 0.16m. by 0.08m., and is separated from other similar fragments by zones of intense alteration, and jasperization probably representing altered glass, and interpillow material

19-10: -in a zone of pillow fragments and altered light blue-green material with much jasperoid material and some sulfide
-appears to be in a zone of maximum alteration perhaps adjacent to a small movement zone
-some bands of sulfide plus jasper-rich ore material
-there are some fluid seeps as well

Note: -the last group of samples are numbers 19-11 to 19-13
-these are further 7.0m. downstream on the west bank also in the subaqueous weathering zone

19-11: -in a large pillow section
-1.3m.(hor.) by 0.6m.(ver.)
-the pillow is not variolitic and is a little fractured internally
-a little jasperoid material occurs on the partings, and there are some white filled vesicles
-the sample is near one end of the pillow perhaps 0.2m. from the nearest margin
-it is in a fresh gray rock away from any major mineralized fractures
-differs only from the massive lava in being relatively fine grained

19-12: -appears to be in a large pillow fragment of fresh gray vesicular lava
-the fragment is 0.7m. long by at least 0.5m. vertically
-the sample is at least 0.25m. from the nearest pillow margin

-the margins are not variolitic, the pillow is overlain by and is included in massive lava

19-13: -the sample is in an interval transitional between large pillow and massive lava
-the material is a uniform medium gray colour with little sign of alteration or fracturing
-the sample is at least 0.2m. from the nearest possible pillow margin

Re-occupation of Stations 20-24 of 1993:June 30,1994

Geological and Magnetic Comments

General Comments for Stations 20-24:
- -in general the state of regional hydrothermal alteration of this section is relatively low

Station 20(Dike) - (71.85,122.60)
- -relatively thick well-jointed fresh medium grey dike
- -is less altered than Dike 21
- -there is a broad maximum grain size plateau in the centre of the dike
- -at the top, the dike chills against a little altered, grey vesicular massive lava screen

20-1:
- -in the grain size transition to the lower contact

20-2:
- -also in this transition, but further into the dike
- -specks of sulfide are visible in the vicinity of these two samples
- -narrow sulfide-rich veins are present elsewhere
- -both 20-1 and 20-2 are in the centre of a large joint block away from any major cracks or veins

20-3:
- -in the central grain size maximum of the dike
- -it is located in a V-shaped zone between two major sulfide bearing fractures, and has a similar sulfide bearing fracture beneath it
- -it is approximately 0.05m. from each of the fractures which may be related to its weak magnetification

20-4, 20-5, and 20-6:
- -all in the central grain size maximum of the dike
- -they are all in the centre of very fresh joint-blocks
- -they are far from the joint fractures, and these fractures do not carry any sulfide or secondary minerals, they are just physical cracks

Station 21(Dike) - (71.85,122.60)
- -a roughly cross-jointed grey-green dike with 0.05-0.1m. thick horizontally rust banded contact intervals

21-1:
- -finer grained and in the lower rust-banded contact interval

21-2, 21-3, and 21-4:
- -in the grey interior of the dike with grain size appearing to increase through 21-2, 21-3, and 21-4

Station 22(Screen) - (71.85,122.60)

-consist of massive lava with occasional included pillow type outlines
-note:these outlines do not obviously correspond to grain size or change of other features of typical pillows
-the rock is a fresh gray colour, massive, jointed with narrow sulfide veins, and individual clots of sulfide
-where it is subaerially weathered, there is distinctive differential weathering with pronounced banding parallel to the screen

22-1: -in the middle of a rectangular joint block 0.3m. by 0.2m.
-the sample is in the centre of the block and joints are simply unmineralized cracks

22-2: -in the middle of a similar joint block 0.22m. by 0.15m.

22-3: -in the middle of a similar joint block 0.2m. by 0.2m.

22-4: -in the middle of a similar joint block 0.25m. by 0.13m.

22-5: -in the middle of a similar joint block 0.12m. by 0.12m.

22-6: -in the middle of a somewhat cracked larger joint block 0.33m. by 0.2m. with a possible curved pillow outline above it

22-7: -fresh joint block
-block is 0.14m. by 0.21m.
-the sample is 0.03m. from one of the joints

22-8: -in a joint block 0.27m. by 0.1m.

22-9: -in a darker brown weathering zone that occurs adjacent to the contact with dike 21
-the grain size is unchanged and sulfide clots are visible throughout
-the only differences from all the other samples from the screen is the slightly darker colour of the fresh rock, and the brown weathering patina

Station 23(Dike) - (71.85,122.60)

-a well jointed dike with an unusual subaqueous weathering appearance
-the appearance is almost black, rounded, pitch-like and pitted
-the interior of the fresh rock is pale to medium gray with small green phenocrysts, and a slightly mottled appearance

23-1: -in the lower fine grained interval adjacent to screen 20

-relatively sulfide rich as well as being finer grained
-this may be due to proximity to mineralized screen 24

23-2: -at the beginning of the grain sized transition to the lower contact

23-3 and 23-4:
-are in the grain size maxima in the interior of the dike

23-5: -in the grain size transition to the upper contact of he dike

Station 24(Screen) - (71.85,122.60)
-a variable unit
-in primary construction it appears to be a welded pillow breccia which is variably mineralized
-where subaerially weathered it looks like an aa-flow

24-1: -in a tightly welded unmineralized pillow breccia that has been subaqueously weathered
-the sample is from the centre of a fragment of solid lava

24-2: -also from a tightly welded subaqueously weathered part of the screen
-differs from 24-1 in being only partly in a fragment of solid lava, and otherwise in interfragment material

24-3: -in a large fragment of solid material in the breccia
-its dimensions are 0.2m. by 0.3m. by at least 0.15m.
-these are also tightly welded and subaqueously weathered

24-4: -in the more mineralized upper part of the unit
-it is in what looks like fragmented massive lava

24-5: -in the fragmented mineralized upper part of the unit

24-6: -in massive fragmented lava with sulfide veins in the upper part of the unit

Note:Two pictures were taken of Screen 24.

Appendix B
Microprobe Analyses

Note: Sulphides and oxides were identified on the basis of petrology.

Microprobe Analysis

Point	SiO2	TiO2	Al2O3	FeO	MnO	MgO	CaO	Na2O	K2O	P2O5	SrO	Total	Mineral
13-007	53.68	0.00	28.67	0.97	0.00	0.13	12.12	4.55	0.02	0.00	0.00	99.97	plag
	54.04	0.21	27.57	1.08	0.04	0.35	11.15	3.92	1.59	0.00	0.00	99.93	plag
	27.13	0.04	16.94	25.89	0.82	15.68	0.05	0.28	0.00	0.00	0.00	86.75	chlorite
	97.75	0.07	0.12	0.46	0.14	0.01	0.04	0.01	0.00	0.12	0.00	98.20	quartz
	44.26	0.10	9.91	13.25	0.41	16.70	4.94	0.44	0.22	0.06	0.00	90.13	plag altered
	99.11	0.00	0.33	0.13	0.09	0.00	0.02	0.04	0.00	0.01	0.00	99.44	quartz
	53.43	0.03	28.93	0.84	0.00	0.22	12.39	4.69	0.03	0.08	0.00	100.50	plag
	27.99	0.03	17.25	23.46	0.84	16.81	0.30	0.26	0.00	0.01	0.00	86.92	chlorite in plag
	54.45	0.08	28.07	0.77	0.01	0.13	11.42	4.91	0.06	0.23	0.00	99.85	plag
	27.36	0.04	16.80	24.13	0.76	16.14	0.18	0.17	0.00	0.00	0.00	85.53	chlorite
15-003	54.36	0.02	28.60	0.89	0.13	0.25	11.57	4.89	0.00	0.00	0.21	100.56	plag
	53.76	0.08	25.14	1.05	0.02	0.23	9.02	5.47	0.07	0.06	0.34	95.01	plag
	54.10	0.00	28.46	0.95	0.10	0.12	11.53	4.86	0.00	0.00	0.31	100.21	plag
	27.17	0.00	18.17	22.43	1.00	17.15	0.27	0.37	0.00	0.16	0.51	87.06	chlorite
	0.69	0.45	0.21	86.18	0.29	0.12	0.20	0.54	0.00	0.00	0.14	88.56	oxide
	26.24	0.06	17.82	21.44	1.06	16.73	0.08	0.36	0.03	0.00	0.19	83.66	chlorite
16-003	64.47	0.12	18.58	0.20	0.00	0.03	0.21	0.33	16.15	0.09	0.00	99.94	k-spar
	53.17	0.11	28.82	0.89	0.07	0.16	12.24	4.43	0.05	0.00	0.00	99.71	plag
	27.27	0.00	17.85	21.18	1.01	18.69	0.00	0.18	0.00	0.06	0.10	86.18	chlorite
	53.70	0.11	28.14	0.84	0.03	0.11	11.93	4.72	0.00	0.06	0.19	99.33	plag
	53.36	0.11	28.34	1.01	0.06	0.19	12.00	4.55	0.02	0.04	0.00	99.45	plag
	27.15	0.10	18.56	20.54	0.94	19.19	0.02	0.29	0.05	0.03	0.04	86.68	chlorite
18-001	53.53	0.08	28.23	1.18	0.00	0.30	12.28	4.41	0.01	0.07	0.24	100.16	plag
	0.63	0.05	0.00	57.75	0.00	0.00	0.00	0.46	0.04	16.83	9.49	85.16	sulphide
	57.90	0.16	26.18	0.68	0.10	0.21	9.45	5.84	0.00	0.05	0.05	100.26	plag
	30.60	35.48	1.87	1.00	0.00	0.13	28.00	0.11	0.00	0.08	0.12	97.09	titanite
	30.50	33.63	2.63	1.82	0.10	0.01	28.18	0.00	0.00	0.00	0.04	96.76	titanite
	53.63	0.10	28.10	1.13	0.03	0.21	12.08	4.58	0.04	0.00	0.27	100.00	plag
	29.24	0.38	16.68	22.98	1.04	15.45	0.10	0.32	0.00	0.01	0.49	86.67	chlorite
	54.04	0.09	28.00	1.17	0.04	0.16	11.84	4.63	0.00	0.00	0.20	99.86	plag
	29.11	0.16	17.47	20.09	1.12	17.60	0.06	0.29	0.00	0.00	0.18	85.67	chlorite
	53.53	0.10	28.91	1.09	0.00	0.25	12.36	4.43	0.02	0.00	0.15	100.58	plag
	28.59	0.16	17.50	21.17	0.95	16.87	0.03	0.17	0.00	0.00	0.23	85.49	chlorite
	99.65	0.01	0.42	0.00	0.04	0.00	0.00	0.07	0.00	0.00	0.16	100.07	quartz

Point	SiO2	TiO2	Al2O3	FeO	MnO	MgO	CaO	Na2O	K2O	P2O5	SrO	Total	Mineral
19-008	52.55	0.04	28.71	1.15	0.00	0.21	12.56	4.17	0.02	0.03	0.00	99.36	plag
	63.72	0.04	18.34	0.34	0.08	0.05	0.12	0.28	16.54	0.02	0.00	99.35	k-spar
	33.83	0.07	16.47	13.09	0.55	17.95	0.55	0.32	0.10	0.04	0.06	82.87	chlorite
	28.61	0.09	16.51	18.08	0.87	20.33	0.26	0.26	0.00	0.03	0.05	84.92	chlorite
	52.69	0.06	28.07	0.93	0.05	0.17	12.23	4.27	0.03	0.00	0.00	98.37	plag
	99.26	0.04	0.39	0.21	0.07	0.02	0.00	0.08	0.00	0.17	0.00	99.85	quartz
	52.87	0.11	28.48	1.00	0.00	0.32	12.28	4.28	0.00	0.02	0.00	99.24	plag
	51.66	0.05	29.23	0.90	0.00	0.20	13.44	3.85	0.00	0.04	0.00	99.28	plag
	0.84	0.52	0.00	55.93	0.02	0.03	0.27	0.55	0.00	16.55	9.43	84.08	sulphide
20-004	0.81	17.27	0.40	70.03	2.51	0.26	0.91	0.24	0.02	0.00	0.03	92.42	oxide
	54.92	0.12	27.89	0.99	0.07	0.19	10.84	5.39	0.04	0.00	0.22	100.45	plag
	28.09	0.00	16.69	22.64	1.13	16.41	0.34	0.34	0.01	0.05	0.21	85.64	chlorite
	55.50	0.13	27.60	0.84	0.00	0.13	10.82	5.20	0.00	0.05	0.29	100.25	plag
	33.97	0.13	14.04	17.99	0.89	18.26	0.76	0.37	0.03	0.00	0.22	86.50	chlorite
	56.54	0.12	27.85	0.76	0.02	0.21	10.54	5.66	0.00	0.00	0.24	102.06	plag
	0.22	17.84	0.16	69.72	3.89	0.08	0.21	0.29	0.00	0.00	0.06	92.33	oxide
	56.36	0.13	27.44	0.97	0.05	0.32	10.12	5.67	0.00	0.01	0.15	100.88	plag
	37.37	0.22	23.76	11.46	1.37	0.36	21.83	0.11	0.00	0.12	0.21	96.37	epidote
21-003	52.49	0.00	29.06	1.01	0.11	0.20	12.61	4.20	0.04	0.01	0.12	99.56	plag
	26.90	0.09	16.61	23.39	1.17	16.20	0.21	0.42	0.00	0.00	0.24	85.13	chlorite
	53.69	0.06	28.32	0.94	0.07	0.22	11.50	4.69	0.00	0.00	0.25	99.60	plag
	26.77	0.07	17.34	25.06	1.24	15.74	0.08	0.26	0.03	0.09	0.27	86.68	chlorite
	34.83	0.13	11.95	14.40	0.55	18.31	1.20	0.34	0.03	0.00	0.35	81.93	chlorite
	53.43	0.00	28.50	0.91	0.03	0.22	12.03	4.57	0.00	0.00	0.39	100.06	plag
	52.95	0.04	29.13	1.25	0.03	0.23	12.53	4.31	0.00	0.00	0.30	100.69	plag
	61.86	0.13	22.48	0.53	0.09	0.30	4.39	5.22	3.88	0.00	0.12	98.66	K, Na, Ca spar
	52.92	0.08	29.15	1.01	0.11	0.19	12.49	4.37	0.00	0.00	0.29	100.43	plag
22-008	55.95	0.02	28.12	0.62	0.00	0.07	11.04	5.22	0.04	0.12	0.00	100.95	plag
	55.92	0.01	27.40	0.69	0.00	0.10	10.31	5.49	0.01	0.04	0.00	99.81	plag
	0.34	15.25	0.15	72.47	1.48	0.12	0.21	0.45	0.00	0.00	0.05	90.34	oxide
	0.61	0.00	0.00	56.55	0.00	0.00	0.02	2.66	0.03	16.76	9.20	85.77	sulphide
	54.22	0.03	28.35	0.66	0.00	0.17	11.64	4.99	0.00	0.10	0.00	100.02	plag
	54.33	0.00	28.39	0.75	0.00	0.01	11.51	4.81	0.00	0.00	0.00	99.79	plag
	99.88	0.16	0.09	0.01	0.00	0.06	0.00	0.06	0.00	0.20	0.00	99.88	quartz
	99.69	0.03	0.03	0.28	0.00	0.04	0.00	0.05	0.00	0.00	0.00	99.97	quartz
	0.32	15.85	0.85	71.61	1.32	0.11	0.09	0.44	0.00	0.00	0.03	90.40	oxide
	54.87	0.09	27.81	0.89	0.11	0.14	11.27	4.90	0.00	0.00	0.00	99.75	plag

Point	SiO2	TiO2	Al2O3	FeO	MnO	MgO	CaO	Na2O	K2O	P2O5	SrO	Total	Mineral
23-002	55.23	0.05	26.78	0.90	0.07	0.26	10.33	5.00	0.00	0.00	0.08	98.58	plag
	25.23	0.04	14.93	18.34	0.87	14.93	0.24	0.41	0.01	0.26	0.52	75.71	chlorite
	53.40	0.00	28.48	0.83	0.00	0.23	11.81	4.66	0.00	0.00	0.10	99.41	plag
	0.62	0.03	0.00	57.24	0.03	0.00	0.08	0.42	0.00	16.70	9.42	84.40	sulphide pyrite
	54.66	0.26	26.71	1.56	0.04	0.33	10.80	5.08	0.03	0.00	0.12	99.40	plag
	0.76	4.16	1.07	81.48	0.14	0.13	0.56	0.49	0.00	0.00	0.12	88.52	oxide
	26.81	0.03	17.76	22.37	1.18	16.84	0.18	0.42	0.02	0.00	0.18	85.57	chlorite
	58.76	0.00	22.71	1.28	0.10	0.91	4.72	7.74	0.07	0.00	0.20	96.12	plag Na, Ca
	26.71	0.00	17.39	23.75	1.01	16.62	0.04	0.28	0.00	0.02	0.09	85.76	chlorite
	53.73	0.21	28.04	0.75	0.09	0.23	11.59	4.75	0.00	0.00	0.36	99.66	plag
24-003	54.75	0.18	27.31	1.21	0.16	0.01	11.35	4.59	0.04	0.09	0.00	99.55	plag
	53.27	0.12	28.48	1.54	0.00	0.27	12.47	4.31	0.03	0.03	0.00	100.34	plag
	53.56	0.05	28.27	1.69	0.03	0.30	12.49	4.45	0.02	0.03	0.00	100.76	plag
	52.94	0.20	28.97	1.36	0.01	0.22	12.76	4.18	0.01	0.07	0.02	100.63	plag
	12.93	0.53	5.95	47.68	0.49	6.32	1.00	0.75	0.02	0.02	0.03	75.64	Fe chlorite
	26.75	0.07	15.93	17.44	0.95	17.96	0.30	0.37	0.03	0.03	0.06	79.83	chlorite
	0.66	5.43	0.27	80.87	0.34	0.19	0.24	0.35	0.00	0.04	0.13	88.36	oxide
	97.56	0.01	0.25	0.24	0.04	0.00	0.00	0.09	0.00	0.00	0.00	98.05	quartz
	27.45	0.00	16.19	19.08	0.88	18.18	0.33	0.33	0.01	0.02	0.00	82.51	chlorite
25-002	57.09	0.05	26.68	0.74	0.10	0.12	9.55	6.15	0.00	0.06	0.21	100.41	plag
	27.97	0.00	16.92	26.46	0.82	13.50	0.48	0.39	0.00	0.00	0.00	86.53	chlorite
	68.55	0.06	21.09	0.14	0.00	0.15	1.12	8.69	0.01	0.00	0.16	99.44	plag Na
	56.30	0.00	27.16	0.95	0.00	0.21	10.08	5.85	0.00	0.03	0.19	100.54	plag
	26.20	0.00	17.45	27.59	0.68	12.79	0.36	0.40	0.02	0.00	0.42	85.88	chlorite
	50.20	0.33	3.65	20.52	0.87	9.62	11.08	0.69	0.04	0.00	0.20	96.96	pyrx augite
	56.12	0.08	27.40	0.76	0.03	0.22	10.25	5.67	0.00	0.00	0.34	101.01	plag
	27.82	0.13	16.98	27.19	0.73	13.34	0.38	0.33	0.00	0.02	0.16	86.78	chlorite
	1.73	0.44	0.57	78.85	0.07	0.06	0.57	0.40	0.03	0.07	0.08	82.55	oxide
	45.50	4.70	3.29	18.01	0.82	7.70	12.76	0.65	0.01	0.00	0.39	94.11	pyrx augite
	48.46	0.30	2.73	28.66	1.52	7.67	5.64	0.80	0.00	0.00	0.25	96.22	pyrx augite
	55.71	0.03	27.43	0.94	0.00	0.24	10.34	5.54	0.00	0.00	0.06	100.20	plag
	0.54	0.41	0.21	86.20	0.08	0.13	0.18	0.42	0.00	0.00	0.03	87.97	oxide
	49.38	0.34	3.50	20.99	0.92	9.38	10.64	0.60	0.00	0.00	0.14	95.76	pyrx augite
	57.37	0.00	26.55	0.58	0.00	0.18	9.25	6.31	0.03	0.00	0.21	100.44	plag

Point	SiO2	TiO2	Al2O3	FeO	MnO	MgO	CaO	Na2O	K2O	P2O5	SrO	Total	Mineral
26-003	54.39	0.05	28.38	1.15	0.02	0.20	11.62	4.91	0.00	0.00	0.17	100.65	plag
	26.63	0.06	17.60	26.53	0.57	14.87	0.06	0.34	0.00	0.00	0.20	86.55	chlorite
	100.01	0.13	0.14	0.17	0.10	0.00	0.00	0.00	0.00	0.00	0.11	100.16	quartz
	26.05	0.00	17.56	26.42	0.55	14.71	0.09	0.29	0.00	0.00	0.15	85.66	chlorite
	57.88	0.00	26.53	0.53	0.08	0.10	8.79	6.08	0.02	0.00	0.11	99.81	plag
	2.32	0.33	0.70	76.76	0.03	0.85	0.33	0.46	0.01	0.00	0.06	81.76	oxide
	53.39	0.05	28.42	0.99	0.00	0.18	11.59	4.79	0.00	0.00	0.36	99.96	plag
	50.89	0.00	0.64	13.48	1.00	9.65	22.54	0.38	0.00	0.00	0.22	98.82	pyrx augite
	54.46	0.00	27.93	0.73	0.04	0.14	11.35	5.04	0.00	0.00	0.34	99.85	plag
27-003	29.14	0.05	16.18	22.09	0.44	18.37	0.21	0.30	0.03	0.04	0.00	86.72	chlorite
	99.36	0.05	0.18	0.08	0.02	0.03	0.01	0.09	0.00	0.09	0.00	99.60	quartz
	53.17	0.02	29.03	0.97	0.06	0.18	12.65	4.25	0.02	0.03	0.00	100.25	plag
	28.91	0.10	16.24	22.44	0.53	18.29	0.21	0.27	0.01	0.00	0.00	86.89	chlorite
	54.40	0.09	28.62	0.95	0.06	0.11	11.71	4.73	0.04	0.00	0.00	100.42	plag
	54.06	0.00	27.92	1.01	0.00	0.14	11.45	4.47	0.00	0.03	0.00	98.91	plag
	98.00	0.00	0.28	0.19	0.03	0.00	0.04	0.04	0.00	0.08	0.00	98.47	quartz
	49.21	0.03	0.80	13.37	0.89	8.96	21.37	0.43	0.00	0.00	0.02	95.04	pyrx augite
	44.72	0.22	2.40	13.99	0.72	10.22	16.72	0.32	0.00	0.02	0.00	89.31	pyrx augite
	54.41	0.05	28.34	0.89	0.00	0.16	11.58	4.91	0.00	0.02	0.00	100.29	plag
	54.62	0.00	28.60	1.22	0.02	0.05	11.69	4.67	0.01	0.00	0.00	100.80	plag core Ca
	65.93	0.07	21.15	0.37	0.01	0.08	2.11	9.33	0.19	0.17	0.00	99.19	plag rim Na
28-002	53.52	0.05	28.10	1.22	0.00	0.07	11.87	4.75	0.00	0.00	0.00	99.45	plag
	0.36	12.19	2.91	72.67	0.27	0.27	0.17	0.68	0.00	0.01	0.00	89.52	oxide
	27.33	0.06	17.35	24.24	0.56	16.53	0.20	0.23	0.00	0.00	0.13	86.45	chlorite
	64.94	0.01	18.56	0.32	0.00	0.03	0.07	0.34	16.19	0.06	0.00	100.36	k-spar
	69.34	0.00	21.14	0.26	0.00	0.13	1.15	6.73	0.03	0.00	0.00	98.62	plag Na
	27.50	0.01	17.59	24.26	0.58	16.57	0.16	0.23	0.00	0.00	0.00	86.89	chlorite
	65.28	0.02	21.32	0.43	0.00	0.04	1.66	9.94	0.03	0.00	0.00	98.63	plag Na
	67.88	0.01	20.39	0.29	0.07	0.06	0.95	11.62	0.05	0.00	0.00	101.12	plag core Na
	55.34	0.03	27.36	1.04	0.00	0.17	10.77	5.22	0.00	0.12	0.00	99.89	plag rim Ca
30-003	26.71	0.00	17.26	25.12	0.51	15.66	0.12	0.22	0.00	0.00	0.00	85.59	chlorite
	54.09	0.01	28.48	1.12	0.00	0.07	11.81	4.76	0.01	0.04	0.00	100.25	plag
	33.56	25.73	6.75	3.81	0.14	2.05	21.81	0.83	0.00	0.13	0.00	94.55	titanite
	53.23	0.10	27.49	1.06	0.06	0.20	11.27	4.56	0.00	0.11	0.00	97.88	plag rim Ca
	30.51	31.31	3.10	2.53	0.03	0.07	27.14	0.01	0.01	0.07	0.00	94.58	titanite
	57.77	0.30	26.05	0.35	0.07	0.03	8.27	6.69	0.00	0.09	0.06	99.43	plag
	64.66	0.04	18.47	0.26	0.00	0.04	0.06	0.10	16.18	0.00	0.00	99.56	k-spar core
	66.30	0.07	20.94	0.29	0.00	0.03	1.71	9.50	0.06	0.00	0.00	98.74	plag rim Na
	51.73	0.09	28.86	0.89	0.00	0.08	12.80	3.91	0.09	0.00	0.12	98.29	plag
	0.65	6.47	0.43	69.08	0.08	0.09	1.04	0.43	0.01	0.78	0.18	79.05	oxide
	26.74	0.00	17.60	23.81	0.65	15.88	0.17	0.31	0.01	0.00	0.21	85.17	chlorite

Point	SiO2	TiO2	Al2O3	FeO	MnO	MgO	CaO	Na2O	K2O	P2O5	SrO	Total	Mineral
31-002	52.58	0.00	29.18	1.39	0.04	0.21	12.54	4.09	0.04	0.00	0.00	99.99	plag
	55.58	0.00	27.30	0.90	0.03	0.10	10.60	5.38	0.01	0.00	0.00	99.75	plag
	52.51	0.36	1.81	9.6	0.00	16.19	18.71	0.22	0.00	0.00	0.00	99.39	pyrx augite
	27.15	0.09	17.09	22.75	0.75	16.86	0.18	0.34	0.02	0.10	0.14	85.12	chlorite
	55.64	0.00	27.00	0.96	0.09	0.19	10.29	5.50	0.06	0.14	0.08	99.57	plag
	15.55	0.58	10.44	53.09	0.27	11.19	0.24	0.46	0.03	0.00	0.19	91.82	Fe chlorite
32-002	26.52	0.00	17.45	24.99	0.68	15.90	0.12	0.30	0.00	0.00	0.03	85.95	chlorite
	26.59	0.11	17.79	25.12	0.93	15.70	0.09	0.31	0.00	0.04	0.00	86.44	chlorite
	66.44	0.07	20.72	0.56	0.00	0.10	1.56	10.56	0.02	0.00	0.00	99.85	plag Na
	58.04	0.00	25.82	0.38	0.00	0.08	7.98	6.93	0.00	0.10	0.03	99.14	plag
	64.54	0.00	20.50	1.15	0.06	0.62	2.39	8.53	0.04	0.02	0.02	97.73	plag Na
	68.86	0.00	19.99	0.35	0.04	0.07	0.38	9.48	0.02	0.01	0.00	99.05	plag core Na
	56.35	0.16	26.58	1.06	0.00	0.14	10.11	5.52	0.00	0.09	0.00	99.63	plag rim Ca
	61.94	0.11	19.39	0.29	0.00	0.24	2.56	3.11	9.43	0.37	0.60	97.94	k-spar
	66.72	0.02	20.32	0.47	0.06	0.21	0.70	9.08	0.15	0.03	0.08	97.65	plag Na
	29.09	0.06	17.39	21.67	0.70	16.18	0.59	0.54	0.03	0.05	0.12	86.17	chlorite
33-003	53.89	0.03	29.13	1.03	0.00	0.32	12.23	4.67	0.00	0.03	0.20	101.26	plag
	51.64	0.03	0.63	13.68	0.62	10.27	22.47	0.23	0.00	0.00	0.08	99.54	pyrx augite
	53.74	0.11	28.78	0.77	0.01	0.16	11.86	4.82	0.03	0.02	0.26	100.39	plag
	27.06	0.18	17.54	25.44	0.65	15.69	0.25	0.30	0.00	0.10	0.16	87.11	chlorite
	51.43	0.10	29.70	1.04	0.00	0.32	13.71	3.78	0.00	0.00	0.17	99.98	plag
	27.30	0.11	17.24	24.74	0.61	15.66	0.17	0.32	0.05	0.00	0.22	86.24	chlorite
	0.21	18.33	1.24	68.80	2.26	0.17	0.21	0.46	0.02	0.00	0.18	92.66	oxide
	53.26	0.06	29.01	0.91	0.00	0.24	12.24	4.50	0.00	0.00	0.20	100.16	plag